



UNIVERSITY *of*
TASMANIA

DOCTORAL THESIS

**Size structured reef ecosystems: linking size
spectrum theory to global field observations
of reef fauna from copepods to sharks**

Author:

Freddie J. HEATHER
(MBiolSci with Hons.)

Supervisors:

Rick STUART-SMITH
Julia BLANCHARD
Graham EDGAR

*A thesis submitted in fulfilment of the requirements for the
degree of Doctor of Philosophy*

Institute for Marine and Antarctic Studies (IMAS)
University of Tasmania

November, 2021

Declaration of Authorship

I, Freddie J. HEATHER, declare that this thesis titled, "Size structured reef ecosystems: linking size spectrum theory to global field observations of reef fauna from copepods to sharks" and the work presented in it are my own. I confirm that:

- This work was done wholly or mainly while in candidature for a research degree at this University.
- Where any part of this thesis has previously been submitted for a degree or any other qualification at this University or any other institution, this has been clearly stated.
- Where I have consulted the published work of others, this is always clearly attributed.
- Where I have quoted from the work of others, the source is always given. With the exception of such quotations, this thesis is entirely my own work.
- I have acknowledged all main sources of help.
- Where the thesis is based on work done by myself jointly with others, I have made clear exactly what was done by others and what I have contributed myself.

Signed:

Date: Wednesday 17th November, 2021

Statement of authority of access

This thesis may be made available for loan and limited copying and communication in accordance with the Copyright Act 1968.

Statement regarding published work

The publishers of the papers comprising Chapters 2 and 3 hold the copyright for that content and access to the material should be sought from the respective journals/publishers. The remaining nonpublished content of the thesis may be made available for loan and limited copying and communication in accordance with the Statement of Access and the Copyright Act 1968.

Due to the inclusion of published material there is unavoidable repetition of material between chapters in this thesis.

Signed:

Date: Wednesday 17th November, 2021

Statement of co-authorship

The following people and institutions contributed to the publication of work undertaken as part of this thesis:

Freddie Heather (FH)¹, Rick Stuart-Smith (RSS)¹, Julia Blanchard (JB)¹, Graham Edgar (GE)¹, Rowan Trebilco (RT)^{1,2}, and Kate Fraser (KF)¹.

1. Institute for Marine and Antarctic Studies, University of Tasmania, 20 Castray Esplanade, Battery Point, Hobart, TAS 7004, Australia
2. Antarctic Climate & Ecosystems CRC, 20 Castray Esplanade, Hobart, TAS 7004, Australia

Contribution of work by co-authors for each paper:

Paper 1 (Located in Chapter 2): Heather, F.J., Blanchard, J.L., Edgar, G.J., Trebilco, R. and Stuart-Smith, R.D., 2021. *Globally consistent reef size spectra integrating fishes and invertebrates*. Ecology Letters, 24(3), pp.572-579.

FH designed the analysis, analysed the data and led the writing of the manuscript. FH, JB, GE, RT and RSS contributed to critical feedback, interpretation and substantial revisions of the paper.

Paper 2 (Located in Chapter 3): Heather, F.J., Stuart-Smith, R.D., Blanchard, J.L., Fraser, K.M., and Edgar, G.J., (2021). *Reef communities show predictable undulations in linear abundance size spectra from copepods to sharks*. Ecology Letters, 24(10), pp.2146-2154.

FH and GE conceptualised the study, FH designed the analysis, analysed the data and led the writing of the manuscript. KF performed epifaunal sampling. FH, JB, RSS, GE and KF contributed to critical feedback, interpretation, and substantial revisions of the paper.

We, the undersigned, endorse the above stated contribution of work undertaken for each of the published (or submitted) peer-reviewed manuscripts contributing to this thesis:

Freddie Heather
Candidate,
Institute for Marine and
Antarctic Studies,
University of Tasmania

Rick Stuart-Smith,
Primary supervisor,
Institute for Marine and
Antarctic Studies,
University of Tasmania

Catriona MacLeod,
Ecology & Biodiversity
Centre Head,
Institute for Marine and
Antarctic Studies,
University of Tasmania

Date: Wednesday 17th November, 2021

UNIVERSITY OF TASMANIA

Abstract

College of Sciences and Engineering
Institute for Marine and Antarctic Studies (IMAS)

Doctor of Philosophy

**Size structured reef ecosystems: linking size spectrum theory to global field
observations of reef fauna from copepods to sharks**

by Freddie J. HEATHER

Across aquatic systems, the body size of an organism is often more important than its species identity in determining how it interacts with its predators, competitors, and habitat. The relationship between body size and abundance is often described by a linear function on the log-log scale (the size spectrum). The size spectrum provides a very simple way to represent an ecological community comprised of potentially many species, life stages and individuals with just two parameters, a slope, and an intercept. The size spectrum slope, for example, can inform us about how energy moves through the system (e.g., feeding behaviours), and deviations from expected slope values can inform us about disturbances (e.g., fishing impacts). To determine 'deviations', we must first characterise a baseline size spectrum, vital to its use as an ecological indicator of reef health.

The study of community size spectra requires individual-level body size and abundance data. Empirical studies of size spectra therefore rarely span multiple taxonomic groups or broad spatial scales, prohibiting more general conclusions about the ecosystem. The Reef Life Survey (RLS) is a global-scale citizen-science program surveying the marine life of both tropical and temperate reefs. The data from this program provides an incomparable resource to test various size spectra theories in reef ecosystems and forms a core basis for the research presented in this thesis.

The primary goal of the thesis was to extend our knowledge on the size structuring of reef communities across taxonomic groups and scales, by combining these global empirical data with novel analytical approaches. Three discrete aims were: 1) Describe the empirical size spectrum of reefs globally, including both fishes and large mobile invertebrates. 2) Investigate the cause of the commonly observed 'dip' in abundance of the small fishes in reef size spectra, which is often assumed to be a result of under-sampling of small reef fishes. 3) Determine how the size structure of reef communities relates to abundance and the number of species, three elements of biodiversity rarely considered together.

The first analytical chapter of this thesis addresses the issue of reef size spectra studies focusing on a single taxonomic group and therefore potentially missing large components of the energy pathway. The study estimated invertebrate body size data based on asymptotic length and combines it with fish body size data to provide the first global-scale

estimates of reef size spectra that extend beyond just the fishes. The study highlights the importance of including invertebrates in reef size spectra, develops a method for estimating invertebrate body size in other data-poor situations, and provides a baseline size spectrum for reefs.

The second analytical chapter addresses the issue of reef size spectra studies ignoring small fishes. Observed reef size spectra including small to medium sized fishes tend to be unimodal on the log-log scale. It has been common practice to remove small-bodied individuals less than the modal body size and fit a linear model to the “descending limb”. This practice has been justified by the potential of under-sampling these small individuals. The study tests this theory of under-sampling by extending the body size range of the size spectrum to incorporate the smallest sized reef fauna – epifaunal individuals down to 0.125 mm in body size. This study provides evidence for this abundance ‘dip’ being a true feature of an underlying nonlinear size spectrum. This study extended the linearity of reef size spectra investigated on reefs to span the entire range of size classes of consumers, for the first time, to my knowledge. Outcomes have important implications for the justification of the removal of the smaller-bodied individuals, and therefore for the estimation of the size spectrum slope.

The final analytical chapter uses size spectra to address a broad question regarding the complex inter-dependencies between body size, abundance, and species richness. The study applies, and further develops, a method originally developed for estimating community size spectra from protist species size distributions to investigate three important macroecological relationships; 1) the abundance size spectrum, 2) the species-richness size spectrum (how species richness varies with body size), and 3) the combination of these; the proposed linear (on the log-log scale) relationship between species richness and abundance within size classes. The study also provides a methodology to accurately reconstruct these three relationships in situations with minimal body size data (e.g., from only the species abundance and an estimate of asymptotic species size), providing a pipeline by which future studies can investigate these relationships using datasets that lack equivalent size detail to the RLS data used here.

The combined outcomes of these three analytical chapters include enhanced understanding of energy flow and size structure of reef ecosystems. In particular, they confirm alignment with theoretical expectations when much of the full ecosystem size spectrum is covered, rather than removing portions of it to confirm theory or extrapolating from a single taxonomic group. The study also provides a means to better progress use of size spectra as ecological indicators of reef health. By describing both the linear and nonlinear aspects of the empirical size spectrum of reefs, we are now better positioned to identify the environmental, ecological, and anthropogenic drivers of variation and deviation in the size spectrum. This PhD project, which benefitted from a highly detailed dataset to generate and test methods, now provides a set of approaches that can be applied by ecologists in other fields, under less data-rich situations.

Acknowledgements

First and foremost, thank you Rick, Julia and Graham. I am so grateful for having the opportunity to work with you three, and I feel very privileged to have had you as my teachers and colleagues. Rick, thank you for your patience with my stubbornness to learn and write my manuscripts in \LaTeX , and for always bringing my rambblings back to the ecological significance. Graham, thank you for your wise insights into whatever is it I am racking my brain over. Julia, thank you for introducing me to Tasmania, I never imagined that the first email I sent you back in Sheffield regarding a Masters project would eventually lead to me completing a PhD with you in Tasmania. It's been an awesome journey.

This PhD would not have been possible without the countless hours of work from all the volunteer divers and the team behind the Reef Life Survey, including all the staff involved with vital data management. Thank you for not only creating an incredible global marine database, but also for making it publicly available. Special thanks to Toni Cooper, Lizzie Oh, Ella Clausius, Just Berkhout, and Scott Ling. This research was supported by the Marine Biodiversity Hub, a collaborative partnership supported through funding from the Australian Government's National Environmental Science Program, and data management support from Australia's Integrated Marine Observing System (IMOS). This research was also made possible by funding of the Australian Research Council (ARC).

Thank you to Shane Richards for helping me with attempts to incorporate bayesian methods into my work. Although they did not make it into the work presented in the thesis, hopefully it will form some component of the planned work together moving forward. Also, thank you Simon Wotherspoon, it may not have seemed like much at the time, but your offer to lunch at the Japanese restaurant across from the Waterfront came at a critical time during my PhD and meant a lot to me. Thank you as well to Asta Audzijonyte for our over-a-cuppa chats about wellbeing and academic-life in general.

The large majority of my time during my PhD was spent in R and RStudio. Thank you to the R core team, RStudio team, and the team behind Tidyverse, you have made the past four more enjoyable, efficient, and satisfying.

I am so thankful to have had such a welcome to Tasmania. From the Pritchard family who first took me in when I arrived, to the Yorkies Xtra that have become my own family over the past four years. Thank you to the OG Yorkies for making me one-of-us at York St, and to introducing me to all the people that later became close friends.

A big shout out to IMAS PhD students from both the Waterfront and Taroona. You have helped me through the rough times, and celebrated the good times, it has been invaluable to have you all there, riding the PhD train together. Thank you especially to the Taroona crew; I live for the 10:30 tea and crossword and weekly Pomodoro snacks. To those that came before, thank you, and to those yet to graduate, good luck and I will be there for your submission party. To all my friends and family that have supported me in the last four years throughout the PhD: Thank you so much.

Thank you very much to Jian Yen and Renato Morais for examining this thesis, I really appreciate the time you put into providing detailed, constructive comments. I would also like to thank the three anonymous reviewers, and James Robinson for their time in reviewing the published papers presented in this thesis.

Contents

Declaration of Authorship	ii
Abstract	v
Acknowledgements	vii
1 General introduction	1
1.1 The distribution of life on earth: A macroecological lens	1
1.2 On animal body size	1
1.3 Why do we care about the size spectrum?	3
1.4 Various representations of the size spectrum	3
1.5 Size structured reefs	5
1.6 Aims of the thesis	6
1.6.1 Aim 1: Describe the empirical size spectrum of reefs globally, including both fishes and large mobile invertebrates.	6
1.6.2 Aim 2: Extend the size spectrum to include small epifaunal invertebrates.	6
1.6.3 Aim 3: Investigate the relationship between body size, abundance, and species richness in reef ecosystems and,	7
1.6.4 Aim 4: Develop a methodology to explore broad-scale size spectra in the absence of detailed body size information.	7
2 Globally consistent reef size spectra integrating fishes and invertebrates	8
2.1 Abstract	8
2.2 Introduction	9
2.3 Methods	11
2.3.1 Survey data	11
2.3.2 Estimation of invertebrate body length distributions	12
2.3.3 From body length to body mass	12
2.3.4 Fitting the normalized abundance size spectrum	13
2.4 Results	13
2.5 Discussion	14
2.6 Acknowledgements	18
2.7 Supplementary material	18
S2.1 Estimating observed body size for invertebrates	18

S2.2	Estimation of invertebrate body mass from body length	22
S2.3	Justification of a cut-off value	24
S2.4	Normalization of the size spectrum	25
S2.5	Invertebrate inclusion effect across latitudinal zones	25
S2.6	Are temperate-tropical differences in size spectra a product of large scale differences in fishing pressure?	27
S2.7	Global patterns of fish-only and combined community size spectra slopes	28
S2.8	Sensitivity analysis	29
3	Reef communities show predictable undulations in linear abundance size spectra from copepods to sharks	32
3.1	Abstract	32
3.2	Introduction	33
3.3	Methods	35
3.3.1	Survey data	35
3.3.2	Combining the datasets	36
3.3.3	Fitting nonlinear size spectra	36
3.3.4	Hypothesis testing	37
3.3.5	Environmental covariates	38
3.4	Results	38
3.5	Discussion	41
3.6	Acknowledgements	44
3.7	Supplementary material	45
S3.1	Linear vs. nonlinear size spectra models	45
S3.2	Environmental variables	47
S3.3	Body size position of peak abundance	48
S3.4	Environmental covariates explaining model parameters	48
S3.5	Model comparison	49
4	Resolving global links between body size, abundance, and species richness on reefs	52
4.1	Abstract	52
4.2	Main	53
4.3	Abundance size spectrum	53
4.4	Richness size spectrum	55
4.5	Richness-abundance spectrum	58
4.6	Predictions in the absence of individual-level data	58
4.7	Methods	60
4.7.1	Data collection	60
4.7.2	Body mass estimation	61
4.7.3	Fitting abundance size spectra	61
4.7.4	Fitting richness size spectra	62

4.7.5	Fitting richness-abundance spectra	62
4.7.6	Size spectrum reconstruction methods	62
	Method 1 (One body size distribution per species)	63
	Method 2 (Asymptotic size for each species)	64
4.7.7	Building the community size spectrum	64
4.7.8	Validating reconstructed size spectra	65
4.8	Acknowledgements	66
4.9	Supplementary material	66
S4.1	Estimating the body mass distribution from asymptotic mass	66
S4.2	Survey-level abundance size spectra	69
S4.3	Survey-level richness size spectra	71
S4.4	Survey-level richness-abundance spectrum	73
5	Synthesis & future research	74
5.1	The size spectrum as an ecological indicator of reef health	74
5.2	Where to next?	77
5.2.1	Question 1. How do environmental variables influence reef size spectra globally?	77
5.2.2	Question 2. How does MPA status influence reef size spectra?	78
5.2.3	Question 3. Does habitat complexity result in a tertiary structure of the reef size spectrum?	78
5.2.4	Question 4. Do peaks in reef size spectra represent trophic guilds?	78
5.2.5	Question 5. Are aquatic species body size distributions lognormal?	79
5.2.6	Question 6. Could the Rossberg et al. (2019) model predict the domes in reef size spectra?	79
5.2.7	Question 7. How do nonlinear reef size spectra vary globally?	80
5.2.8	Question 8. Are reconstructed size spectra sufficiently accurate to broadly reflect local-scale disturbance (e.g., fishing)?	80
5.2.9	Question 9. Can we reconstruct the size spectrum using eDNA only?	83
5.2.10	Question 10. Could global species distribution data be used to reconstruct size spectra?	83
5.3	Concluding remarks	84
5.4	Code availability	84

List of Figures

1.1	Normalisation of the size spectrum	4
2.1	Hypothesized effect of including invertebrates in the size spectrum	11

2.2	Invertebrates steepen the normalized abundance size spectrum	14
2.3	Globally consistent size spectra	15
2.4	Size spectrum slope and spatial scale	16
S2.5	The relationship between asymptotic and mean body size	20
S2.6	The relationship between asymptotic and variance in body size	21
S2.7	Estimating invertebrate length	22
S2.8	Invertebrate length-weight relationships	23
S2.9	Justification of a lower-bound cut-off	24
S2.10	Ecoregion-level normalized abundance size spectrum	26
S2.11	Tropical vs Temperate invertebrate effect	27
S2.12	Invertebrate inclusion effect in MPAs	28
S2.13	Global patterns of fish-only and combined size spectra	29
S2.14	Length-weight sensitivity analysis	31
3.1	Conceptual diagram of hypotheses	35
3.2	Sinusoidal patterns in linear model residuals	39
3.3	Example linear and nonlinear size spectrum fits	40
3.4	Comparison of AIC values of three models	41
S3.5	Extended size spectra for 45 sites	45
S3.6	Linear vs. nonlinear size spectrum models	46
S3.7	Abundance peaks vs. Temperature	48
4.1	Empirical relationships between M, N and R	55
4.2	Global patterns in M, N and R	57
4.3	Reconstructed relationships between M, N and R	60
4.4	Summary of the reconstruction approach	63
4.5	Methods summary	65
S4.6	Predicting meanlog from asymptotic mass	67
S4.7	Predicting sdlog from asymptotic mass	68
S4.8	Survey-level abundance size spectra (25 surveys)	69
S4.9	Goodness-of-fit distributions for abundance size spectra	70
S4.10	Survey-level richness size spectra (25 surveys)	71
S4.11	Goodness-of-fit distributions for richness size spectra	72
S4.12	Richness-abundance spectra (25 surveys)	73
5.1	Size spectrum in the full context	76
5.2	Future directions	77
5.3	Ways to build a power-law community size spectrum	82

List of Tables

S2.1	Length-weight sensitivity analysis values	30
S3.1	Details of environmental variables	47
S3.2	Variation explained by environmental variables	49
S3.3	Comparison of the three models AIC values	49

List of Abbreviations

RLS	Reef Life Survey
AIC	Akaike Information Criterion
RMSE	Root Mean Squared Error
SST	Sea Surface Temperature
MPA	Marine Protected Area
NEOLI	No take, Enforced, Old, Large, and Isolated MPAs
MLE	Maximum Likelihood Estimation
SSD	Species Size Distribution
eDNA	environmental DNA

List of Symbols

N	abundance	m^{-2}
m, M	body mass	g
l, L	body length	cm
l_{∞}, L_{∞}	Asymptotic length	cm
m_{∞}, M_{∞}	Asymptotic mass	g
R	Species richness (number of species)	
R_m	Species richness within mass class, m	
N_m	Abundance within mass class, m	
k	species ID	
s	site ID	
e	ecoregion ID	
c	taxonomic class ID	
a	Power-law coefficient	
b	Power-law exponent	
u	Linear model random variable coefficient	
$p(x)$	Probability of x	
λ	size spectrum slope	
$\bar{\lambda}$	mean size spectrum slope	
μ_x	lognormal meanlog paramater ($x = \text{length or mass}$)	
σ_x^2	lognormal sdlog paramater ($x = \text{length or mass}$)	

*To Mum,
Thank you for always being there, and for believing in me.
I made it happen.*

Chapter 1

General introduction

1.1 The distribution of life on earth: A macroecological lens

It has long been recognised that life is not evenly distributed across the globe, yet the causal explanations for this remain disputed. Why, for example, are there so many species in the tropics (Brown, 2014)? Or, why do we also observe a longitudinal gradient in marine species richness, peaking in the Coral Triangle (Edgar et al., 2017)? Questions of this nature require a global lens. Macroecology is the study of broad scale (both temporal and spatial) ecological patterns and processes (Brown and Maurer, 1989, Brown, 1995), and is based upon the assumption that the current state of an ecological community is a net outcome of complex underlying processes (Brown et al., 2002). The statistical description of global- or regional-scale empirical patterns in abundance, species richness, and body size allows for the identification of universal patterns or ‘laws’, not possible by analysing the individual components of a system alone. A combination of broad-scale statistical descriptions and fine-scale analyses of individual components is required to inform theoretical approaches and to develop a better understanding of structuring of ecological communities (Connolly et al., 2017, Gaston and Blackburn, 2000). Macroecological methods are therefore one component to understanding these fundamental questions of the partitioning of energy and distribution of life on earth.

Body size has long been recognised as a fundamental characteristic of an organism. The relative ease of measuring body size and the fact that body size scales with so many ecologically important traits (Peters, 1983, also discussed below) has led to body size being a central component of macroecological research. One of the overarching aims of this thesis is to better understand the generality of body size related patterns in the context of biodiversity and ecosystem structure for reefs. Using a global-scale reef database, I focus on understanding the universality of body size and abundance relationships and broaden the range of taxonomic groupings and diversity of sizes compared to work that has been previously been carried out for reefs.

1.2 On animal body size

“One hill cannot shelter two tigers” – Chinese proverb

The above quote prefaces a chapter from Charles Elton's 1927 book *Animal Ecology* (Elton, 1927). It introduces the idea that carnivorous animals at or near the top of an ecological food chain require large geographical areas to support their food requirements. With this idea, Elton developed a fundamental concept in ecology; animals higher up the food chain are less abundant in comparison to those at the base, which Elton termed the Pyramid of numbers. Elton posed another way to view this relationship – that smaller animals are more common in general, assuming that animal body size and trophic position are related. These concepts make intuitive sense (e.g., there are more plankton than there are whales in the ocean), yet the underlying mechanisms behind these patterns were only speculative.

Around this time, Huxley et al. (1932) showed that body size was correlated to many physiological variables that could be described by the power-law relationship,

$$Y = a \cdot M^b$$

where, a and b are constants, M is body mass and Y is some dependent variable such as growth rate or metabolic rate, later termed allometric equations. The same year, Kleiber (1932) showed that an animal's basal metabolic rate was proportional to its body mass to the power of $\frac{3}{4}$, which later went on to form the basis of the metabolic theory of ecology (Brown et al., 2004).

Despite the importance of body size in determining an animal's vital rates, much of trophic ecology for the following four decades focused on the roles of species and taxonomic niches over body size-based methods (see Sprules and Barth, 2016). An exception to this was a relatively forgotten, yet very important, study by Ghilarov (Ghilarov, 1944). Ghilarov showed a predictable decline in abundance of soil organisms, irrespective of taxonomy, with logarithmic body size. This result was later recognised as equivalent to consistent biomass within logarithmic body size bins and the first example in any ecosystem of what was later termed the "biomass equivalence rule" (Polishchuk, 2019, Polishchuk and Blanchard, 2019).

In the late 1960s and early 1970s, Sheldon, Parsons and colleagues, with the aid of a new cell counting technology, the Coulter counter (Sheldon and Parsons, 1966), began observing similar patterns of biomass equivalence in planktonic organisms in the ocean, apparently unaware of the patterns Ghilarov (1944) observed in soil. With a series of studies spanning large spatial scales and a range of planktonic body sizes (Sheldon and Parsons, 1967, Sheldon et al., 1967, 1972), Sheldon and colleagues came to the famous hypothesis that equal concentration of biomass occurs from bacteria to whales (Sheldon et al., 1972). This incredible relationship between logarithmic body size and biomass, irrespective of taxonomic identity, termed the biomass size spectrum, opened the field of study of the size spectrum in aquatic ecology, and led to a concerted effort to classify the biomass size spectrum in a range of aquatic systems (see Sprules and Barth, 2016), including freshwater lakes (Sprules et al., 1983), open ocean (Rodriguez and Mullin, 1986), and intertidal estuaries (Schwinghamer, 1981).

1.3 Why do we care about the size spectrum?

Body size is often described as the single most important trait determining how an individual interacts with its environment and community (Peters, 1983, Schmidt-Nielsen, 1984). Animal body size has been empirically related to many ecological and physiological rates (Peters, 1983) such as growth rate, metabolic rate (Brown et al., 2004, Kleiber, 1932), swimming rate (Ware, 1978), and trophic level (Jennings et al., 2001, 2002). The distribution of individual body sizes within a community, irrespective of species identity, i.e., size spectrum, can therefore provide important information about how energy (i.e., biomass) is partitioned in the community and how it moves throughout the food web.

The size spectrum is often represented as a linear relationship between body mass and biomass (or abundance) on the log-log scale. The linear size spectrum is a very simplistic way to describe a complex community, with only an intercept and slope, and yet is a useful indicator of ecosystem health and relative human exploitation of the system (Nash and Graham, 2016, discussed further in the section *Size structured reef ecosystems* below).

Species-based food web models often represent individuals within species as a single entity, where body size is represented by a single value per species (Brose et al., 2017). Traditionally, terrestrial ecology has focused on taxonomic compositions of communities and favoured species-based approaches over purely size-based, such as the size-spectrum approach (Cyr et al., 1997), possibly due to the relatively small change in ecosystem function with change in the body size of terrestrial species (Trebilco et al., 2013). Aquatic ecologists, however, have readily adopted size-based methods in ecological modelling due to well described ontogenetic niche shifts and size-based predation (Cohen et al., 1993).

To propose that any single method (e.g., size-based or species-based) is sufficient to model a complex ecosystem would be an oversimplification, yet size-based and species-based approaches have generally been considered separately. More recently however, there have been increased attempts to combine these size-based and species-based approaches (Andersen and Pedersen, 2010, Blanchard et al., 2014, Hartvig et al., 2011, Purves, 2013, Trebilco et al., 2013, White et al., 2007). Chapter 4 of this thesis also attempts to combine these fields by relating the abundance size spectrum to the relationship between body size and species richness (discussed in more detail in the section *Aims of the thesis* below).

1.4 Various representations of the size spectrum

There are many representations of community body size-abundance relationships in the literature (White et al., 2007). Two of the most common approaches are 1) the logarithmic biomass within logarithmic body size classes (the biomass size spectrum) (e.g. Boudreau and Dickie, 1992, Kerr and Dickie, 2001), and 2) the logarithmic abundance within logarithmic size classes, also known as the numerical or abundance size spectrum (Blackburn and Gaston, 1997). Both relationships are often represented as linear relationships on the log-log scale with slopes of approximately zero (i.e., biomass equivalence) (Figure 1.1A)

and -1 (decreasing abundance with body size)(Figure 1.1C) for biomass and abundance size spectra, respectively (Blanchard et al., 2017, Trebilco et al., 2013).

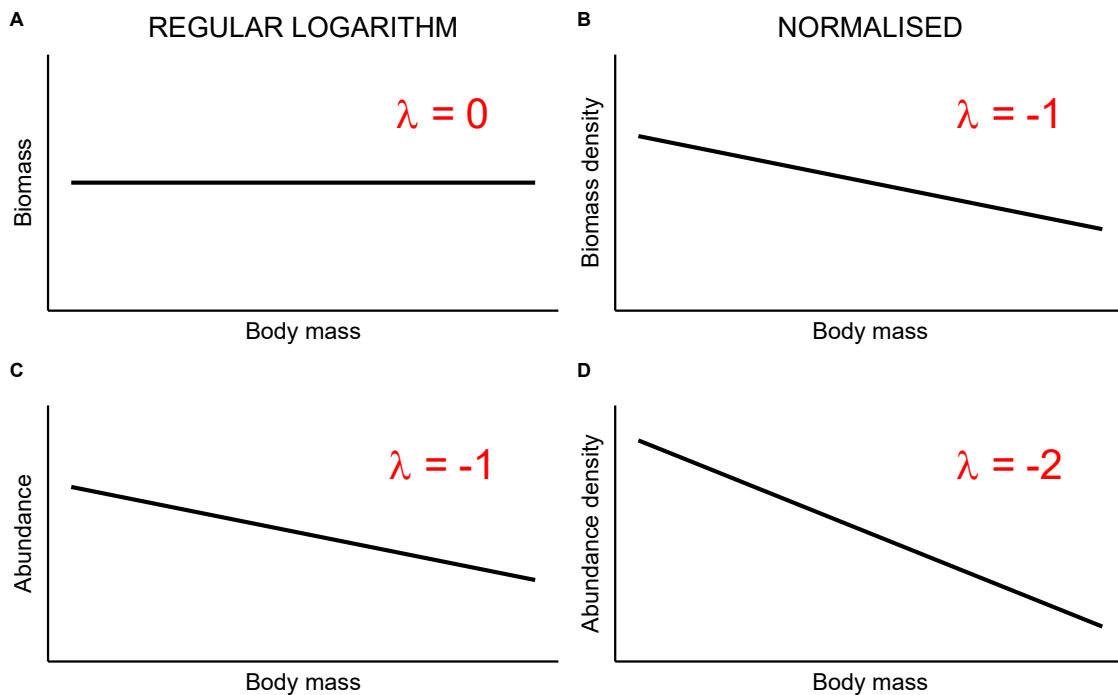


FIGURE 1.1: A comparison of the approximate slope (λ) estimates of individual-level community size spectra. Comparing normalised (Platt and Denman, 1977) and non-normalised abundance and biomass size spectra.

To allow better comparison between studies, Platt and Denman (1977) accounted for the variable logarithmic bin widths by dividing the abundance (or biomass) by the width of the bin, providing an estimate of abundance (or biomass) per unit body size, i.e., abundance density (or biomass density). This procedure of dividing by bin width is known as normalisation of the size spectrum and is now commonly used in size spectra studies (Kerr and Dickie, 2001). Normalisation of the size spectrum reduces the size spectrum slope by 1 (Figure 1.1B, D), which in turn provides a direct estimate of the exponent value (b) of the non-logarithmic (power-law; White et al., 2008) relationship. Normalisation of the size spectrum therefore promotes the comparison of slopes between studies. Despite this, confusion still remains with various representations of size spectra (White et al., 2007), which often convey the same information (Trebilco et al., 2013).

Edwards et al. (2017) used a simulation approach to compare various representations of size spectra to determine the best approach for estimating the size spectrum slope. Edwards et al. (2017) show that using maximum likelihood estimation to fit a bounded pareto distribution to the rank-frequency relationship of individual body size provides the best estimate of the slope (and therefore exponent) of the size spectrum. A rank-frequency relationship does not, however, provide an estimate of the intercept of the size spectrum, which can signify ecologically important information such as primary production. In contrast, linear regression methods, whilst potentially flawed (Edwards

et al., 2017), provide the ability to easily incorporate spatial scale as a random effect of slope estimates (Heather et al., 2021a).

1.5 Size structured reefs

Human impacts are altering the structure and function of reef ecosystems (Hughes, 2003, Mellin et al., 2016, Morais et al., 2020a, Stuart-Smith et al., 2021), both directly (e.g., through fishing; Jennings and Lock, 1996, Robinson et al., 2017), and indirectly (e.g., climate change; Cheal et al., 2017, Hughes et al., 2018). The total impact of these ecosystem stressors, however, is not consistent across the size spectrum. Not only are larger-bodied individuals at greater risk to broad scale ecosystem disturbance due to their reduced rate of turnover (Reynolds et al., 2001) but fishing practices are often highly size-selective, often targeting the largest bodied individuals (Jennings et al., 1999, Pauly, 1998). Further, with larger individuals often at higher trophic levels (Jennings et al., 2002), and predation levels in aquatic systems typically driven by body size, reductions in the abundance of larger individuals can result in size-dependant flow-on effects through the food web (Rossberg et al., 2019, Salomon et al., 2010). The distribution of individual body sizes of a reef community, irrespective of species (i.e., the size spectrum), has therefore been suggested as a potentially useful ecological indicator (e.g. Graham et al., 2005), but its use relies on its strength to detect ecosystem disturbances.

Despite the simplicity of the linear size spectrum, there exists a wealth of literature on its use as an ecological indicator, across not only reefs but a range of ecological communities (Shin et al., 2005). The slope of the size spectrum for example, has been shown to vary with fishing pressure on reefs (Dulvy et al., 2004, Graham et al., 2005, Nash and Graham, 2016, Robinson et al., 2017) and across a range of other aquatic ecosystems (Bianchi et al., 2000, Rice and Gislason, 1996, Blanchard et al., 2005). In order to quantify the level of disturbance of an ecosystem however, it is necessary to have a baseline from which to compare (Jennings and Blanchard, 2004).

Although empirical size spectra across aquatic ecosystems are generally fitted with a linear model, peaks at certain body sizes (aka. “domes”; Boudreau et al., 1991) are commonly observed (e.g. Sprules et al., 1983). The exact cause of this nonlinearity is currently under question (Rossberg et al., 2019); hypotheses include the physical environment providing body size-specific niches or refugia (Rogers et al., 2014, Schwinghamer, 1981), bottom up or top-down trophic cascades (Andersen and Pedersen, 2010, Benoît and Rochet, 2004, Rossberg et al., 2019), or even simply sampling biases associated with visual survey methods on reefs (Ackerman et al., 2004, Ackerman and Bellwood, 2000). Chapter 3 of this thesis empirically tests these hypotheses (discussed more in the section *Aims of the thesis* below).

Many theories have been proposed to explain the consistency in the size spectrum slope (depending on the method used, see Figure 1.1). These theories range from simple ecological principles, such as the metabolic theory of ecology (i.e., abundance (N) scales with body mass (M) to the power of -0.75: $N \propto M^{-0.75}$) and inefficient energy transfer

between trophic levels (therefore $N \propto M^{-0.75}$) (Trebilco et al., 2013) to complex process-based models (see Blanchard et al., 2017). This thesis does not aim to answer the question of which of these theories, or combination of theories, give rise to the apparently universal pattern of the size spectrum. This thesis does however aim to describe the empirical size spectrum of reefs globally, allowing for the validation of these theories and the further development of empirically-based mechanistic and statistical approaches. Below I outline the specific aims of this thesis.

1.6 Aims of the thesis

Despite the importance of body size in determining an individual's life history traits and vital rates, a purely size-based approach does not provide a complete picture of ecosystem structure, particularly in reefs; which are amongst the most species-rich ecosystems. Mechanistic approaches have moved towards combined species and size based approaches (Andersen, 2019, Reuman et al., 2014) yet they require foundations based on empirical observations. The primary goal of this thesis is to extend our knowledge on the size structuring of reef ecosystems across taxonomic groups and scales, by combining global empirical data (Edgar et al., 2020, Edgar and Stuart-Smith, 2014, RLS, 2021) with novel analytical approaches. Four discrete aims of this thesis are:

1.6.1 Aim 1: Describe the empirical size spectrum of reefs globally, including both fishes and large mobile invertebrates.

Historically, studies of reef size spectra focus on a single taxonomic group (e.g., fishes) and thus the contribution of other taxa in the system remains uncertain. Chapter 2 of this thesis aims to address this uncertainty, determining the reef size spectra across all large, mobile consumers in a system. The study presented in Chapter 2 estimates invertebrate body size data based on asymptotic length and combines it with fish body size data to provide the first global-scale estimates of reef size spectra that extend beyond just the fishes. The study highlights the importance of including invertebrates in reef size spectra, develops a method for estimating invertebrate body size in other data-poor situations, and provides a baseline size spectrum for reefs. This chapter is published in Ecology Letters (Heather et al., 2021a).

1.6.2 Aim 2: Extend the size spectrum to include small epifaunal invertebrates.

Chapter 3 addresses the issue of reef size spectra studies often ignoring small fishes. Observed reef size spectra including small to medium sized fishes tend to be unimodal on the log-log scale (Ackerman et al., 2004). It has been common practice to remove small-bodied individuals less than the modal body size and fit a linear model to the "descending limb" (e.g. Robinson et al., 2017, Trebilco et al., 2015, Wilson et al., 2010). This practice has been justified by the potential of under-sampling these small individuals. The study presented in Chapter 3 tests this theory of under-sampling by extending the body

size range of the size spectrum to incorporate the smallest sized reef fauna – epifaunal individuals down to 0.125 mm in body length. This study provides evidence that this abundance ‘dip’ is a true feature of an underlying nonlinear size spectrum. This study extended the scope of reef size spectra investigated on reefs to span the entire range of size classes of consumers, for the first time to my knowledge. The results of this study have important implications for the justification of the removal of the smaller-bodied individuals, and therefore for the estimation of the size spectrum slope. This chapter is published in Ecology Letters (Heather et al., 2021b).

1.6.3 Aim 3: Investigate the relationship between body size, abundance, and species richness in reef ecosystems and,

1.6.4 Aim 4: Develop a methodology to explore broad-scale size spectra in the absence of detailed body size information.

Chapter 4 uses size spectra to address a broad question regarding the complex interdependencies between body size, abundance, and species richness. The study applies, and further develops, a method originally developed for estimating community size spectra from protist species size distributions (Giometto et al., 2013, Rinaldo et al., 2002) to investigate three important macroecological relationships; 1) the abundance size spectrum, 2) the species-richness size spectrum (how species richness varies with body size), and 3) the combination of these; the proposed linear relationship between log species richness and log abundance within size classes. The study also provides a methodology to accurately reconstruct these three relationships in situations with minimal body size data (e.g., from only the species abundance and an estimate of asymptotic species size), providing a pipeline by which future studies can investigate these relationships using datasets that lack equivalent size detail to the global empirical data used here (Edgar et al., 2020, Edgar and Stuart-Smith, 2014).

These chapters contribute to an enhanced understanding of the size structure, and ultimately the energy flow, of global reef ecosystems. By describing both the linear and nonlinear aspects of the empirical size spectrum of reefs, we are now better positioned to identify the environmental, ecological, and anthropogenic drivers of variation in the size spectrum. This PhD project, which benefitted from a highly detailed dataset to generate and test methods, now provides a set of approaches that can be applied by ecologists in other fields, under less data-rich situations.

Chapter 2

Globally consistent reef size spectra integrating fishes and invertebrates

Freddie J. Heather¹, Julia L. Blanchard¹, Graham J. Edgar¹, Rowan Trebilco^{1,2}, Rick D. Stuart-Smith¹

1 – Institute for Marine and Antarctic Studies, University of Tasmania, 20 Castray Esplanade, Battery Point, Hobart, TAS 7004, Australia

2 – Antarctic Climate & Ecosystems CRC, 20 Castray Esplanade, Hobart, TAS 7004, Australia

Code availability: Code for the analysis, and to recreate all figures, is available at https://github.com/FreddieJH/inverts_size_spec.

2.1 Abstract

The frequency distribution of individual body sizes in animal communities (i.e., the size spectrum) provides powerful insights for understanding the energy flux through food webs. However, studies of size spectra in rocky and coral reef communities typically focus only on fishes or invertebrates due to taxonomic and data constraints, and consequently ignore energy pathways involving the full range of macroscopic consumer taxa. We analyse size spectra with co-located fish and mobile macroinvertebrate data from 3,369 reef sites worldwide, specifically focusing on how the addition of invertebrate data alters patterns. The inclusion of invertebrates steepens the size spectrum, more so in temperate regions, resulting in a consistent size spectrum slope across latitudes, and bringing slopes closer to theoretical expectations based on energy flow through the system. These results highlight the importance of understanding contributions of both invertebrates and fishes to reef food webs worldwide.

2.2 Introduction

Body size is arguably the most important single factor determining an individual's vital rates and how it interacts with its environment (Brown et al., 2004). Body size distributions therefore provide rich insights into size-dependent relationships between animals and underlying energy flow of communities. One such distribution links individual body size and abundance in a community (the community size spectrum). This relationship has been extensively studied in both marine and terrestrial realms (e.g., Reuman et al., 2008), following early conjectures of a "biomass equivalence rule": that biomass is approximately equal across logarithmic size bins spanning sizes of the smallest to the largest creatures (Ghilarov, 1944, Sheldon et al., 1972). This results in a negative power-law relationship between abundance concentration (N) and body size (M) (Andersen and Beyer, 2006), $N \propto M^\lambda$, where $\lambda \approx -2$. Because of the important information concerning system-wide energy movements (Brown and Gillooly, 2003, Trebilco et al., 2013), methods used to estimate the power law exponent have been extensively evaluated in the literature (White et al., 2008, Edwards et al., 2017).

Although remarkable consistencies in empirical size spectra have been observed (Sprules and Barth, 2016), substantial deviations can also occur. These deviations provide important information about ecosystem structure and perturbations. For example, the selective removal of larger individuals through fishing has been shown to steepen the negative slope of the size spectrum in both pelagic (Daan et al., 2005, Pope and Knights, 1982, Blanchard et al., 2005) and reef ecosystems (Dulvy et al., 2004, Graham et al., 2005, Wilson et al., 2010, Robinson et al., 2017). By contrast, seasonal competition for resources (Edgar, 1994) and energy subsidies from outside the reef ecosystem (Trebilco et al., 2013, 2016, Morais and Bellwood, 2019) can potentially result in shallower size spectra, while habitat complexity can cause deviations of the size spectra from the expected power law (Rogers et al., 2014). For a community of individuals feeding on a common resource, i.e., at a single trophic level, such as herbivorous fishes (Robinson et al., 2016), abundance may also scale less steeply with body size, following the allometric scaling of body size with metabolic rate and energetic equivalence (Damuth, 1981, Kleiber, 1932, Nee et al., 1991). However, most aquatic communities are comprised of a trophic chain or web, whereby individuals feed upon one another as well as the basal resource. Consequently, due to inefficiencies in the transfer of energy between trophic levels (Lindeman, 1942), fewer individuals can be sustained when feeding at higher trophic levels. Given the strong relationship between an individual's size and its trophic position (Jennings et al., 2001), this is consistent with fewer large-bodied individuals in a community arising from individuals feeding in a size-based way (i.e., a food chain or web) (Brown and Gillooly, 2003, Jennings and Mackinson, 2003, Trebilco et al., 2013, Andersen, 2019). Although the general pattern of declining abundance with body size holds in many places, particularly at very large spatial scales, there has been no global test of the "biomass equivalence rule" at the community scale for reefs or any other large system (Polishchuk and Blanchard, 2019).

Global datasets available to test the “biomass equivalence rule” for marine systems have been previously lacking. The Reef Life Survey (RLS) program has quantified the abundance and size distribution of all conspicuous species on reef habitats globally (Edgar and Stuart-Smith, 2014) and provides the best available means for exploring biomass equivalence at this scale. It is the largest single database, terrestrial or marine, in terms of its taxonomic, spatial and temporal coverage with a basis of standardized quantitative methods. The high resolution yet global coverage of the data enables us to investigate size spectra at varying spatial scales.

Another challenge relates to the major missing component of reef community size spectra: benthic invertebrates. Whilst most previous empirical work on reef size spectra has focused solely on fish communities, large mobile benthic invertebrates can play fundamental roles in reef ecosystems, even to the point of dominating the animal biomass present. For example, in some temperate reefs, we observed communities in which over 90% of individuals >1 cm body size, were invertebrates (see also Edgar et al., 2017). Furthermore, considerable overlap exists in resource use between fishes and invertebrates, with overlap in the diets of many fishes and invertebrates, and many fish predators relying heavily on invertebrate prey (i.e., fishes and invertebrates do not necessarily occupy separate energy pathways)(Barneche et al., 2014). As such, to better understand the size structure of whole reef communities and food webs that are not artificially constrained by taxonomic group, data on both fishes and invertebrates are needed. Several previous studies have recognized the potential importance of invertebrates in reef size spectra (e.g., Donovan et al., 2018), but body size data were lacking. Here, we use invertebrate body size data to test the “biomass equivalence rule” for size spectra of reef communities, comparing fish-only data and fish and invertebrate data for the same sites globally.

We hypothesize that: 1) The inclusion of invertebrates will change the slope (i.e., exponent) of the community size spectrum (Figure 2.1). If invertebrates are relatively smaller bodied than their fish counterparts in a community (e.g., Figure 2.1A), we would expect their inclusion in the size spectrum to have a steepening effect (Figure 2.1B). Likewise, if invertebrates are relatively larger bodied than the fishes in the community (e.g., Figure 2.1C), we would expect a shallowing effect when they are included (Figure 2.1D). This also might correspond to a situation where herbivorous or detritivorous invertebrates occupy a single trophic level, which would result in shallower slopes (Dinmore and Jennings, 2004, Maxwell and Jennings, 2006). We further hypothesize that: 2) This invertebrate inclusion effect will be greater in temperate communities compared to tropical communities due to a relatively greater proportion of invertebrates in temperate reefs (Edgar et al., 2017). 3) The broad geographic span and fine transect-level grain allows us to consider multiple spatial scales, and thereby test our third hypothesis; spatial scale of sampling contributes to variation around slope estimates. A λ of -2 is expected in the absence of human impacts, such as fishing. Because few reefs worldwide are beyond the reach of fishers, we expect to find a steeper (more negative) slope overall. This study provides improved understanding on the variability of reef size spectrum slopes globally, which is crucial for the development of size spectra as indicators for reef ecosystem health (e.g., Nash and

Graham, 2016, Trebilco et al., 2016, Zgliczynski and Sandin, 2017, Morais et al., 2020a).

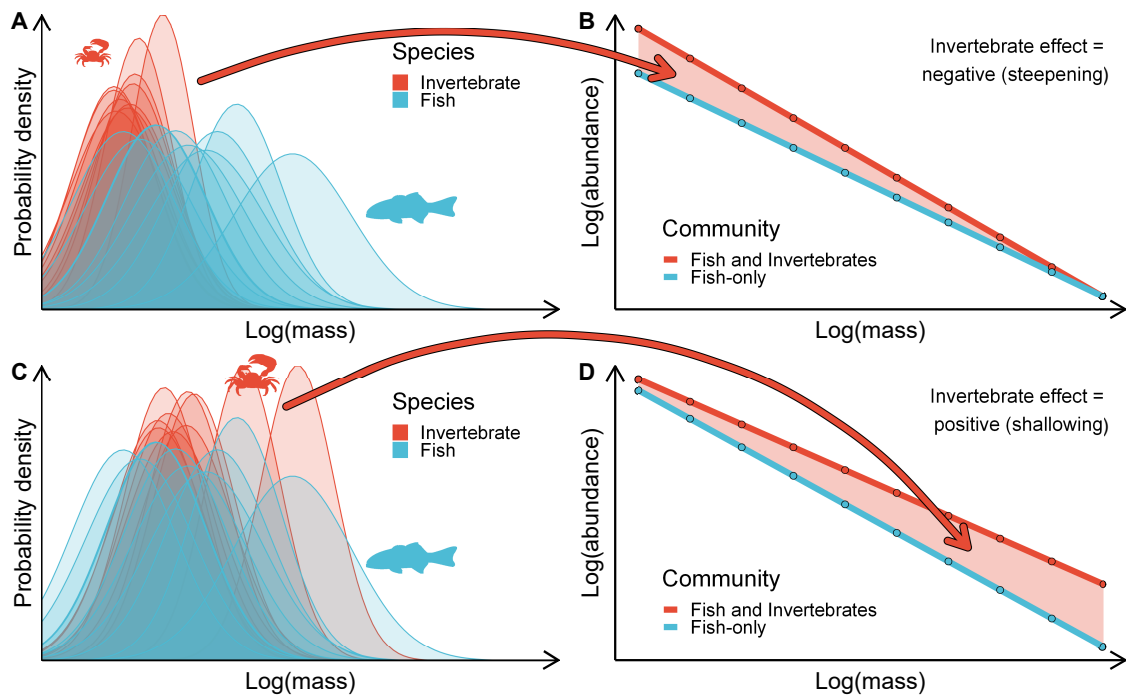


FIGURE 2.1: Hypothesized effect of including invertebrates in the size spectrum: 1) A steepening effect (A, B), and 2) a shallowing effect (C, D). The steepness of the size spectrum arises from the relative abundances of larger and smaller bodied individuals. If invertebrates have a steeper size spectrum slope (i.e., relatively fewer large-bodied individuals) compared to their co-located fish (A), we would expect the slope of the size spectrum of the combined community (fish and invertebrates) to be steeper than the slope of the fish only (B). A shallowing effect (D) would be expected if invertebrates have a relatively greater number of large-bodied individuals compared to the fish-only community (C).

2.3 Methods

2.3.1 Survey data

Applying the RLS protocol (available at <https://www.reeflifesurvey.com/>), trained divers swim along a 50 m transect and identify to species level the fishes and invertebrates they encounter (Edgar and Stuart-Smith, 2014). A single survey ($n = 11,936$ surveys) consists of two separate methods undertaken on the same transect line. Method 1 involves recording any fish species ($n = 2,608$ species) within 5 m wide blocks either side of the line, whilst method 2 involves searching along the bottom, underneath kelp and in cracks in 1 m wide blocks either side of the line, recording invertebrates ($n = 1,184$ species) and cryptic fishes ($n = 951$ species). Abundance of each species within the defined block area is counted directly or estimated when necessary for highly abundant species. Size is estimated for all fishes, and by experienced biologists for invertebrates at some sites. Animals are estimated to belong to one of 13 size categories: 2.5, 5, 7.5, 10, 12.5, 15, 20, 25,

30, 35, 40, 50, and 62.5 cm. Lengths greater than 62.5 cm are estimated to the nearest 12.5 cm. For a full description of the survey methods, see [RLS \(2021\)](#). Abundance from method 2 records were standardized to the equivalent area covered by method 1 by multiplying abundance by five, standardizing all records as densities per 500 m^2 . A site ($n = 3,369$ sites) usually contained multiple surveys undertaken along at least two depths on the same day. Sites are nested in 'locations', which are nested within ecoregions ($n = 91$ ecoregions), as defined by the Marine Ecoregions of the World ([Spalding et al., 2007](#)).

2.3.2 Estimation of invertebrate body length distributions

All invertebrates encountered on surveys were identified to species level (or the highest taxonomic resolution possible) and counted within 1 m wide blocks either side of each 50 m transect line surveyed for fishes. At a small subset of surveys, body length of the invertebrates was estimated or measured. Species body length distributions with sufficient observations ($n > 10$ per species, spanning a sufficient range of body length bins for distribution fitting) were therefore available for only 167 invertebrate species ($\approx 14\%$ of total invertebrate species in the data) from seven taxonomic classes. For these species, individual body lengths were best described by a lognormal distribution, consistent with the body length distributions of the fish species and previous body length distribution literature (e.g., [Blackburn and Gaston, 1994](#)). For each species, we fitted a lognormal distribution to the body lengths using the 'fitdistrplus' package ([Delignette-Muller and Dutang, 2015](#)) in R ([R Core Team, 2020](#)). We then fitted two linear regression models estimating the two parameters of the lognormal distribution (mean and variance) using the asymptotic length of the species and its taxonomic class as predictor variables (Equations S2.3, S2.4). For the remaining species with only asymptotic length available, we were then able to reconstruct the lognormal body length distribution by estimating the two lognormal distribution parameters using these two regression models. Asymptotic sizes for all invertebrate species were obtained from SealifeBase ([Palomares and Pauly, 2019](#)).

2.3.3 From body length to body mass

Conversion to individual body mass distributions was achieved using published length-weight allometric relationships derived from SealifeBase ([Palomares and Pauly, 2019](#)) and FishBase ([Froese and Pauly, 2010](#)) and observed (where available) or estimated individual body length. For each species we calculated the asymptotic mass (M_∞) given asymptotic body length (L_∞) and the species' length-weight relationship. Where species-specific individual length-weight information was unavailable, body mass was estimated from one of two linear regression models: a class-level and an overall length-weight regression model (Appendix S2.2).

To assess the effect of including invertebrates into the size spectrum on the estimation of the slope, all further analyses were carried out firstly with only fish species included,

and secondly with invertebrates also included. Differences in the size spectrum slopes between these two analyses is referred to as the ‘invertebrate inclusion effect’ ($\Delta\lambda$).

2.3.4 Fitting the normalized abundance size spectrum

Relationships between N and M are generally estimated from a linear regression of binned size data on a log-log scale Newman (2005). Size spectrum analyses often ‘normalize’ the y-axis by dividing the abundance within each mass bin by the actual width of the x-axis bin to account for varying bin widths. This normalization procedure has the effect of reducing the size spectrum slope by 1 and results in the slope being comparable with the power law exponent λ . Here we use the slope of the normalized abundance size spectrum to estimate the exponent λ . We chose a linear regression method over a maximum likelihood estimation of the exponent (see Edwards et al., 2017), due to the simplicity of incorporating the spatially-hierarchical nature of the data (sites nested within ecoregions).

For each survey, individuals were binned into \log_2 mass bins, and the abundance within each bin calculated as the number of individuals in each bin. Ackerman and Bellwood (2000) found that the abundances of 75% of fish smaller than 5 cm were underestimated in reef visual census data. To avoid biases associated with under-sampling of small individuals, we applied a lower bound cut-off of 32 g body mass, which represented the modal \log_2 mass bin (Appendix S2.3, see also Ackerman et al., 2004). Abundances were divided by 500 to obtain abundance per m^2 .

We normalized the abundance by dividing by the width of the logarithmic mass bin (Appendix S2.4). We then fitted linear mixed effects models of \log_2 abundance (N) as a function of the \log_2 mass bin mid (M) and with ecoregion (e) and site (s) as random effects, both having a random slope and intercept, and with site nested within ecoregion (Equation 2.1).

$$\log_2(N) = \beta_0 + u_{0,e} + u_{0,s|e} + (\beta_1 + u_{1,e} + u_{1,s|e}) \cdot \log_2(M) + \epsilon \quad (2.1)$$

where, $u_{0,e}$, $u_{0,s|e}$, $u_{1,e}$, and $u_{1,s|e}$ are normally distributed random effects, and where β_1 represents the overall (global-level) slope, $u_{1,e}$ is the ecoregion-level variation and $u_{1,s|e}$ the site level variation (given the ecoregion variation) in the slope estimates of the model (Appendix S2.4). Linear mixed models were fitted using the lme4 package (Bates et al., 2015) in R (R Core Team, 2020). Confidence intervals around the overall slope estimate were estimated using the Wald method in the ‘confint’ function of the lme4 package (Bates et al., 2015).

2.4 Results

For fish-only communities, we estimated the overall mean site-level slope of the normalized abundance size spectrum (λ) as $-1.88 (\pm 0.06, 95\% \text{ CI})$. The inclusion of invertebrates steepened (i.e., decreased) λ from -1.88 to $-2.04 (\pm 0.06, 95\% \text{ CI})$ (Figure 2.2, One sample t-test: $\overline{\Delta\lambda} = -0.07, df = 3371, p < 0.001$).

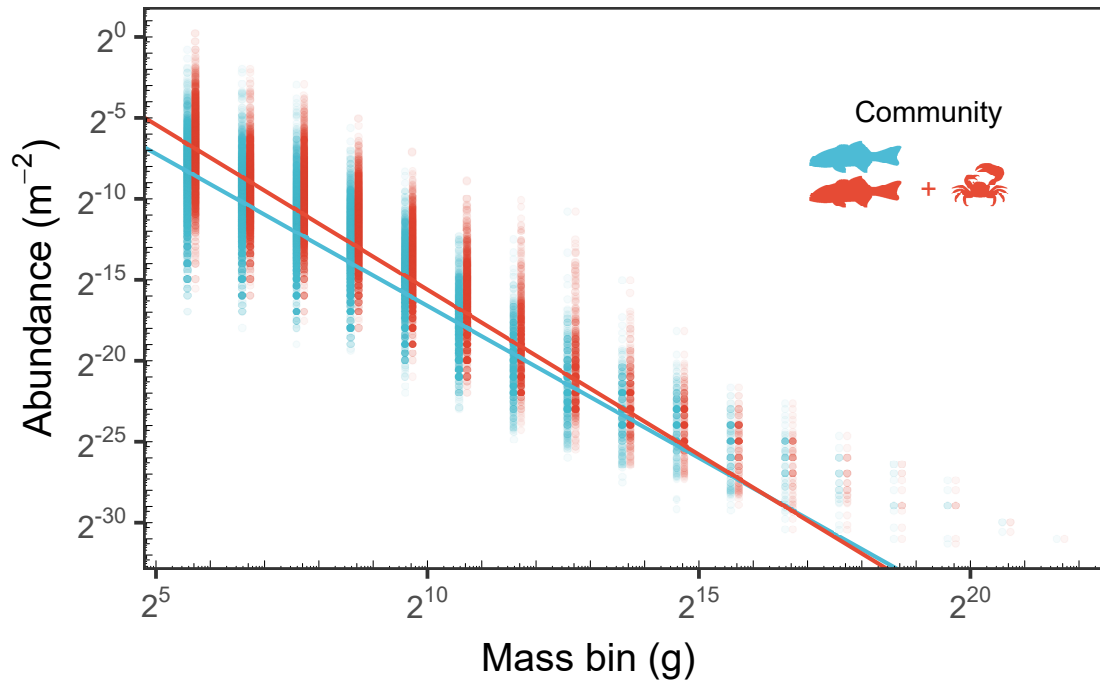


FIGURE 2.2: Invertebrates steepen the normalized abundance size spectrum. Separate normalized abundance size spectra are shown for the fish-only and combined (fish and invertebrate) communities, with solid lines representing fits from linear mixed effects models for the global data (“Site” nested within “Ecoregion” as random effects). Fish-only slope = -1.88 ± 0.06 , combined slope = -2.04 ± 0.06 . Points have been offset on the x-axis for clarity.

Absolute latitude explained 13% of the variation in the invertebrate inclusion effect ($\Delta\lambda$), with a greater steepening at higher latitudes (linear regression model: $\Delta\lambda \sim \text{abs}(\text{latitude})$; $R^2 = 13\%$, $p < 0.001$) (Figure 2.3B, C). Slopes for fish-only communities were shallower at high latitudes, while slopes for the combined fish and invertebrate data were remarkably consistent across latitudes (Figure 2.3A) (see also S5). This greater steepening by invertebrate inclusion, in higher latitude regions was also observed in sites with the greatest protection from fishing pressure (see Appendix S2.6).

Variation in the slope estimates were explained at both the ecoregion and site (given the ecoregion) scales (Figure 2.4). More of the variation in the slope was evident across ecoregions (Combined community: $\sigma_e = 0.25$, 14% total variation), than among sites within ecoregions (Combined community: $\sigma_{s|e} = 0.17$, 9% of total variation). The total variation explained, across all sites and ecoregions, is the sum of these two variation components, and hence shows that variation declines with increasing spatial scale overall.

2.5 Discussion

This study provides the first global test of the generality of the “biomass equivalence rule” for reef communities, analyzing size spectra of 3,369 reef communities worldwide. Our analyses resulted in three key findings: 1) The inclusion of invertebrates, as opposed to a purely fish-centric approach generally used previously, brought the global estimate of

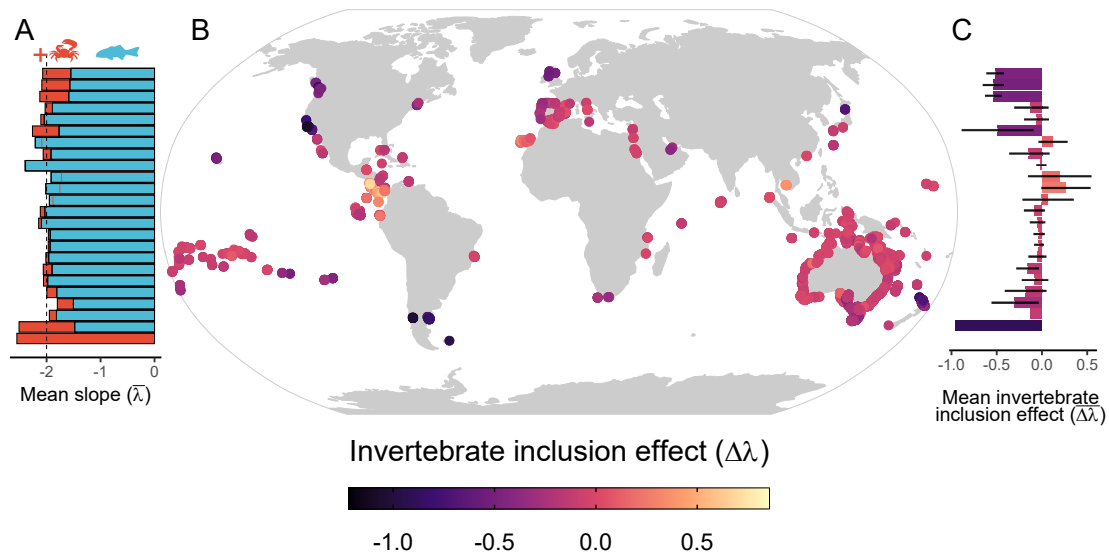


FIGURE 2.3: The inclusion of invertebrates results in a consistent community size spectrum slope of ~ -2 . (A) The size spectrum slope for fish-only communities (blue) and when including invertebrates (orange) – orange vertical lines have been used to indicate the top of the orange bar when obscured. (B) A map of the invertebrate inclusion effect ($\Delta\lambda$) across the globe. (C) The latitudinal variation of the ‘invertebrate inclusion effect’ ($\Delta\lambda$). The steepening effect when including invertebrates is greatest at high latitudes. Each bar in A and C represents the mean over 5° of latitude. Error bars in C represent the 95% confidence intervals, and missing error bars represent insufficient data.

size spectrum slopes closer to the theoretical exponent of -2, the value expected under the biomass equivalence rule; 2) The effect of including invertebrates was most marked for temperate reefs, where invertebrates contribute a substantial fraction of reef animal biomass; and 3) The contributions to variance in slope estimates were comparable at both the ecoregion (14%) and site scales (9%). Many studies of size spectra aggregate observations to larger spatial scales, whereas our work shows that accounting for hierarchical sampling at the local community scale is important for informing the overall processes driving estimates of size spectra as well as testing the generality of theoretical expectations.

Size spectrum theory, that encompasses detailed mechanistic models describing size-based feeding and physiological constraints (Andersen, 2019, Blanchard et al., 2017) to simple scaling theory that summarises these processes via transfer efficiency and predator prey mass ratios (Brown and Gillooly, 2003, Jennings and Mackinson, 2003) both predict normalized abundance size spectrum slopes of approximately -2. However, many processes can affect both of these assumptions and could contribute to the variation around this theoretical value, even in the absence of fishing (Trebilco et al., 2016, Eddy et al., 2020). The empirical consistency of the size spectrum slope across many different

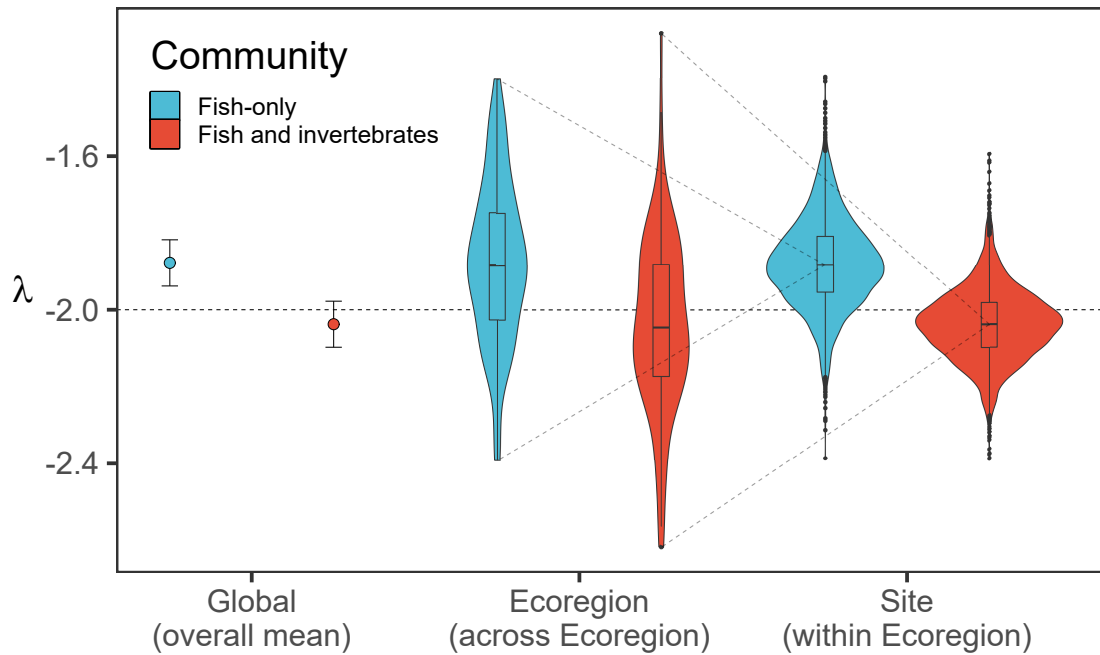


FIGURE 2.4: The contribution of spatial scale to abundance size spectra slope estimates. “Ecoregion” refers to the variation among ecoregions globally in the linear mixed effects model and “Site” refers to the variation among individual reef sites within ecoregions. Dotted lines between the violins are added to emphasize that the variation at the site level represents the added variation after accounting for the variation at the ecoregion level. A horizontal dotted line at -2 is added to highlight the slope in previous studies based on pelagic studies.

aquatic ecosystems (Sprules and Barth, 2016), and sensitivity to the effects of impacts such as fishing (Shin et al., 2005, Petchey and Belgrano, 2010), has led to its proposed use as an ecological indicator of ecosystem health for reefs (Nash and Graham, 2016). However, its uptake for reefs has been hampered by lack of knowledge of an appropriate baseline, due to apparent discrepancies between the simplifying assumptions of size spectrum theory and lack of consistency across reef fish size spectra. Previous studies on local reef fish communities have shown slopes shallower than -2 (e.g., -1.13 to 1.95, Robinson et al., 2017; -1.75, Ackerman et al., 2004; -1.58, Robinson et al., 2016), potentially due to energetic subsidies (Trebilco et al., 2013, 2016), relatively greater levels of herbivory (Steneck et al., 2017), or size-dependent habitat refugia (Rogers et al., 2014), but still within the range of slopes estimated here for fish-only communities. Although not all these studies specifically aimed to test theory related to energy flow, the exclusion of invertebrates in these studies would have likely changed the slopes found. On average globally, we found that the inclusion of invertebrates into the community size spectrum steepened λ from -1.88 to -2.04 ($\Delta\lambda = -0.16$), closer to the value of -2 that would be expected according to the “biomass equivalence rule”. All sites in this study are subject to varying levels of human disturbance (e.g., fishing), and therefore we might expect that in the absence of fishing pressure, reef communities would have shallower size spectra than this -2 estimate.

The effect of including invertebrates varied geographically, with a much greater effect at higher latitudes. At the highest latitudes considered here (approx. 60° N or S), fish-only size spectra had slopes that were more consistent with an inverted biomass pyramid (Trebilco et al., 2013), where biomass increases with body size and trophic level. The opposite was true for invertebrate-only size spectra, whereby the steepest slopes were observed at the highest latitude (Figure 2.3A). These two taxonomic groups, however, are not independent food web entities and interact through competition and predation. Combining these two groups into the size spectrum led to consistency in the slope across latitudes. The resultant pattern translates to an even distribution of log-log biomass across all body sizes and across latitudes, supporting previous conjectures of biomass equivalence holding from bacteria to whales and from the tropics to the poles (Sheldon et al., 1977, Kerr and Dickie, 2001). The latitudinal difference of including invertebrates is likely due to their dominance on temperate reefs, compared to more fish-dominated tropical reefs (Edgar et al., 2017). Whilst fishing pressure is non-random across the globe (Anticamara et al., 2011), it is unlikely to be the cause of the observed latitudinal patterns in the invertebrate inclusion effect, as we observe similar latitudinal patterns in sites within the most highly effective marine protected areas (Figure S6.1). Herbivores are also important on tropical reefs, and previous work has suggested that communities with a high biomass of herbivores, which do not feed according to size, should produce shallower size spectra (Robinson et al., 2017), as a result of being able to obtain relatively larger body sizes due to less energy lost through transfer efficiency (Brown and Gillooly, 2003). Larger-bodied herbivores also have the added advantage of reduced predation risk from gape-limited predators (e.g., Mumby, 2006), leading to a relatively greater number of large-bodied individuals and a shallower slope. In this study, across the globe, the slope was steeper than would be expected according to that reasoning. These steeper slopes could be due to a combination of functionally distinct trophic pathways affecting energy availability (Dinmore and Jennings, 2004, Maxwell and Jennings, 2006), greater human impacts affecting tropical reefs (Graham et al., 2005, Robinson et al., 2017) (see also Figure S6.1), or other factors affecting local variation in reef size spectra (Edgar, 1994, Rogers et al., 2014), and require further study.

A better understanding of the mechanisms underlying consistency and variability of slopes needs information on the spatial scales at which variability arises (Polishchuk and Blanchard, 2019). Investigation of different processes acting at local (e.g., sites) and larger spatial scales (e.g., ecoregions, global) should help to inform whether macroecological patterns are scale invariant (Rahbek, 2004, Connolly et al., 2017). A first step is to assess how much variation occurs at each scale. Here, we found that variation from the overall global size spectrum slope was explained about equally at both the ecoregion and site scales. Despite this scale-invariance of slope, the drivers of this variation still probably differ with scale, and our work opens the door for further studies into the factors shaping the size spectrum slope at different scales. At the ecoregion scale, drivers of variation likely include commercial fishing practices (e.g., Blanchard et al., 2005), large-scale habitat loss (e.g., Morais et al., 2020b), changing climate (e.g., Robinson et al., 2019a,b), and

environmental forcing (e.g., [Heenan et al., 2020](#)). Potential drivers at the site scale include population processes (e.g., [Barneche et al., 2014, 2016](#)), local community interactions, eutrophication (e.g., [Turner, 2001](#)), coastal pollution (e.g., [Azzurro et al., 2010](#)), and small-scale patchiness in fishing pressure related to human access (e.g., [Robinson et al., 2017, Campbell et al., 2020](#)).

Changes in size spectra slopes through time and space, have been used previously to assess changes in community and ecosystem health associated with the intensity of human activities ([Shin et al., 2005, Dulvy et al., 2004, Wilson et al., 2010, Graham et al., 2005](#)). Here, we used time-averaged size spectra on fished reefs, but future work on how size spectrum slopes vary with human activities (e.g., fishing and pollution) across time and space is needed. Reefs are also under pressure from the multifaceted effects of climate change ([Graham et al., 2007](#)). Integrative modelling, and empirical and mechanistic studies (e.g., [Barneche et al., 2014, Morais et al., 2020a](#)), are all needed to disentangle the combined and relative influences of multiple anthropogenic stressors when contrasted with natural ecological variation affecting size spectra. Advancing this research goal would assist development of predictive modelling tools for mapping changes on reefs, giving us a better idea of baseline reef size spectra and thus helping improve marine biodiversity policy and management ([Stuart-Smith et al., 2017](#)).

In order to use the size spectrum slope as an indicator of reef health across systems, we must first understand the theoretical baseline slope ([Jennings and Blanchard, 2004](#)), from which environmental, ecological and anthropogenic drivers of the remaining variation in slopes can be estimated. Our study highlights the importance of including invertebrates in reef size spectrum analyses for both the estimate of the baseline and for reducing variability in the slope estimates. When accounting for the invertebrates in the reef community, we show extremely high consistency in the size spectrum slope, supporting the generality of the biomass equivalence rule for reef communities at the global scale.

2.6 Acknowledgements

This research was supported by the Marine Biodiversity Hub, a collaborative partnership supported through funding from the Australian Government's National Environmental Science Program, and used the NCRIS-enabled Integrated Marine Observing System (IMOS) infrastructure for database support and storage. This research was also made possible by funding of the Australian Research Council (ARC), and the data from the Reef Life Survey Foundation. The authors also thank data support from Antonia Cooper, Just Berkhout, Diego Barneche, Scott Ling, Ella Clausius and Elizabeth Oh.

2.7 Supplementary material

S2.1 Estimating observed body size for invertebrates

Adequate body size measurements ($n > 10$ observations per species) were available for 248 invertebrate species over seven classes (Asteroidea, Cephalopoda, Crinoidea, Echinoidea,

Gastropoda, Holothuroidea, and Malacostraca). We found a lognormal distribution best described the body length distributions,

$$\log(L) \sim \mathcal{N}(L_\mu, L_\sigma) \quad (\text{S2.2})$$

consistent with previous literature on animal body length distributions (e.g., [Blackburn and Gaston, 1994](#)). For 167 of these 248 species, we were able to fit a lognormal distribution using the ‘fitdistcens’ function in the ‘fitdistrplus’ package ([Delignette-Muller and Dutang, 2015](#)) in R ([R Core Team, 2020](#)), designed for fitting univariate distributions to binned data. The remaining 81 species ranged an insufficient number of body length bins to fit a lognormal distribution and were therefore excluded from the body length estimation analyses.

Using asymptotic lengths (L_∞) obtained from SealifeBase ([Palomares and Pauly, 2019](#)) as a predictor variable, we fitted two linear models, each predicting one of the two parameters of the fitted species lognormal distribution (L_μ, L_σ). The first model estimated the mean of the lognormal distribution of species, L_μ , given the species asymptotic length, L_∞ , and the class to which the species belongs, C (Equation S2.3, Figure S2.5).

$$\log(L_\mu) = \beta_0 + \beta_1 \log(L_\infty) + C + \epsilon \quad (\text{S2.3})$$

where the fitted parameters were,

$$\beta_0 = 0.54$$

$$\beta_1 = 0.40$$

$$C = \begin{bmatrix} \textit{Asteroidea} & = & 0.00 \\ \textit{Cephalopoda} & = & 0.92 \\ \textit{Crinoidea} & = & -0.07 \\ \textit{Echinoidea} & = & 0.17 \\ \textit{Gastropoda} & = & 0.29 \\ \textit{Holothuroidea} & = & 0.65 \\ \textit{Malacostraca} & = & 0.27 \end{bmatrix}$$

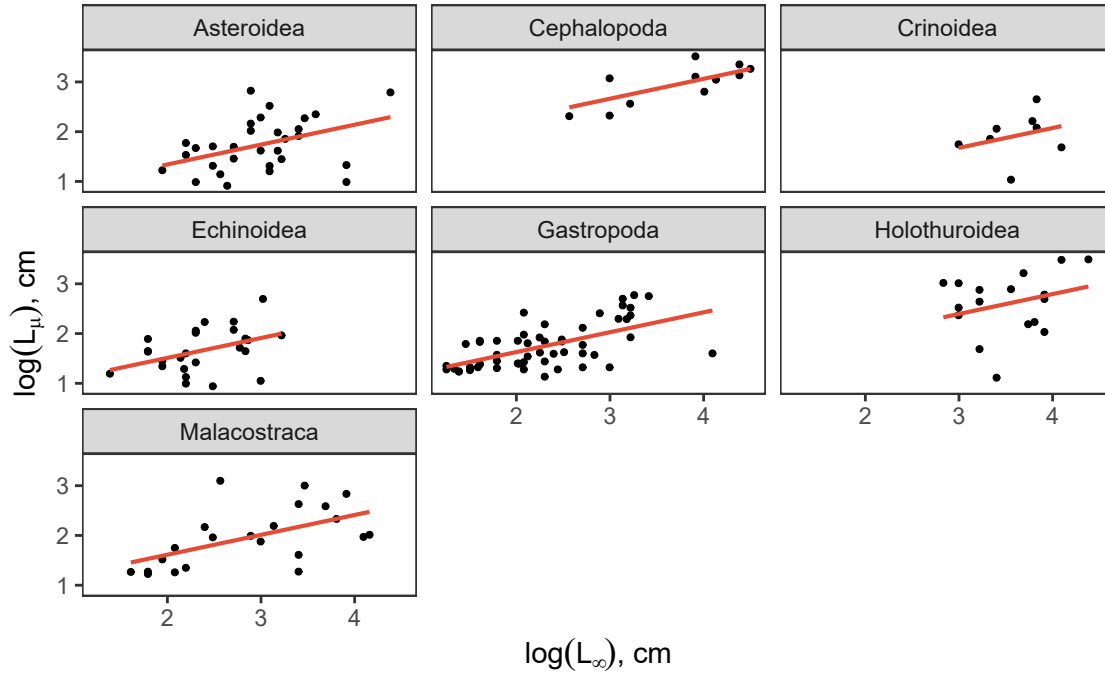


FIGURE S2.5: The relationship between asymptotic size, L_∞ , and the mean of the lognormal distribution, L_μ , for 167 invertebrate species across seven classes, with a fitted linear model ($R^2 = 51\%$, Equation S2.3).

The second model estimated the standard deviation of the lognormal distribution of species, L_σ , given the species' asymptotic length, L_∞ (Equation S2.4, Figure S2.6). The inclusion of class as a fixed effect in this model did not improve the fitting (determined by the Akaike information criterion, AIC (Akaike, 1974)) and was therefore not included.

$$\log(L_\sigma) = \beta_0 + \beta_1 \log(L_\infty) + \epsilon \quad (\text{S2.4})$$

where the fitted parameters were,

$$\beta_0 = 0.06$$

$$\beta_1 = 0.11$$

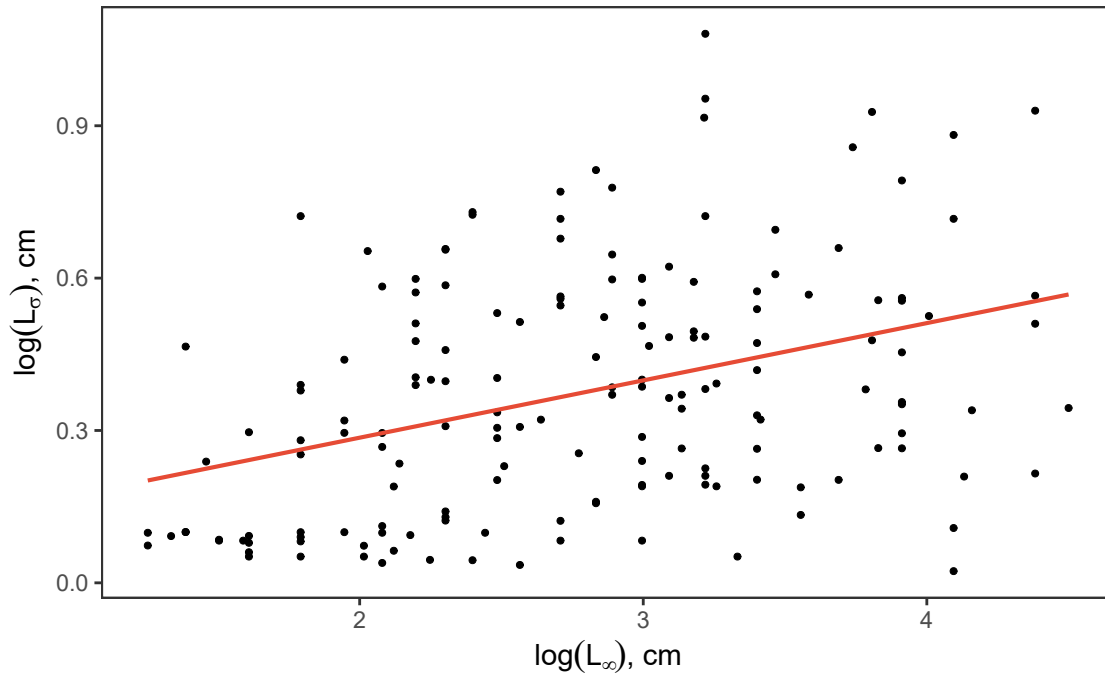


FIGURE S2.6: The relationship between asymptotic size, L_∞ , and the standard deviation of the lognormal distribution, L_σ , for 167 invertebrate species across seven classes, with a fitted linear model ($R^2 = 14\%$, Equation S2.4).

For the remaining invertebrate species, for which we had information on their asymptotic body length and class, but insufficient observed body length data, we used equations S2.3 and S2.4 to estimate the lognormal distribution. For each species we therefore have an estimate of the two lognormal parameters and thus could reconstruct the body length distribution. To validate the method, we compared the body length distributions fitted to the observed data, with the predicted body length distributions (if we only had asymptotic length and taxonomic class available) (Figure S2.7).

To estimate the body sizes of a given invertebrate species at a single survey, we integrated the predicted lognormal distribution into the length bins of the original survey method, to obtain the probability of occurrence within each bin. We then multiplied the bin probability by the abundance of the species to get an estimate of the abundance, and rounded to the nearest whole number. This way both the fishes and invertebrates were in the same format for further analyses; abundance per observational length bin.

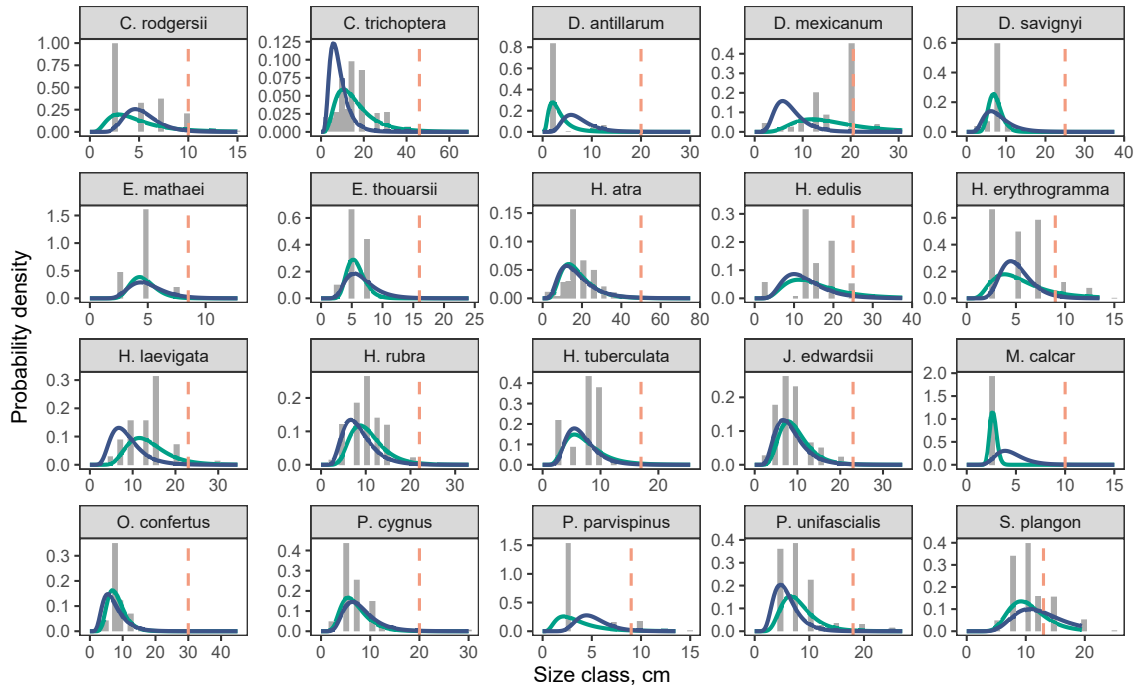


FIGURE S2.7: Estimating invertebrate body size distributions. The observed body length distributions (grey bars) of the 20 invertebrate species with the greatest number of body length estimates. The green line indicates the lognormal distribution fitted to the observed body length data, whilst the blue line represents the estimated lognormal distribution based solely on the asymptotic body length (L_{∞} , orange dashed line) of the species and its taxonomic class.

S2.2 Estimation of invertebrate body mass from body length

For fishes, species length-weight relationships were available from previous analyses (Edgar and Stuart-Smith, 2009). For invertebrates, body mass was estimated from body length using published length-weight relationships (Palomares and Pauly, 2019) in the form $M = a \cdot L^b$, where, M is body mass and L is body size (maximal length measure), and a and b are either empirically derived or modelled constants. Estimates for a and b were available for 76 invertebrate species belonging to six taxonomic classes (Asteroidea, Cephalopoda, Echinoidea, Gastropoda, Holothuridea, and Malacostraca).

To estimate the parameters a and b for the remaining invertebrate species, we fitted two linear regression models. The first linear regression model included taxonomic class (C) as a fixed factor. This model was used to estimate the class-level length-weight relationship for species belonging to one of the six taxonomic classes for which the data were fitted (Equation S2.5, red line in Figure S2.8).

$$\log(M) = \beta_0 + \beta_1 \log(L) + C + \epsilon \quad (\text{S2.5})$$

where,

$$\begin{aligned} a &= \exp(\beta_0 + C) \\ b &= \beta_1 \end{aligned} \quad (\text{S2.6})$$

and the fitted parameters were,

$$\begin{aligned} \beta_0 &= -2.49 \\ \beta_1 &= 2.75 \\ C &= \begin{bmatrix} \textit{Asteroidea} & = & 0.00 \\ \textit{Cephalopoda} & = & 2.15 \\ \textit{Echinoidea} & = & 2.04 \\ \textit{Gastropoda} & = & 1.17 \\ \textit{Holothuroidea} & = & -0.26 \\ \textit{Malacostraca} & = & 1.72 \end{bmatrix} \end{aligned}$$

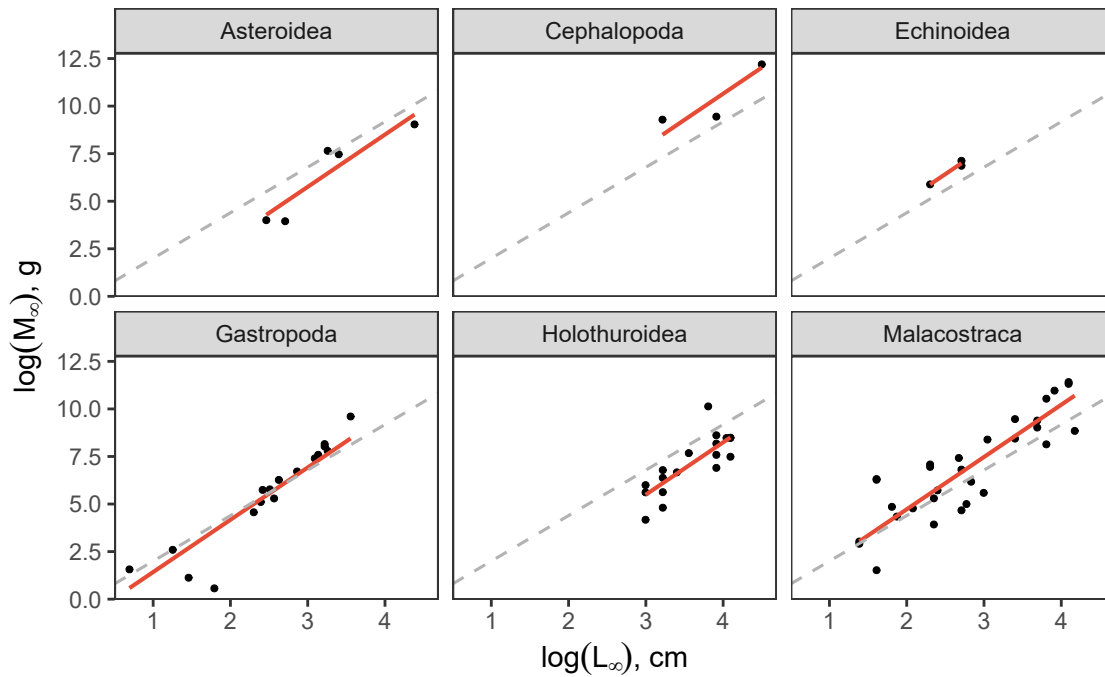


FIGURE S2.8: The relationship between body length and body mass for 85 invertebrate species. Two linear models are shown, the first with taxonomic class included as a predictor variable (solid red line, Equation S2.5) and the second without (dashed grey line, Equation S2.7).

For invertebrate species that did not belong to one of these six classes (Crinoidea species), the length-weight relationship was estimated from a second general linear model, without class as a fixed factor (Equation S2.7, dashed grey line in Figure S2.8).

$$\log(M) = \beta_0 + \beta_1 \log(L) + \epsilon \quad (\text{S2.7})$$

where,

$$\begin{aligned} a &= \exp(\beta_0) \\ b &= \beta_1 \end{aligned} \quad (\text{S2.8})$$

and the fitted parameters were,

$$\begin{aligned} \beta_0 &= -0.39 \\ \beta_1 &= 2.39 \end{aligned}$$

S2.3 Justification of a cut-off value

A cut-off is necessary when using linear regression methods due to the downward turning of the size spectrum at the smallest size classes (Figure S2.9).

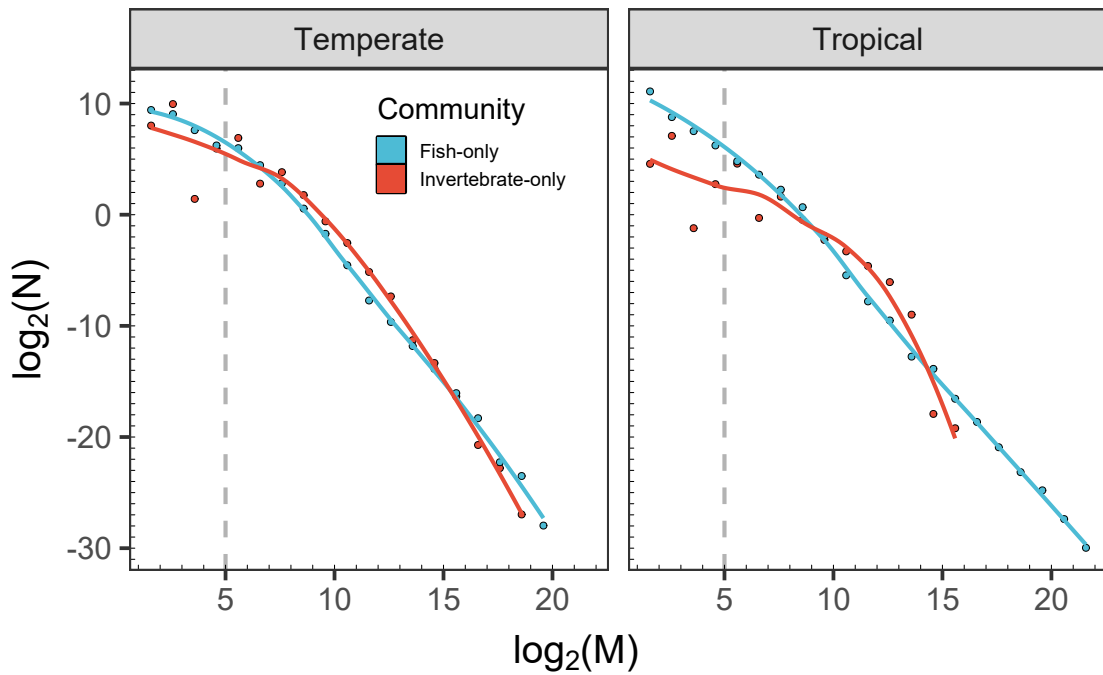


FIGURE S2.9: Entire size spectra for invertebrate-only and fish-only reef communities. Dotted grey vertical line at 2^5 (= 32 g) indicates the lower-bound size bin used as the cut-off. A smooth line is fitted using locally estimated scatterplot smoothing (LOESS).

S2.4 Normalization of the size spectrum

Abundance (m^{-2}) was calculated as the number of individuals per square meter of seabed. Where multiple surveys were conducted at a single site, the mean abundance was calculated per logarithmic mass bin to create a time-averaged size spectrum at the site-level. To account for bin widths within each logarithmic mass bin, we divided the abundance by the width of the bin, a common normalization procedure (Platt and Denman, 1977).

We then fit a global linear mixed effects model to the normalized \log_2 abundance, $\log_2(N)$, against the \log_2 mass bin mid, $\log_2(M)$, with site (s) nested within Ecoregion (e) as random factors with their own random slope and intercept (Equation S2.9). The model was fitted using the lmer function in the lme4 package (Bates et al., 2015) in R (R Core Team, 2020)(see Figure S2.10).

$$\log_2(N) = \beta_0 + u_{0,e} + u_{0,s|e} + (\beta_1 + u_{1,e} + u_{1,s|e}) \cdot \log_2(M) + \epsilon \quad (\text{S2.9})$$

β_0 is the overall intercept, β_1 is the overall slope, $u_{0,e}$ and $u_{1,e}$ represent the normally distributed ecoregion random intercept and slope, respectively. $u_{0,s|e}$ and $u_{1,s|e}$ represent the normally distributed random intercept and slope, respectively, of the site given the ecoregion random effect. The model was fitted to the fish-only dataset, and the combined (fish and invertebrate) dataset, separately.

S2.5 Invertebrate inclusion effect across latitudinal zones

We observe a greater invertebrate inclusion effect in temperate sites than tropical sites (Figure S2.11).

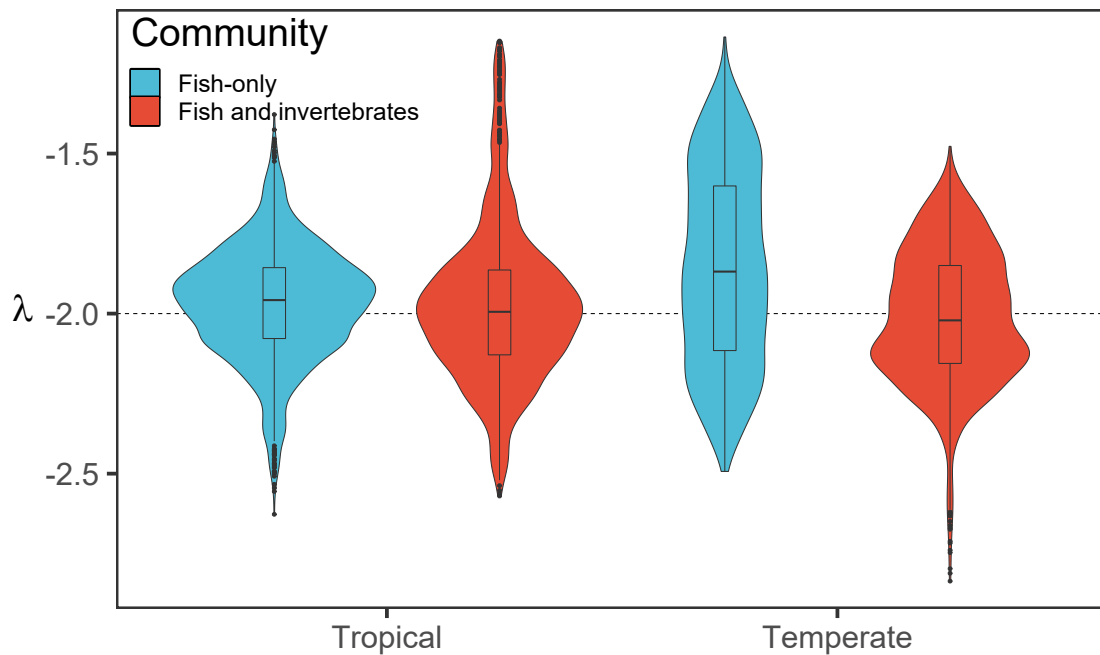


FIGURE S2.11: Reef size spectra slope estimates by latitudinal zone. Distribution of estimates of the site-level normalized abundance size spectrum slope (λ) for temperate and tropical sites. A dotted line at -2 is added to highlight the theoretical expected value.

S2.6 Are temperate-tropical differences in size spectra a product of large scale differences in fishing pressure?

Fishing pressure is non-random across the globe (Anticamara et al., 2011). To test if the pattern of a greater invertebrate effect in temperate than tropical sites was driven by broad differences in regions in the removal of large fishes or invertebrates through exploitation, we used a subset of data from surveys in the most effective Marine Protected Areas (MPAs) globally. We used 192 sites surveyed in MPAs that met four or five of the NEOLI features identified by Edgar et al. (2014), and compared their distributions of 'invertebrate effect' (Figure S2.12). Figure S2.12 shows that even in the least impacted sites by fishers, the invertebrate effect remains clearly of greater magnitude in temperate sites than in tropical sites.

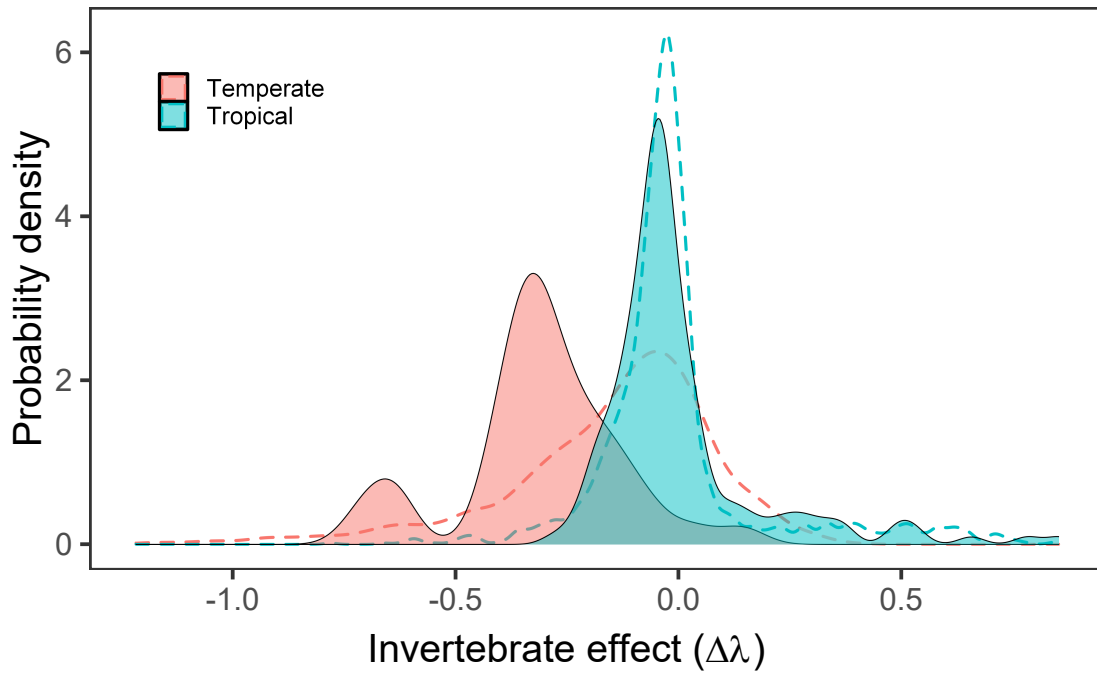


FIGURE S2.12: Comparing the effect of including invertebrates ($\Delta\lambda$) on 40 temperate sites and 152 tropical sites that met four or five of the NEOLI features that define a successful marine protected area. A more negative invertebrate effect refers to a greater steepening of the size spectrum when invertebrates are included. For comparative purposes, dotted lines represent the distributions for all sites (inside and outside MPAs).

S2.7 Global patterns of fish-only and combined community size spectra slopes

We can see in Figure S2.13A that there is a latitudinal pattern in the slope of the fish-only size spectrum, with shallower slopes at higher latitudes. When we include invertebrates (Figure S2.13B) we remove this latitudinal pattern, resulting in a greater consistency in size spectrum slopes.

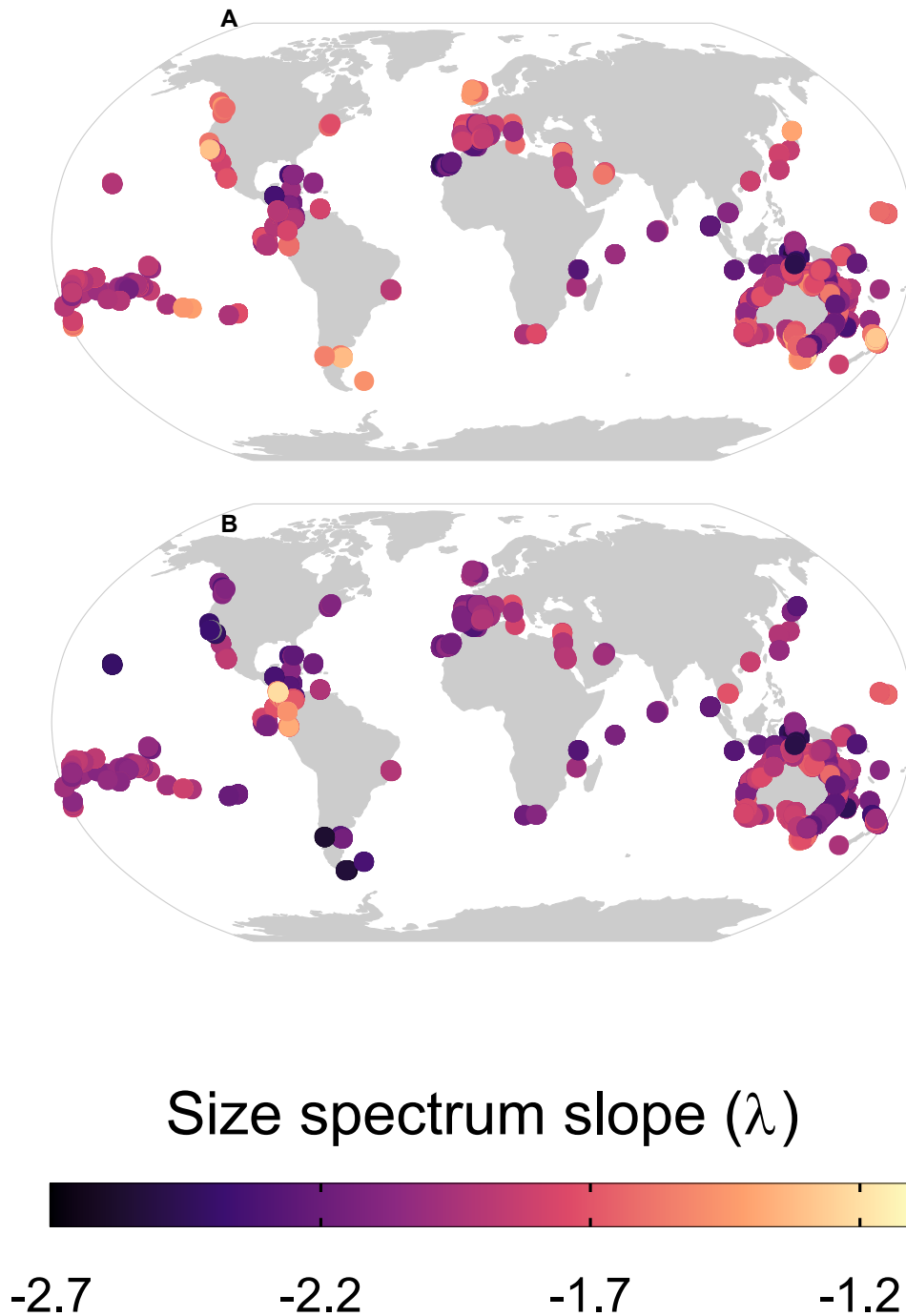


FIGURE S2.13: Size spectrum slopes of the A) fish-only reef community and B) fish and invertebrate community, across the globe. We observe greater consistency in size spectrum slopes when including invertebrates.

S2.8 Sensitivity analysis

To test the robustness of invertebrate body size estimation, we re-ran all analyses but using the 2.5th and 97.5th percentiles of the coefficients of the models to estimate invertebrate

body length (Equations S2.3, S2.4) and the models to estimate body mass (Equations S2.5, S2.7), to test the impact on the final result (Table S2.1). The overall result of the steepening invertebrate effect ($\Delta\lambda$) appears to be very insensitive to extreme coefficients (2.5th and 97.5th percentiles) of body length estimation. Only when using extreme coefficients of mass estimation do we observe a change in the outcome. When using the 2.5th percentile, in mass calculation, we observe a more pronounced steepening invertebrate effect. On the other hand, when using the upper extreme coefficient (97.5th percentile) of mass estimation we observed both minor steepening and shallowing. However, when using the fitted coefficients of body length estimation, and varying only the coefficients of mass estimation over a range of confidence intervals, we observed a steepening invertebrate effect across all the confidence intervals tested (Figure S2.14). Only at the extreme upper end of these estimates does the combined slope approaches that of the fish-only slope. This is due to the over-estimation of invertebrate body mass for a given body length, resulting in a shallower slope. We therefore have high confidence in the overall outcome of steepening ‘invertebrate effect’ using the methods in this paper. Despite this, we still recommend the collection of more invertebrate body length data and length-weight data to further improve these methods and fit to finer scale taxonomic resolution.

TABLE S2.1: Sensitivity analysis of the body length and body mass estimation methods on the ‘invertebrate effect’ on the size spectrum slope ($\Delta\lambda$). Using the 95% confidence intervals in equations S2.3 and S2.4 for body length estimation, and equations S2.5 and S2.7 for body mass estimation, as well as the combinations between these values.

Length confint	Mass confint	λ_{fish}	$\lambda_{combined}$	$\Delta\lambda$
fit (50%)	fit (50%)	-1.88	-2.04	-0.16
fit (50%)	lower (2.5%)	-1.88	-2.09	-0.21
fit (50%)	upper (97.5%)	-1.88	-1.88	0.00
lower (2.5%)	fit (50%)	-1.88	-2.06	-0.18
lower (2.5%)	lower (2.5%)	-1.88	-2.08	-0.20
lower (2.5%)	upper (97.5%)	-1.88	-1.91	-0.03
upper (97.5%)	fit (50%)	-1.88	-1.99	-0.11
upper (97.5%)	lower (2.5%)	-1.88	-2.06	-0.19
upper (97.5%)	upper (97.5%)	-1.88	-1.83	0.05

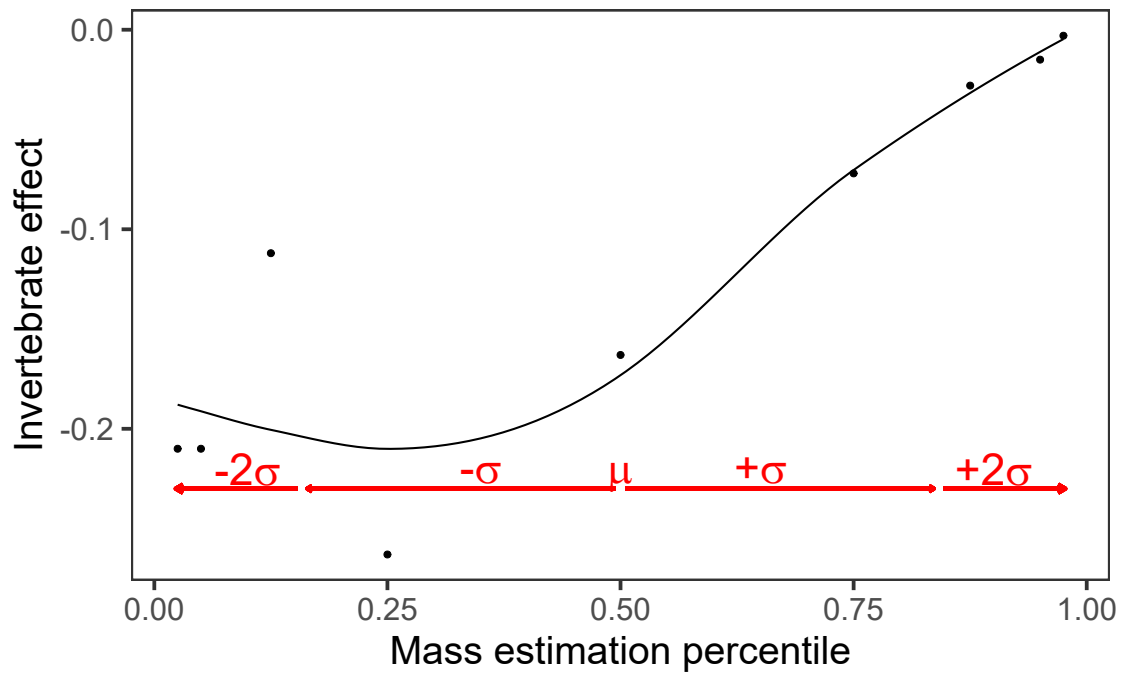


FIGURE S2.14: Sensitivity analysis of the mass estimation method, showing the robustness of the mass estimation method to even extreme coefficient values. μ represents the fitted value of the mass estimation coefficient, σ represents the standard deviation around this estimate. Within one standard deviation either side of the estimated coefficients (μ), we still observe a significant steepening invertebrate effect.

Chapter 3

Reef communities show predictable undulations in linear abundance size spectra from copepods to sharks

Freddie J. Heather¹, Rick D. Stuart-Smith¹, Julia L. Blanchard¹, Kate M. Fraser¹, Graham J. Edgar¹

1 – Institute for Marine and Antarctic Studies, University of Tasmania, 20 Castray Esplanade, Battery Point, Hobart, TAS 7004, Australia

Code availability: Code for the analysis, and to recreate all figures, is available at https://github.com/FreddieJH/sinusoidal_size_spec.

3.1 Abstract

Amongst the more widely accepted general hypotheses in ecology is that community relationships between abundance and body size follow a log-linear size spectrum, from the smallest consumers to the largest predators (i.e., “bacteria to whales”). Nevertheless, most studies only investigate small subsets of this spectrum, and note that extreme size classes in survey data deviate from linear expectations. In this study, we fit size spectra to field data from 45 rocky and coral reef sites along a 28° latitudinal gradient, comprising individuals from 0.125 mm to 2 m in body size. We found that 96% of the variation in abundance along this ‘extended’ size gradient was described by a single linear function across all sites. However, consistent ‘wobbles’ were also observed, with subtle peaks and troughs in abundance along the spectrum, which varied with sea temperature, as predicted by theory relating to trophic cascades.

3.2 Introduction

The body size of an organism is often regarded as the single most important factor determining how it interacts with its environment (Brown et al., 2004, Peters, 1983, Gillooly et al., 2002, Schmidt-Nielsen, 1984). At the community level, the relationship between an individual's body size and abundance can provide important insights into how energy, and hence biomass, moves through the food chain (Brown and Gillooly, 2003, Trebilco et al., 2013). Similar biomass across logarithmic body size classes is often observed in marine communities (Sprules and Barth, 2016), which equates to decreasing abundance with increasing body size, termed the abundance size spectrum (Trebilco et al., 2013).

In marine communities, the faunal abundance size spectrum is often described by a linear function on the log-log scale. The intercept and slope of this function can provide information about nutrient availability (e.g., Sprules and Munawar, 1986, Boudreau and Dickie, 1992), human disturbance (Dulvy et al., 2004, Shin et al., 2005, Wilson et al., 2010, Graham et al., 2005) and feeding strategies of the individuals (Robinson et al., 2016) in the community. In pelagic systems, a consistent size spectrum is commonly observed, often attributed to strict size-based predation (Jennings et al., 2001) and trophic level inefficiencies (Lindeman, 1942), in combination with the relationship between body size and metabolic rate (Kleiber, 1932).

Deviations from size spectrum linearity, for example peaks of abundance at specific body sizes, have been described in lake systems (e.g., Sprules et al., 1983), intertidal (Schwinghamer, 1981) and subtidal (Edgar, 1994) benthic communities. Schwinghamer (1981) attributed these peaks in abundance to the physical environment, whereby sediment grain size created size-based habitat niches. Rogers et al. (2014) showed a similar pattern on coral reefs, whereby deviations from linearity reflected habitat complexity via habitat refugia for prey. These abundance peaks have also been attributed to trophic interactions, with early studies proposing that peaks in abundance correspond to outcomes of interacting functional groups (Dickie et al., 1987). More recent work has shown mechanistically that peaks in abundance can arise from bottom-up (e.g., food limitation) and top-down (e.g., predation mortality) trophic cascades (Benoît and Rochet, 2004, Andersen and Pedersen, 2010, Rossberg et al., 2019). Whilst a combination of these influences is likely, no clear consensus exists on the drivers of these nonlinear patterns in faunal size spectra.

Reef studies tend to focus on fishes, where observed size spectra are often unimodal, with a peak in abundance at a small to intermediate body size (e.g., Ackerman et al., 2004). Due to theoretical expectations of decreasing abundance with body size, and the potential for under-sampling smaller individuals, many reef size spectra studies have routinely excluded individuals less than the modal size, or equivalent size, from the linear modelling analyses (Wilson et al., 2010, Trebilco et al., 2015, Robinson et al., 2017, Heather et al., 2021a) (See Figure 3.1A). Ignoring the small fishes and fitting a linear model to the size spectrum has the benefit of simplicity and has also been shown to be useful in detecting fishing pressure on reefs (Robinson et al., 2017). These studies have typically used visual survey methods to collect data, which are known to under-represent densities

of some species (Bozec et al., 2011), particularly for small (Ackerman and Bellwood, 2000), cryptic (Stewart and Beukers, 2000, Willis, 2001), and nocturnal fishes (Azzurro et al., 2007). For example, Ackerman and Bellwood (2000) found their visual survey methods underestimated the abundance of reef fishes < 5 cm by 75%.

In this study we use individual body size data spanning 0.125 mm to 2 m across 28° of latitude to systematically test the a) generality of a linear size spectrum on reefs, and b) the presence and cause of the dip in abundance at the small to medium size classes. We applied two distinct methods to collect field data on abundance and size of consumer taxa on 45 reefs from 14.7°S to 43.3°S along the eastern coastline of Australia, including macroalgal covered temperate rocky reefs and coral reefs in the tropics. One method involved sampling of animals associated with benthic habitat (“epifauna”: 0.125 mm to 22 mm body size), while the other involved visual census of larger mobile invertebrates and fishes along underwater transect lines (“visual survey data”: 0.01 m to 2 m body size). Together these approaches provided density estimates for all mobile species that could readily be surveyed by divers at a given patch of reef.

The inclusion of invertebrates in smaller and overlapping size classes to the fishes allows for testing of three hypotheses about causes of the abundance dip in the size spectrum observed in reef fishes (Figure 3.1A): 1) It arises from disproportionate under-sampling of small fishes in visual census surveys, as has been assumed in previous studies the rationale for removal of this part of the spectrum. This would be seen through a ‘gap’ in the size spectrum (Figure 3.1B); 2) It is part of a consistent curve in the overall size spectrum of reef consumers, which would be seen in a continuous, but curved size spectrum (Figure 3.1C); 3) It is an artefact of only considering fishes in isolation, and that part of the spectrum is filled by invertebrates that are usually neglected (Heather et al., 2021a). This would be seen by a strongly linear overall spectrum (Figure 3.1D). These competing hypotheses each assume the overarching principles of size-based feeding (Jennings et al., 2001) and transfer inefficiency (Lindeman, 1942) are operating in reef systems, which have been well supported by previous studies (see Sprules and Barth, 2016).

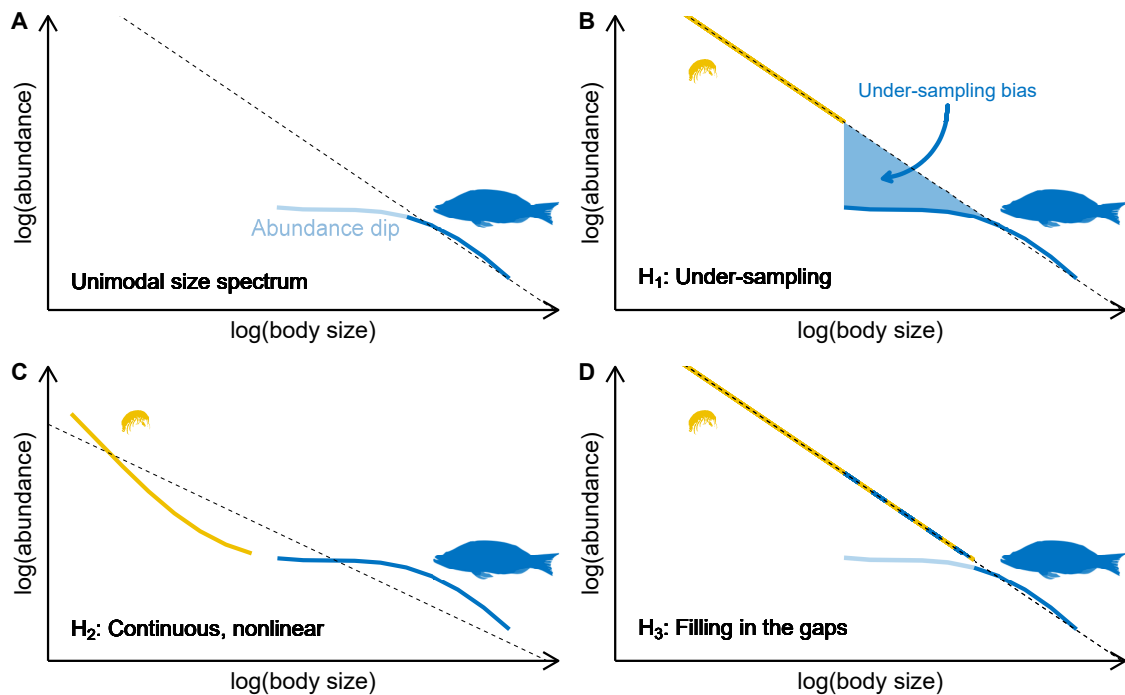


FIGURE 3.1: Conceptual diagram showing the dip in abundance of small fishes typically observed in studies of reef fish size structure (A), and three alternative hypothetical spectra (B-D) that account for the pattern observed in (A). Where the size spectrum is unimodal (A), a linear function is generally fitted to the descending limb (darker blue), with smaller size classes assumed to be under-sampled (lighter blue) and excluded. A linear overall size spectrum with a substantial gap (B) would indicate under-sampling is likely to be the cause, while a continuous curve with a smooth transition through the size classes where the fishes and invertebrates overlap (C) would suggest ecological interactions drive a real non-linearity. A continuous strongly linear spectrum (D) would indicate that epifaunal invertebrates fill the gaps left by fishes.

3.3 Methods

3.3.1 Survey data

Data collection was performed using two distinct methods: 1) Collection of benthic habitat samples with associated invertebrate epifauna and, 2) underwater visual surveys of fishes and large mobile macro-invertebrates. Together, these datasets allowed construction of size spectra from small meiofaunal invertebrates (predominantly harpacticoid copepods, [Fraser et al. \(2021\)](#)) to the largest fishes including sharks ([Edgar et al., 2014](#)).

Epifauna were sampled from 45 sites spanning the eastern coast of Australia, from tropical (Lizard Island; 14.7°S) to temperate (Southern Tasmania; 43.3°S) reefs, between the years of 2015 and 2018. Sample collection involved firstly characterising the habitat at the site by taking 20 evenly spaced photographs of benthos and substrata along each of two 50 m survey transects. Photographs were taken from approximately 50 cm above the substrata to depict approximately 30 cm x 30 cm of seabed. These photographs were assessed to derive an estimate of the relative abundance of different habitat types at each

site (Cresswell et al., 2017). Habitat selected for sampling was then covered with a 25 cm x 25 cm grid-marked quadrat and photographed in situ to quantify its planar area. Habitat and epifaunal samples were bagged in situ after detachment by removing soft habitat (e.g., macroalgae, sponges) with a knife and hard coral habitat with a chisel (Fraser et al., 2021). Habitat that could not easily be removed (e.g., turfing algae, encrusting coral) was vacuum sampled using a venturi air-lift. Each habitat sample was flushed with freshwater to remove mobile epifauna, which were then passed through a set of logarithmic (log base = $\sqrt{2}$) mesh size sorting sieves. Animals retained on each sieve were counted and identified to the highest possible taxonomic resolution. For more detailed methodology see Fraser et al. (2021). Abundance of epifauna by size and taxa were standardised to 1 m² planar area by multiplying the number of individuals per unit area of sampled habitat type with transect area photographed comprising this habitat type.

Fish and large mobile invertebrate species (> 2.5 cm maximum recorded length) were surveyed using the standardized Reef Life Survey visual census methods (Edgar and Stuart-Smith, 2014, Edgar et al., 2020, see also <https://reeflifesurvey.com/>), in which SCUBA divers swim along a 50 m transect line and record all fishes and invertebrates observed within 5 m and 1 m wide belts, respectively. Divers estimate body size of animals observed to the closest of 13 size categories (2.5, 5, 7.5, 10, 12.5, 15, 20, 25, 30, 35, 40, 50, and 62.5 cm) or to the nearest 12.5 cm for body sizes greater than 62.5 cm. Potential biases in visual data collected using this methodology are discussed by Edgar et al. (2020). For large mobile invertebrates, of which body size was not always estimated at the time of observation, body size was estimated using the lognormal probability distribution of body size based on the asymptotic size of the species (see Heather et al., 2021a). Densities of fishes and invertebrates were standardised to abundance per m² by dividing the individual number counts by the respective area surveyed.

3.3.2 Combining the datasets

The body size of individuals from the two datasets overlapped at some sites. To combine these data, we binned both datasets into log bins with a base of $\sqrt{2}$ and summed the abundance of the bin to obtain a total abundance within the size bin. A log base of $\sqrt{2}$ was chosen as this represented the logarithmic sieve mesh sizes of the epifaunal sampling. Normalised density was calculated as the density (abundance per m²) divided by the width of the body size bin (Platt and Denman, 1977).

3.3.3 Fitting nonlinear size spectra

Due to clear sinusoidal patterns in the residuals of linear functions between log body size and log abundance, we fitted a nonlinear size spectrum model proposed by Rossberg et al. (2019) (Equation S3.1). This model included both a linear function with an additional sinusoidal function to allow for the quantification of both the linear and secondary structure aspects of the size spectrum.

$$\log(N) = \beta_0 + \lambda \cdot \log(L) + A \cdot \sin\left(\frac{2 \cdot \pi \cdot \log(L)}{D} - P\right) \quad (\text{S3.1})$$

Where, N is the normalised density (m^{-2}), L is the middle of the size bin (mm), β_0 is the size spectrum intercept, λ is the slope, and A , D and P represent the amplitude, wavelength, and phase of the sine wave, respectively. The size spectrum model (Equation S3.1) was fitted using the ‘nlrq’ function (Koenker, 2010) in R (R Core Team, 2020). The amplitude (A) represents the ‘strength’ of the sine wave, and therefore the deviation from linearity in the size spectrum. Rogers et al. (2014) used the pareto distribution to detect deviations from linearity, due to the body size data being resolved to the individual level rather than in logarithmic size bins. Individual level body size data would allow for the detection of finer-scale deviations from linearity, however, this was not feasible in this study due to the inherent binning nature of data collection (both sieving and visual survey methods). The ratio of abundance from the top of one peak to the bottom of a trough was calculated as the log base to the power of two times the amplitude ($\sqrt{2}^{2A}$). The body size ratio of individuals occupying neighbouring peaks was calculated as the log base to the power of the wavelength ($\sqrt{2}^D$), and the distance between consecutive peaks and troughs was therefore estimated as the log base to the power of half the wavelength ($\sqrt{2}^{\frac{D}{2}}$). If the peaks and troughs in the size spectrum are driven by trophic cascades, then the distance between consecutive peaks and troughs ($\sqrt{2}^{\frac{D}{2}}$) relates to the ratio between the body size of predators and prey.

Due to the difficulty of interpreting the phase parameter (P) of the nonlinear size spectrum when the wavelength (D) is not fixed (Rossberg et al., 2019), we identified the body size in which local peaks and troughs occurred in the size spectrum model using the ‘optimize’ function in R (R Core Team, 2020).

3.3.4 Hypothesis testing

To test the three competing hypotheses (Figure 3.1) we fit three models at each site to the combined dataset (epifaunal and visual survey data); 1) a linear model, 2) a nonlinear model (Equation S3.1), and 3) a linear model excluding size classes within the ‘abundance dip’ (Figure 3.1A). If the inclusion of the epifaunal data fills the size classes with reduced relative abundance (i.e., the abundance dip) (Hypothesis 3, Figure 3.1D), then we would expect the resultant size spectrum to be best described by a simple linear model at the site (Equation SS3.2). If the removal of the data points corresponding to the size bins within the abundance dip (defined as visual survey data size classes smaller than the modal body size class), results in an overall better linear model (Equation S3.2) fit than when all size bins are included, this supports our first hypothesis (Figure 3.1B), that these size classes are potentially under-sampled. If the nonlinear model provides a better fit than the other two linear models, this supports the second hypothesis; that the inclusion of epifauna results in a size spectrum with the region referred to as the abundance dip being an inherent part of an overall nonlinear size spectrum (Hypothesis 2, Figure 3.1C). The

goodness-of-fit of the three models was determined by the Akaike information criterion (AIC) value (Akaike, 1974)(See Supplementary material S3.5).

3.3.5 Environmental covariates

We fitted a series of maximal linear models (Supplementary material S3.4) to identify the most important covariates in estimating the parameters of the size spectrum model (Equation S3.1). These site covariates included mean sea surface temperature ($^{\circ}\text{C}$), mean chlorophyll level (mg m^{-3}), phosphate and nitrate levels (mmol l^{-1}), all extracted from Bio-ORACLE, (Tyberghein et al., 2012), and categorical indices of wave exposure, habitat relief, currents, and reef floor slope, scored on a 1 to 4 scale by divers at the survey sites. Details on these environmental variables can be found in Supplementary S3.2. Using a best subset regression approach (Hebbali, 2020) we selected the environmental variables that minimised the AIC value (Table S3.2).

3.4 Results

When combining the epifaunal and visual survey datasets, 96% of the variation in logarithmic normalised abundance (N) was explained by a linear function of logarithmic body size (L)(linear regression: $\log(N) \sim \log(L)$; all sites combined, Equation S3.3). More variation was explained when combining these datasets (Adjusted $R^2 = 95.8\%$), than when a linear model was fitted to the datasets separately (Epifaunal data, Adjusted $R^2 = 90.1\%$; Visual survey data, Adjusted $R^2 = 84.3\%$). At the majority of sites we observed no individuals in the range of 5 mm to 22 mm (size bins $\sqrt{2}^5$ to $\sqrt{2}^8$ in Figure S3.5).

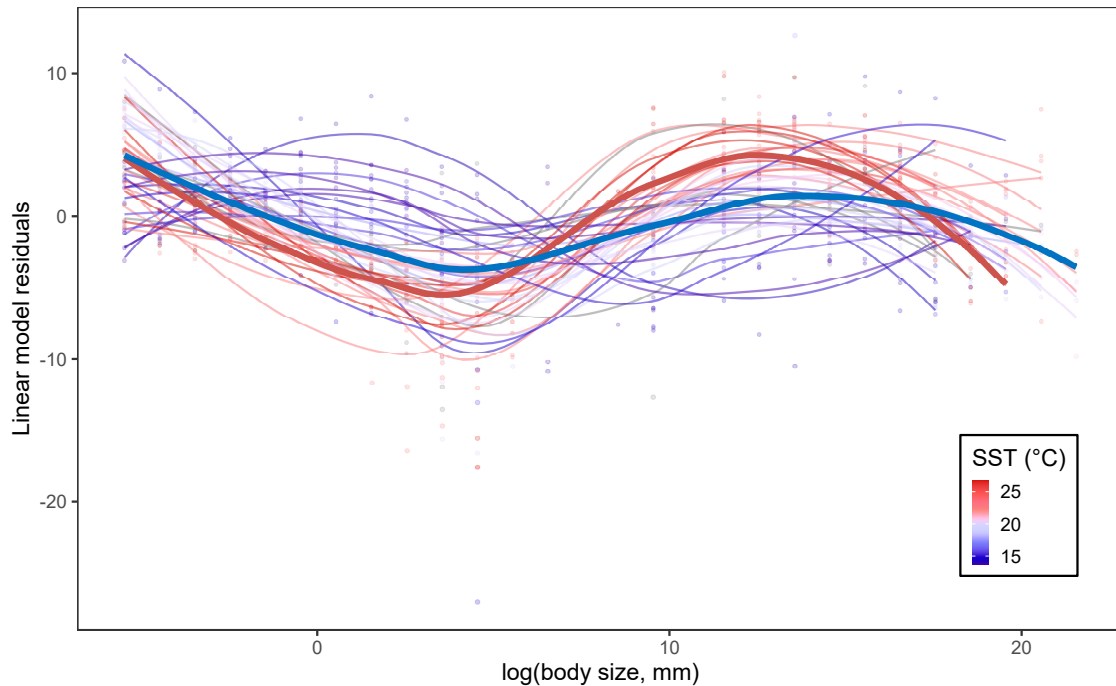


FIGURE 3.2: Sinusoidal patterns in the residuals of the linear model of the size spectrum. Each line represents a LOESS fit for a given site. Each thin line represents a site, with the colour of line representing the mean annual sea surface temperature (SST) at the site. The two thick lines represent the combined LOESS fit for tropical (red) and temperate sites (blue).

Clear sinusoidal patterns were present in the residuals of the linear model fits (Equation S3.2) (Figure 3.2). At 41 of the 45 sites (Figure 3.4), the nonlinear size spectrum model (Figure 3.3, Equation S3.1, Figure S3.6) provided a better fit (lower AIC) than either a linear model (Equation S3.2) incorporating all data (epifaunal and visual survey) and a linear model (Equation S3.2) with all data but excluding the size bins making up the visual survey 'abundance dip'. At three of the 45 sites (Figure 3.4, Table S3.3), the best fitting model was the linear model excluding size classes within the abundance dip (Figure 3.4, Table S3.3); suggesting potential under-sampling of these size classes at these three sites. The size spectrum of one site (EMR47, Figure S3.5, Figure 3.4, Table S3.3) was best described by a linear function. There was no apparent abundance dip at this site, which therefore did not support any of the three hypotheses.

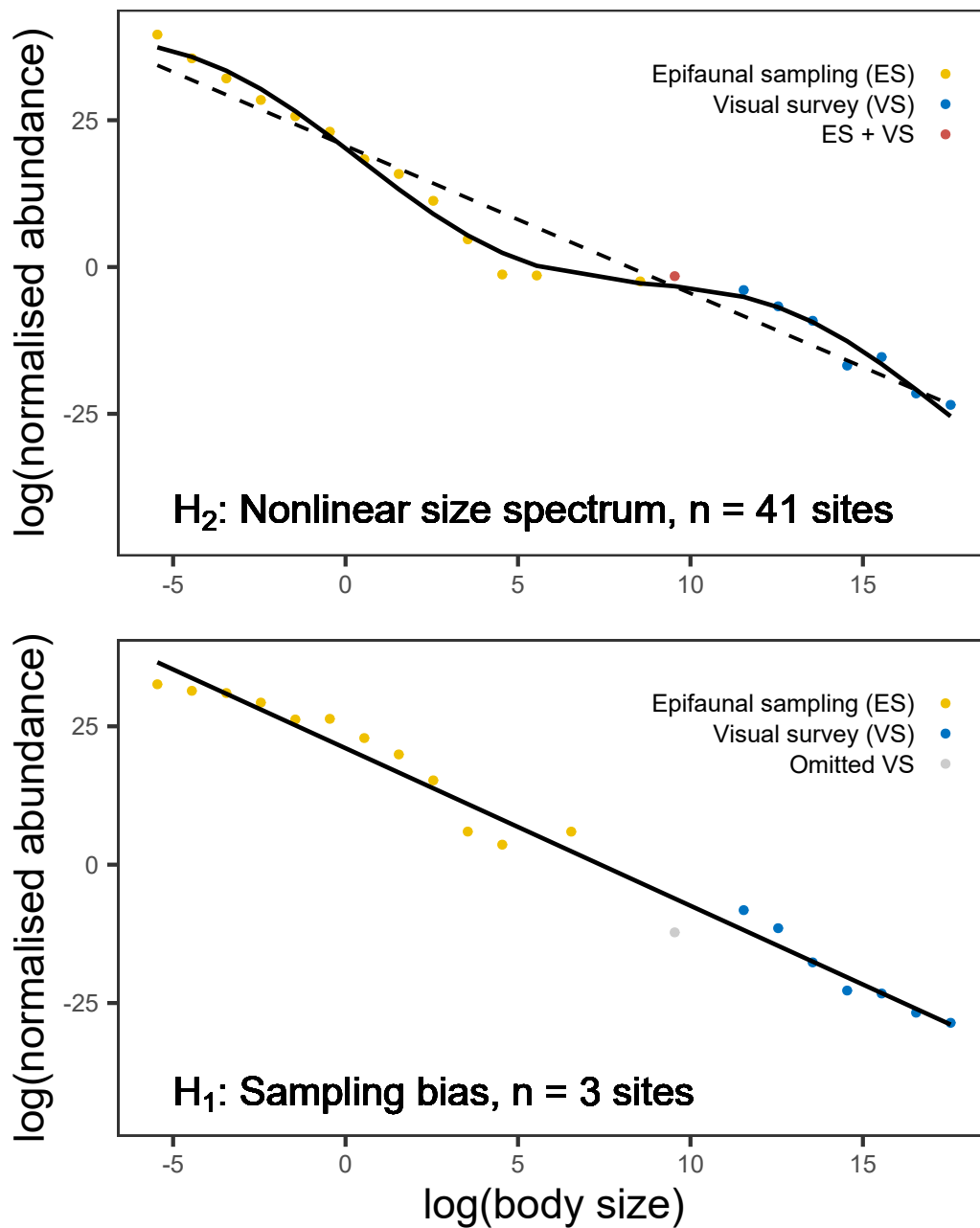


FIGURE 3.3: Abundance size spectra for two example reefs, each providing support for one of the proposed hypotheses. The upper panel shows the size spectrum of a single reef (GBR27) where a nonlinear continuous size spectrum model better describes the community than a linear model, this was observed in 41 of the 45 sites. The lower panel shows an example reef (NIN-S1) where there is potentially under-sampling of the smallest body size class of the visual survey data. The datapoint colour represents the sampling method of the individuals that make up the size class.

The mean community level predator-to-prey size ratio, calculated as the log base to the power of half the wavelength ($\sqrt{2}^{\frac{D}{2}}$), was estimated to be 28.1 (± 10.3 , 95% confidence interval). That is, a predator is expected to be 28.1 times the body length of its prey.

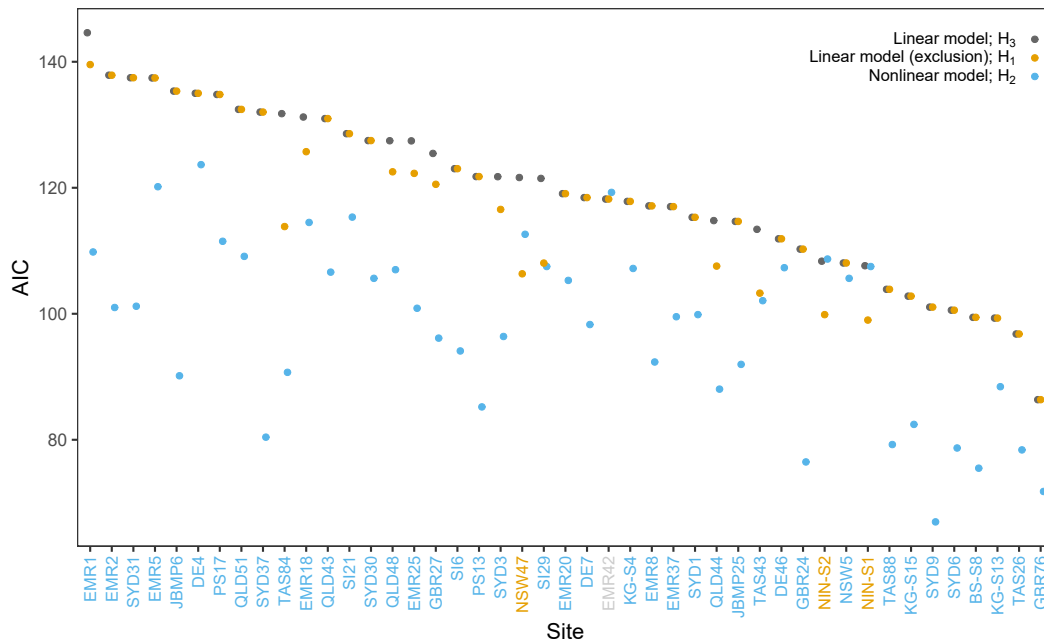


FIGURE 3.4: Comparison of the goodness-of-fit of three models fit to 45 reef size spectra; the Akaike information criterion (AIC) value for a linear model (dark grey points), a linear model excluding size bins within the abundance dip (orange points) and a nonlinear sinusoidal model (blue points). Points have been horizontally jittered to avoid data point overlap. Each model provides support for one of three hypotheses (H_1 , H_2 , and H_3). The colour of the x-axis text refers the best fitting model (lowest AIC) at the site and the hypothesis it supports, which are ordered by linear model (dark grey) AIC values for illustrative purposes. One site (EMR42, light grey text) does not support any of the three hypotheses. Geographical locations of the sites can be found in Figure S3.5.

The fitted nonlinear size spectrum parameter values at the site were regressed against the site-level environmental variables (see Table S3.2 and Equations S3.4-S3.7 for the full fitted models). These combinations of environmental variables explained 31% of the variation (as determined by the R^2 value of Equation S3.4) in size spectrum amplitude, 19% of variation in size spectrum wavelength, 60% of the variance in the size spectrum slope and 35% of the variance in the body size where relative peak abundance occurs (see peaks in Figure 3.2).

The slope of the size spectrum (λ) increased (i.e., became shallower) with increasing site mean sea surface temperature (SST). The position of the peak abundance was also dependent on the site SST, whereby the peak abundance occurred at around 19.8 cm in temperate sites compared to around 7.4 cm at tropical sites (Figure 3.2).

3.5 Discussion

Whilst there was an extremely strong linear component to the size spectra, the addition of a sinusoidal component resulted in better model fitting at 41 of the total 45 sites. This supported our second hypothesis (Figure 3.1C) that the abundance dip commonly

assumed to be solely a sampling artefact is part of a nonlinear size spectrum. A few sites nevertheless provided evidence of under-sampling of small to medium sized fauna (e.g., NIN-S1, NIN-S2, NSW47, lower panel in Figure 3.3). Thus, some support for the first hypothesis (Figure 3.1B) also exists, with under-sampling of smaller sized fishes indicating that the visual methods used cannot cover fishes with equal probability of observation along the size spectrum. Regardless, the data suggest that under-sampling is not likely the primary reason for the non-linearity in reef fish size structure, potentially affecting conclusions of previous studies where smaller size classes had been removed.

The dip in abundance in the range of 2.5 cm to 10 cm for visual survey data observed here (blue datapoints in Figure S3.5, see also Figure 3.1A), is consistent with the patterns observed in previous reef size spectra studies (Ackerman and Bellwood, 2000, Ackerman et al., 2004). Ackerman et al. (2004) used rotenone poisoning sampling to comprehensively sample all reef fauna and observed a similar dip in abundance in this size range. Our results also suggest the dip in abundance is a true feature in an overall size spectrum (Figure S3.1) that is nonlinear (i.e., supporting H_2 , Figure 3.1C). We also note the complete absence of individuals in the size bins ranging 5 mm to 22 mm was observed at many sites (Figure S3.5). This absence is likely due to individuals missed in both sampling methods, for exemplifying small mobile individuals, missed by both habitat-associated epifaunal sampling, and below the visible limit of visual surveys.

Wave-like patterns in size spectra have been previously observed in lake studies (e.g., Sprules et al., 1983, Boudreau and Dickie, 1992), and have been reproduced in mechanistic modelling studies (e.g., Rossberg et al., 2019, Andersen and Pedersen, 2010). The mechanistic approaches indicate trophic cascades driven by fishing pressure (Andersen and Pedersen, 2010) and nutrient enrichment (Rossberg et al., 2019) can result in wave-like patterns in size spectra. Both studies found that a combination of bottom-up (food availability) and top-down (predation mortality) pressures drove the observed patterns. Further, both studies found wave amplitude to increase with body size (i.e., greater linearity in the size spectrum at smaller body sizes), similar to the patterns observed here (Figure 3.3). This could be formally tested with a model that allows amplitude to vary with body size, however this was not applied here due to potential for overparameterization of the model (see also Rossberg et al., 2019). A test to assess whether nutrient enrichment drives sinusoidal patterns in lakes (Rossberg et al., 2019) requires a greater range of available nutrients (phosphates and nitrates) than was available at the reef sites in this study. If the sinusoidal patterns observed in this study are driven by trophic interactions, we would expect the distance between peaks and troughs to correspond to a mean predator-to-prey size ratio (PPSR) at the community level. Using the wavelength to calculate PPSR, we estimated a mean community PPSR of 28.1, which corresponds to a predator-to-prey mass ratio (PPMR) of $10^{4.3}$ ($= 28.1^3$; if we assume isometric growth, $W \propto L^3$), which is consistent with previous estimates of community-level PPMR (Trebilco et al., 2013), further supporting the hypothesis that these sinusoidal patterns are driven by trophic interactions. A dietary study of 88 seagrass inhabiting fishes found predator length to be 13.3x prey length on average, suggesting slightly higher community PPMR on reefs than in seagrass

habitats (Edgar and Shaw, 1995).

Another theory explaining nonlinearity in size spectra assumes habitat complexity provides refugia that favour particular body sizes (e.g., Rogers et al., 2014). The fact that we observed no significant relationship between the survey site relief (a broad-scale measure of habitat complexity) and the size spectrum amplitude (A in Equation S3.1; a measure of nonlinearity) does not necessarily disprove this theory. Complex habitats are likely to provide a wide range of refugia of varying scales (Hixon and Beets, 1989, 1993, Shulman, 1985, Menge and Lubchenco, 1981) and associated potential niches. Site relief was classified categorically into four levels to describe the broad-scale habitat structure, but these categories would unlikely encompass the finer-scale crevices used as prey refugia. Further, wave amplitude is a measure of the strength of the sine curve, not necessarily a measure of fine-scale deviations from linearity that would be expected from fine-scale habitat complexity. Therefore, the potential mismatch in the broader-scale of the relief measures and the finer-scale of prey refugia may result in their non-significant relationship observed here. Based on the observed peaks in the size spectrum ranging from 7 to 20 cm, one might hypothesise that refugia for fishes in this size range may be most important, and that smaller refugia in tropical areas support peaks in abundance at smaller sizes than on temperate reefs. The latter is plausible with more finer scale complexity likely amongst the coral structures on tropical reefs compared to the cover provided by kelps on a rocky base in temperate zones (see below). If the wave amplitude (A) is primarily driven by alternative mechanisms (such as trophic cascades), then analysing the residuals of this nonlinear sinusoidal model may identify a “tertiary structure” of the size spectrum, potentially driven by finer-scale drivers, such as habitat niches and refugia.

Environmental variables explained a large portion of variability in the size spectra; both the linear (λ) and nonlinear components (A , D , and position of peak abundance). Figure 3.2 indicates that the peak in abundance occurs at larger body sizes in cooler sites compared to warmer sites: using Equation S3.7 we estimate a relative peak in abundance at 19.8 cm with 14°C SST, whilst a peak at 7.4 cm with 26°C SST (Figure S3.7). These peaks approximately correspond to the mean body size of the dominant large invertebrate-feeding fishes in temperate regions (e.g., wrasses) and the sometimes hyper-abundant small planktivorous fishes on coral reefs. Numerous explanations potentially account for latitudinally-dependent body size preference. Firstly, the dominant energy pathways may vary with latitude, whereby a higher mean PPMR in temperate reefs leads to less energy lost through trophic inefficiencies and therefore a peak in abundance at larger body sizes. As described above, habitat composition also varies latitudinally and has been shown to play an important role in latitudinal variation in the body sizes of the smallest invertebrates studied here (Fraser et al., 2021, Yamanaka et al., 2012).

Size spectra are widely used as ecological indicators of reef health, for detecting and quantifying ecosystem disturbances such as fishing pressure (Robinson et al., 2017, Dulvy et al., 2004, Graham et al., 2005, Wilson et al., 2010). This application of empirical size spectra as ecological indicators often relies on the assumption that relationships between log abundance (or biomass) and log body size are linear (Nash and Graham, 2016, Graham

et al., 2005, [Dulvy et al., 2004](#)). Here, we show that 96% of the variation in log abundance can be explained by a linear function of log body mass in individuals ranging from 0.125 mm to 2 m, irrespective of taxonomy or location. Our detailed empirical support for consistency of marine size spectra supports the generality of early conjectures of linear size spectra holding from “bacteria to whales” ([Sheldon et al., 1972](#)). However, in order to use size spectra as ecological indicators for reefs we must identify a counterfactual baseline representing an ‘unimpacted’ reef, from which to compare ([Jennings and Blanchard, 2004](#), [Petchey and Belgrano, 2010](#)). Although we observed remarkable consistency in the linearity of the size spectra, subtle nonlinearities are evident. These sinusoidal nonlinearities are similar to those previously observed (e.g., [Sprules et al., 1983](#)) and modelled ([Rossberg et al., 2019](#)) in lake ecosystems. Whether the inflections reflect disturbances to reefs or are an inherent part of reef size spectra remains speculative. While temperature was found here to be a strong driver of sinusoidal patterns, this factor is likely related to multiple interacting direct and indirect effects on body size, including through changes in habitat composition ([Fraser et al., 2021](#)). Trophic cascades potentially also contribute to inflections ([Rossberg et al., 2019](#), [Andersen and Pedersen, 2010](#)). Mechanistic models trained with empirical data are needed to test this hypothesis and to identify the main drivers of the nonlinear patterns. Data presented here for remote highly protected reefs (e.g., Middleton Reef, “EMR”) provide a baseline for reef size spectra, and for their expanded use as ecological indicators of reef health.

3.6 Acknowledgements

This research was supported by the Marine Biodiversity Hub, a collaborative partnership supported through funding from the Australian Government’s National Environmental Science Program, and used the NCRIS-enabled Integrated Marine Observing System (IMOS) infrastructure for database support and storage. This research was also made possible by funding of the Australian Research Council (ARC), and the data from the Reef Life Survey Foundation. The authors also thank data support from Antonia Cooper, Just Berkhout, Scott Ling, Ella Clausius and Elizabeth Oh.

3.7 Supplementary material

S3.1 Linear vs. nonlinear size spectra models

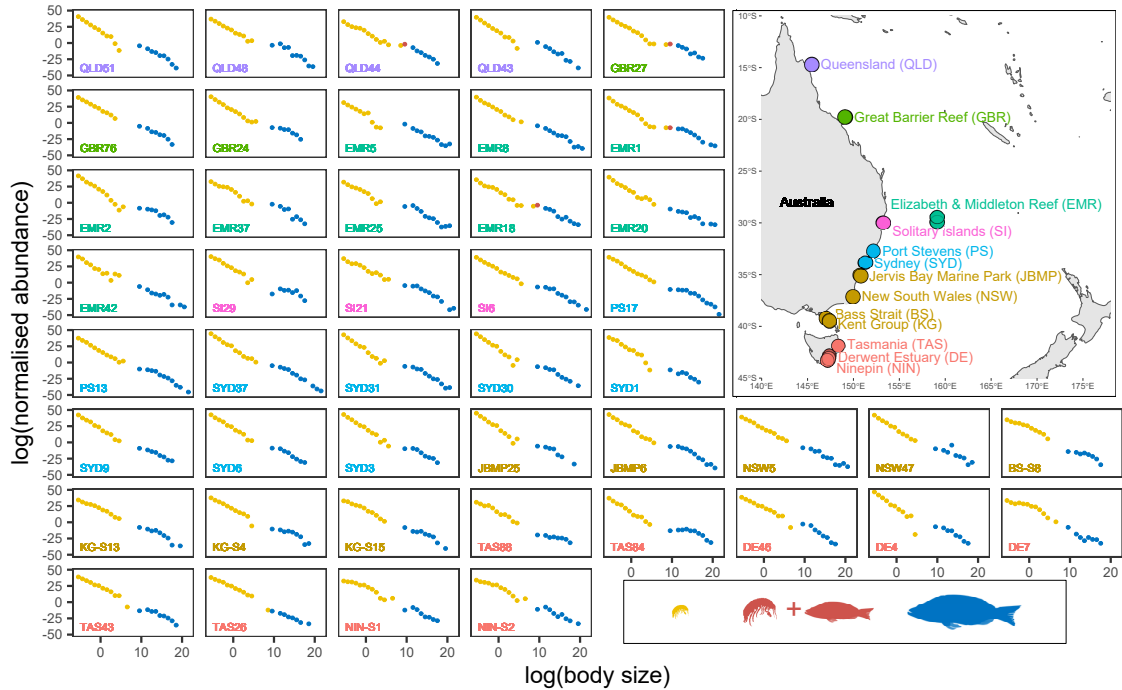


FIGURE S3.5: Size spectra for rocky and coral reef ecological communities, with body size ranging from 0.125 mm to 2 m, at 45 sites along the 28° latitude along the eastern coast of Australia (sites ordered by latitude). Yellow data points represent data from epifaunal sampling, blue data points represent individuals from visual surveys and red data points represent mass bins that contain animals from both sampling methods.

A linear model (Equation S3.2) was fitted to the size spectrum data within each survey site (s). The residuals of these fits were used to re-create Figure 3.3 (main text), and also to compare the goodness-of-fit to the nonlinear size spectrum fits.

$$\log(N) = \beta_{0,s} + \lambda_s \cdot \log(L) \quad (\text{S3.2})$$

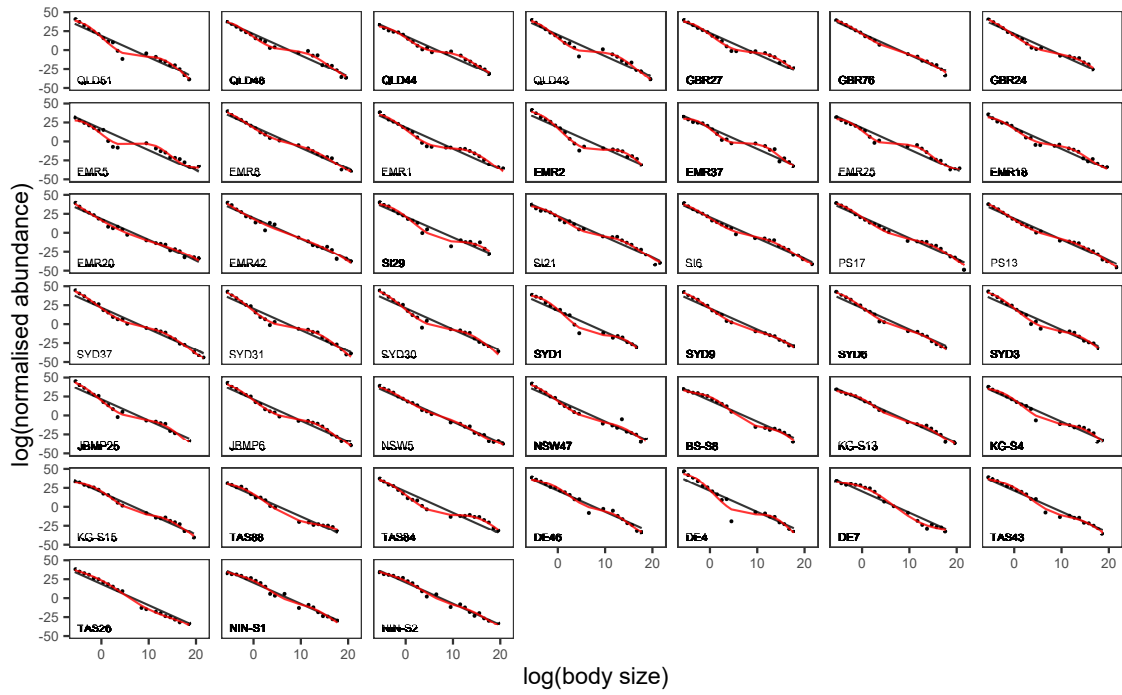


FIGURE S3.6: Continuous abundance size spectrum with a fitted linear model (black, Equation S3.2) and nonlinear model (red, Equation S3.1 in main text).

We also fit a single linear model to all sites, to answer the question about how much variability in abundance is explained by body size alone (at all sites)(Equation S3.3).

$$\log(N) = \beta_0 + \lambda \cdot \log(L) \quad (\text{S3.3})$$

S3.2 Environmental variables

TABLE S3.1: Summary table of the environmental variables used in the study. The four oceanographic variables were remotely sensed with pixel span = 9.2 km, [Edgar et al. \(2014\)](#); categorical variables relate in situ diver assessment at site.

Name	Units	Details
Mean sea surface temperature (SST)	°C	Bio-ORACLE (Tyberghein et al., 2012)
Phosphate	mmol l ⁻¹	Bio-ORACLE (Tyberghein et al., 2012)
Nitrate	mmol l ⁻¹	Bio-ORACLE (Tyberghein et al., 2012)
Mean Chlorophyll A	mg m ⁻³	Bio-ORACLE (Tyberghein et al., 2012)
Wave exposure	Categorical	(1) Sheltered, wind waves < 1 m (2) Waves 1 – 3 m (3) Ocean swell < 3 m (4) Open swell from prevailing direction
Currents	Categorical	(1) None (2) Weak (3) Moderate (4) Strong
Reef slope	Categorical	(1) < 1:10 (2) 1:10 – 1:4 (3) 1:4 – 1:2 (4) > 1:2
Relief	Categorical	(1) < 0.5 m (2) 0.5 – 1 m (3) 1 – 2 m (4) > 2 m

S3.3 Body size position of peak abundance

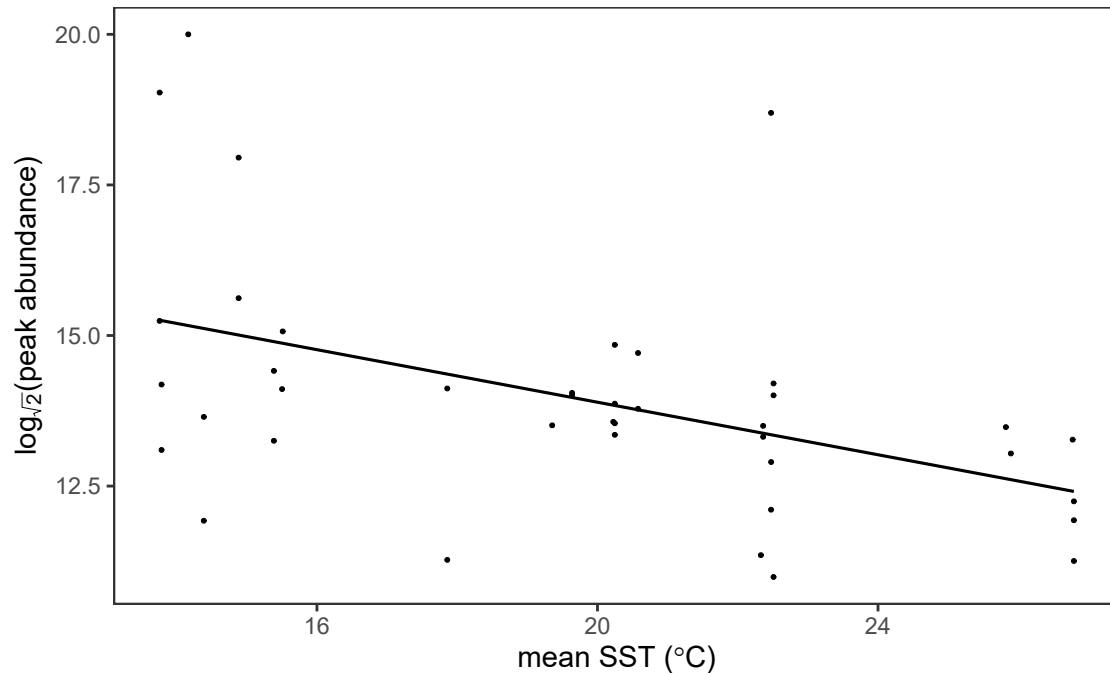


FIGURE S3.7: Relative peaks in abundance occur at certain body sizes in the size spectrum. The body size at which these peaks occur is related to the sea surface temperature (SST) of the site.

S3.4 Environmental covariates explaining model parameters

We used a best subset regression method to identify the combination of environmental drivers that resulted in the best fitting models determined by the lowest AIC value (Akaike, 1974). explained most variation in (S3.2) of the variation in the five nonlinear model coefficients (β_0 , λ , A , D , and position of peak abundance). We fit four linear models, one linear model for each of the nonlinear model coefficients (amplitude, A ; wavelength, D ; slope, λ ; and the body size of relative peak abundance, 'Peak') as the response variable, and with the selected environmental variables as predictor variables. Environmental variables were selected based on a 'best subset' approach. Whereby the best combination of environmental variables that minimised the Akaike information criterion (Akaike, 1974) of the model were chosen. The best subset regression approach was performed using the 'ols_step_best_subset()' function in the 'olsrr' package (Hebbali, 2020) within R (R Core Team, 2020). The models representing the lowest AIC values are shown in Table S3.2. The phase parameter (P) was excluded as did not represent a meaningful feature of the nonlinear model when the wavelength (D) is not fixed (see main text). The intercept (β_0) was excluded as it is highly correlated to the slope of the size spectrum (λ).

TABLE S3.2: Summary of the most important environmental variables explaining the variance each nonlinear model parameter and the amount of variation explained from a multiple linear regression.

Parameter	Predictor variables	R ²
Amplitude (A)	Reef slope, Chlorophyll A, Nitrate, Phosphate, Wave exposure	31%
Wavelength (D)	Reef slope, Wave exposure, Relief, Chlorophyll A, Phosphate	19%
Slope (λ)	Wave exposure, SST, Chlorophyll A, Currents, Nitrate	60%
Peak abundance	SST, Wave exposure, Reef slope, Relief, Chlorophyll A	35%

The four models from Table S3.2 in equation form are:

$$A \sim \beta_0 + \beta_1 S + \beta_2 C_A + \beta_3 N + \beta_4 P + \beta_5 W \quad (\text{S3.4})$$

$$D \sim \beta_6 + \beta_7 S + \beta_8 W + \beta_9 R + \beta_{10} C + \beta_{11} P \quad (\text{S3.5})$$

$$\lambda \sim \beta_{12} + \beta_{13} W + \beta_{14} T + \beta_{15} C_A + \beta_{16} C + \beta_{17} N \quad (\text{S3.6})$$

$$Peak \sim \beta_{18} + \beta_{19} T + \beta_{20} W + \beta_{21} S + \beta_{22} R + \beta_{23} C_A \quad (\text{S3.7})$$

where, A , D , λ and $Peak$ refer to the parameter outputs of the nonlinear size spectrum model (Equation S3.1 in main text), amplitude, wavelength, slope and body size of peak abundance, respectively. The predictor variables are reef slope (S), mean chlorophyll A (C_A), nitrate (N), phosphate (P), wave exposure (W), relief (R), currents (C), mean sea surface temperature (T). Units for these environmental variables can be found in Table S3.1.

S3.5 Model comparison

At each site we fit three models to test each of the three hypotheses of the study, the first model (“lm”, Equation S3.2) to all data (epifaunal and visual census data), the same linear model but excluding size bins within the abundance ‘dip’ (“lm, exclusion”), and a nonlinear size spectrum model (“nls”, Equation S3.1 in main text). A comparison of the AIC values of the models can be seen in Table S3.3.

TABLE S3.3: Comparison of the goodness-of-fit of three models. Goodness-of-fit is determined by a lower Akaike Information Criterion (AIC) value (Akaike, 1974). AIC_{lm} is the AIC value for the overall linear model. AIC_{nls} represents the AIC for the nonlinear size spectrum model and $AIC_{lm,exclusion}$ represents the AIC for the overall linear model with the abundance “dip” excluded. The *Hypothesis* column indicates which hypothesis (see Main text) is supported. See Figure 3.4 in the main text for a graphical representation of this table.

Site code	$AIC_{nls} - AIC_{lm}$	$AIC_{lm,exclusion} - AIC_{lm}$	Hypothesis
BS-S8	-23.9	0	H2

DE4	-11.3	0	H2
DE46	-4.6	0	H2
DE7	-20.2	0	H2
EMR1	-34.8	-5.1	H2
EMR18	-16.7	-5.5	H2
EMR2	-36.9	0	H2
EMR20	-13.8	0	H2
EMR25	-26.6	-5.2	H2
EMR37	-17.5	0	H2
EMR42	1.1	0	NA
EMR5	-17.3	0	H2
EMR8	-24.8	0	H2
GBR24	-33.8	0	H2
GBR27	-29.3	-4.9	H2
GBR76	-14.6	0	H2
JBMP25	-22.7	0	H2
JBMP6	-45.2	0	H2
KG-S13	-10.9	0	H2
KG-S15	-20.4	0	H2
KG-S4	-10.6	0	H2
NIN-S1	-0.1	-8.6	H1
NIN-S2	0.3	-8.5	H1
NSW47	-9	-15.3	H1
NSW5	-2.4	0	H2
PS13	-36.6	0	H2
PS17	-23.3	0	H2
QLD43	-24.4	0	H2
QLD44	-26.8	-7.2	H2
QLD48	-20.5	-4.9	H2
QLD51	-23.3	0	H2
SI21	-13.2	0	H2
SI29	-14	-13.4	H2
SI6	-28.9	0	H2
SYD1	-15.4	0	H2
SYD3	-25.4	-5.2	H2
SYD30	-21.9	0	H2
SYD31	-36.3	0	H2
SYD37	-51.6	0	H2
SYD6	-21.9	0	H2
SYD9	-34.1	0	H2
TAS26	-18.4	0	H2
TAS43	-11.3	-10.1	H2

TAS84	-41.1	-17.9	H2
TAS88	-24.6	0	H2

Chapter 4

Resolving global links between body size, abundance, and species richness on reefs

Freddie J. Heather¹, Graham J. Edgar¹, Rick D. Stuart-Smith¹, Julia L. Blanchard¹

1 – Institute for Marine and Antarctic Studies, University of Tasmania, 20 Castray Esplanade, Battery Point, Hobart, TAS 7004, Australia

Code availability: Code for the analysis, and to recreate all figures, is available at https://github.com/FreddieJH/building_size_spec.

4.1 Abstract

Links between biodiversity and ecosystem functioning are commonly described using relationships between species richness and measures of total abundance or biomass of communities. Body size, abundance and species richness are known to be interrelated in ecological communities, yet detailed knowledge of the nature and generality of these interrelationships across scales is missing. Previous work has debated whether or not species richness peaks at an intermediate body size or whether there is a continual decline in richness with increasing body size. However, testing the generality of this conjecture requires individual body size and abundance data for many species. Here, we use a global dataset on 16.9 million fish and invertebrate individuals across 3,064 species to investigate these three linked relationships. Further, we also develop a method for predicting these patterns when only species abundance and maximum body size data are available. Our method allows for accurate reconstruction of abundance-size, species richness-size and species richness-abundance relationships. Both abundance-body size ($N \sim M^{-1.57}$) and species richness-body size ($R \sim M^{-1.22}$) relationships followed an approximately linear relationship on the log-log scale. Observations and models further indicated a 0.74 scaling coefficient between species-richness and abundance within size classes (i.e., $R_m \sim N_m^{0.74}$). Which we show to be broadly consistent with insect communities, suggesting a general relationship that may apply across terrestrial and aquatic realms globally.

4.2 Main

The basis of the spatial patterns of biodiversity across the globe is a central question within the fields of ecology and evolutionary biology (Fine, 2015). Species richness, abundance and body size are clearly linked across ecological communities, yet no consensus exists on the mechanisms behind these relationships (Fine, 2015, Gislason et al., 2020). An organism's body size is a key predictor of many attributes (Peters, 1983), from metabolic rate (Brown et al., 2004) to trophic position (Jennings et al., 2001), as well as both abundance (e.g. Elton, 1927, Sheldon et al., 1972) and species richness (e.g. May, 1986).

In this study we used a global dataset of 16.9 million reef-associated fish and invertebrate individuals across 3,064 species to investigate these three linked relationships: 1) abundance vs body size ($N \sim M$, the abundance size spectrum), 2) species richness vs body size ($R \sim M$, richness size spectrum), and 3) abundance vs richness within log body size bins ($R_m \sim N_m$, here termed the "diversity-abundance spectrum"). The paucity of individual level body size data at broad geographical scales is usually a limiting factor in determining these relationships. We therefore also developed a method, available for future studies, to reconstruct the three relationships in two levels of body size data availability; 1) when only species-level abundance body size distributions are available and 2) when only a single value of body size is available for each species (asymptotic size).

4.3 Abundance size spectrum

The relationship between body size and abundance in a community, also termed the abundance size spectrum or the individual size distribution, can provide important information about the partitioning and movement of energy within a community (Trebilco et al., 2013). On the log-log scale, size spectra are often described by a linear function, with slopes that are remarkably consistent across marine (Sprules and Barth, 2016), freshwater (Sprules et al., 1983) and terrestrial realms (Ghilarov, 1944). In reef abundance size spectra analyses, it is common practice to remove the smallest body sizes (e.g., <10 cm body length) due to potential sampling biases involved with visual survey methods (Ackerman and Bellwood, 2000) and to conform to the theory of linearity (Trebilco et al., 2015, Wilson et al., 2010). This practice however is debatable, as removal of the smallest bodied individuals may be removing a true, nonlinear, feature of the size spectrum of reefs (Heather et al., 2021b).

The slope of the community abundance size spectrum can convey much information about how energy (and biomass) is distributed in the food web as well as reflecting size-based anthropogenic disturbances, such as fishing (Robinson et al., 2017, Graham et al., 2005, Wilson et al., 2010). Here we show an approximately linear relationship between log body size and log abundance (Figure 4.1a) across the entire range of body sizes that are feasible to assess from visual survey methods (> 2.5cm). By accounting for the variable bin widths, we calculate the abundance per unit body mass within logarithmic body mass bins (Figure 4.1b), commonly referred to as 'normalising' the axis in size spectrum analyses

(Platt and Denman, 1977). Here, we estimate a global mean abundance size spectrum slope of -0.41 (Equation 4.1, normalised = -1.41), corresponding to a relationship between abundance (N) and body mass (M) of $N \propto M^{-1.41}$, and is drastically shallower than previous estimates on reefs (Heather et al., 2021a). Despite the approximate linearity in the abundance size spectrum observed here, we still observe fewer individuals in the smallest body size classes than would be expected assuming a linear decline in log abundance with log body size. On reefs, the smallest bodied individuals have been reportedly observed to be relatively less abundant than would be expected under linear size spectrum theory (e.g. Ackerman et al., 2004, Ackerman and Bellwood, 2000), hence their inclusion in the analyses here unsurprisingly results in a shallower size spectrum compared to previous estimates that ignore these individuals before fitting linear models (Heather et al., 2021a). This highlights the need for a better understanding of the nonlinear patterns in reef abundance size spectra.

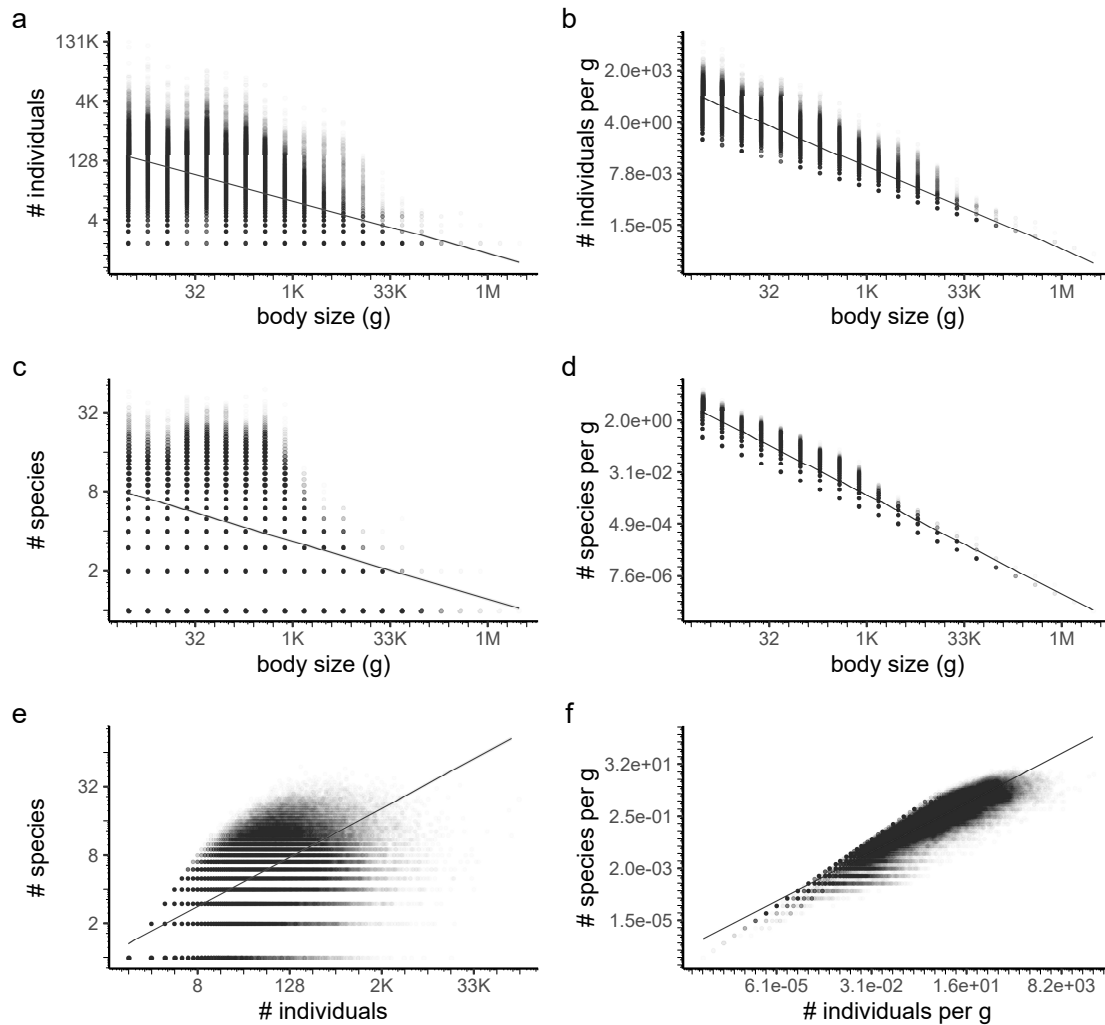


FIGURE 4.1: The empirical relationships between body size, abundance and species richness for 11,935 visual census surveys of reefs globally. A negative linear relationship between log body size and log abundance (a), between log body size and log species richness (b), and a positive linear relationship between log number of species in a logarithmic mass bin and the log number of species within a logarithmic mass bin (c). By accounting for the variable logarithmic bin widths, we calculate the abundance at a given body mass (b, aka. abundance density), richness at a given body mass (d, aka. richness density) and the relationship between abundance density and richness density within body mass bins (f). The model fits are linear mixed effects models with a random slope and intercept for each survey nested within the site.

4.4 Richness size spectrum

Extinction vulnerability is related to body size (Cardillo, 2003, Gaston and Blackburn, 1995, Olden et al., 2007), therefore it is important to consider body size, and not just species identity, in relations to biodiversity loss (Brose et al., 2017). The empirical relationship between body size and species richness has long been discussed yet remains comparatively less studied than the relationship between body size and abundance. Early terrestrial

macroecological studies predicted a right-skewed unimodal relationship between log body size and log species richness, with a roughly linear right tail (Blackburn and Gaston, 1994, Brown and Nicoletto, 1991, Hutchinson and MacArthur, 1959, Loder et al., 1997), whereas Marquet et al. (2005) found the relationship in mammals to be linear across all body sizes. These studies focused on a specific clade or taxonomic group, however, precluding conclusions on whether the pattern remained when other elements of the ecosystem were included (e.g., which may share resources or occupy different size classes or trophic groups to the study group). Reuman et al. (2014, 2008) made the first attempts relating body size to species richness across all the species within a region, defining the “diversity size spectrum” as the frequency distribution of species-level asymptotic size. Here, we describe the “richness size spectrum”, i.e. the species richness within logarithmic body size classes, where a single species may occupy multiple logarithmic mass bins.

Similar to previous estimates (Siemann et al., 1996, May, 1986, Hutchinson and MacArthur, 1959), our results show a peak in species richness at an intermediate logarithmic body mass bin (Figure 4.1c). Investigators often fit a linear model to the right tail of this distribution (e.g. Loder et al., 1997, May, 1986), however, when we account for the varying bin widths (i.e., “normalisation” of the axis), that is, species per unit body mass, we observe a monotonically decreasing relationship (Figure 4.1d) between log body mass and log species richness per unit body mass. The difference between richness peaking at a specific body size and monotonically decreasing is an important distinction to make as it determines the diversity of the smallest bodied individuals. We show that the same information can convey two messages. Whilst species richness for a given body size does monotonically decrease with increasing body size (Figure 4.1d), we also observe localised peaks in this relationship (Figure 4.1c, d).

It is well known that there exists a latitudinal variation in species richness, with both aquatic and terrestrial biodiversity peaking in the tropics. Interestingly, we observe a latitudinal pattern in the slope of the richness size spectrum (Equation 4.2, Figure 4.2b), with the steepest slope in the tropics. Further, a similar pattern in the slope of the abundance size spectrum is observed, with steeper slopes in the tropics (Figure 4.2a), apparently opposing the longitudinally consistent relationship by Heather et al. (2021a). Heather et al. (2021a) however, ignores smaller-bodied individuals (<32 g) in their slope estimates, which is likely the cause of the difference in latitudinal-slope patterns and highlights the importance of including these individuals. A steeper richness size spectrum slope (here observed in the tropics) corresponds to greater number of smaller-bodied species relative to the number of larger-bodied species, likewise a steeper abundance size spectrum slope (here observed in the tropics) represents a greater number of smaller bodied individuals relative to larger-bodied individuals. The similar latitudinal relationship between the richness size spectrum slope and the abundance size spectrum slope (Figure 4.2a,b) suggests the greater relative abundance of smaller-bodied individuals in the tropics may be the driver of the greater species richness.

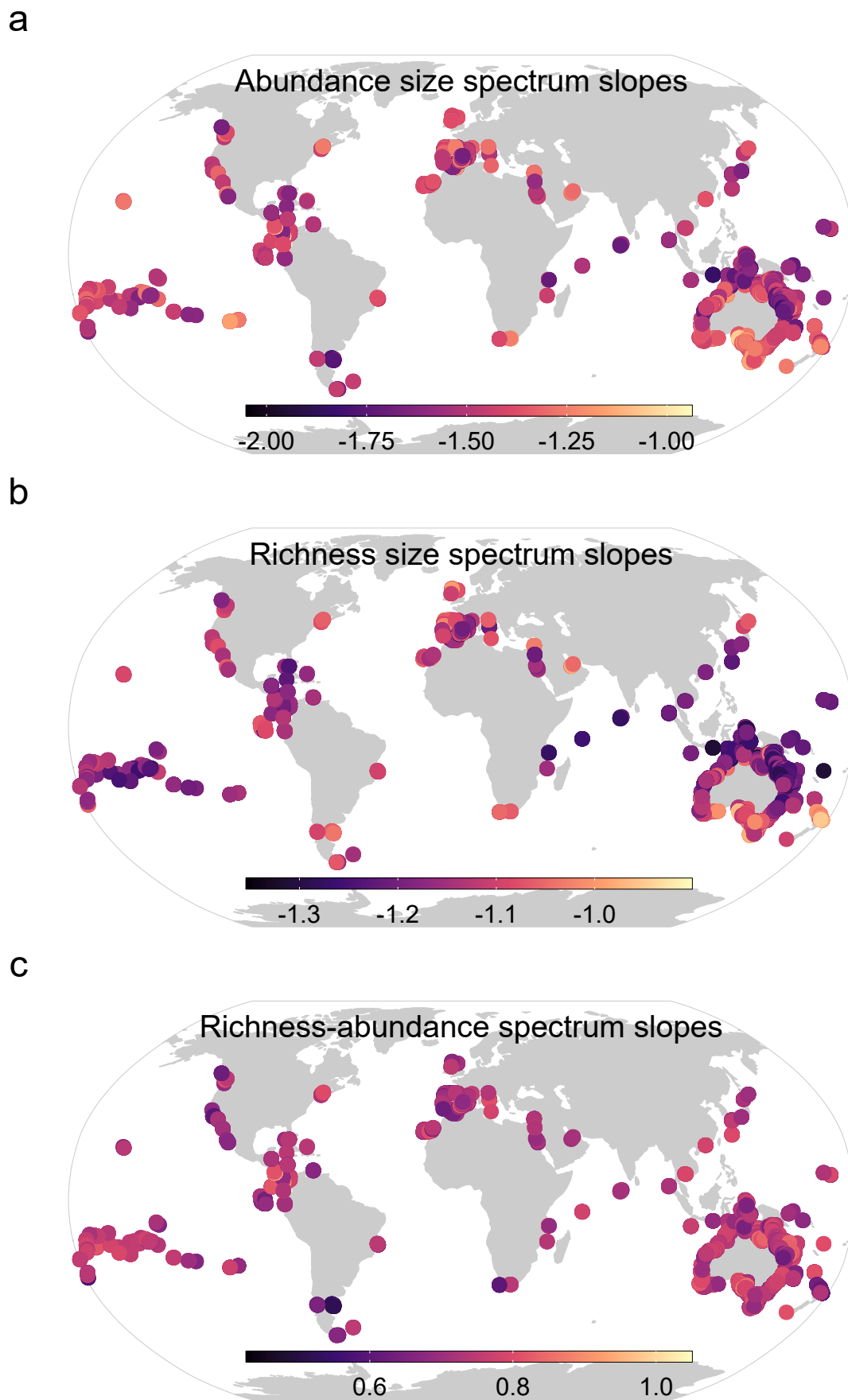


FIGURE 4.2: The global variation in normalised abundance size spectrum slopes (a), the normalised richness size spectrum slopes (b), and the normalised diversity-abundance spectrum slopes (c) for 11,935 reef surveys.

4.5 Richness-abundance spectrum

A previous study (Siemann et al., 1996) on a grassland insect community showed a linear relationship between number of species in a logarithmic body mass class (R_m) and the total number of individuals within the same logarithmic body mass class (N_m). Siemann et al. (1996) speculated a general rule in ecology with $R_m \propto N_m^{0.5}$. In the period since this hypothesis was proposed, the three-way relationship between body size, abundance and richness remains surprisingly understudied, with some notable exceptions (Fa and Fa, 2002, Labra et al., 2020, McClain, 2004). This paucity may be due to the high data requirements of individual-level data spanning many body size classes. Following the methods of Siemann et al. (1996), we show that a relationship of $R_m \propto N_m^{0.37}$ for reef communities (Figure 4.1e), suggesting fewer species given the abundance within a body size class. This discrepancy roughly corresponds to five fewer species in reefs in a mass bin containing 100 individuals, or 20 fewer species in a mass bin containing 1000 individuals, compared to the grassland insect community (Siemann et al., 1996). The unimodal relationships of insect abundance and richness size spectra reported by Siemann et al. (1996) are consistent with the relative drop in abundance and richness at the smallest size classes observed in this study for reefs (Figures 4.1a, c). Similarly however, regressing log abundance and log richness within a body mass class (Figure 4.1e), we observe an approximately positive linear relationship, albeit with a large portion of unexplained variance.

When we account for the varying logarithmic bin widths, i.e., regressing the richness per unit body mass and abundance per unit body mass, we observe a scaling relationship between species richness and abundance of $R_m \propto N_m^{0.74}$ (Equation 4.3, Figure 4.1f). One might expect if metabolic theory is driving this relationship, then temperature would be an important factor in determining the number of species given the number of individuals. Interestingly, we observe no latitudinal patterns in this relationship (Figure 4.2c), i.e. the relationship between abundance and richness within body size classes in reef communities consistent globally.

4.6 Predictions in the absence of individual-level data

The reliance on broad-scale, individual-level body size and abundance data on observing these relationships is a major hindrance to further exploration. We therefore developed a method to reconstruct these three relationship in the absence of individual-level body size data.

Studies using empirical data of protist communities in lakes (Giometto et al., 2013, Rinaldo et al., 2002) showed that the summation of lognormally distributed species body sizes can result in a power-law relationship between body size and abundance. Developing upon this idea, we show that, 1) species-level body size information is sufficient to accurately reconstruct the community abundance and richness size spectra and 2) capture the nonlinear patterns (reduced abundance and richness of smallest logarithmic body

mass bins) of reef size spectra, often ignored when relationships are modelled as linear on the log-log scale.

Using 1000 surveys as a test dataset, we show that the reconstructed abundance size spectra based upon the weighted summation of species body size distributions (Method 1: one body size distribution per species, fitted using the remaining surveys as a training dataset, $n = 10935$ surveys, Figure 4.3a) explained more of the observed data than a linear model in 51% of the test surveys (Both a lower RMSE, and higher R^2 value, Supplementary material, Figure S4.9). Further, when only using a single estimate of body size for each species (asymptotic body size) and a single relationship between asymptotic size and body size distribution (Method 2, Figure 4.3a), we explain more of the observed data than a linear model in 32% of the test surveys (Supplementary material, Figure S4.9). These results suggest that in the absence of individual-level data, we can reasonably accurately reconstruct the abundance size spectrum. This method allows us to partition the variation due to the global-mean body size distribution expected of the species and the variation explained by survey-level deviations and allows for us to test assumptions about the underlying species distributions that give rise to the observed community size spectrum.

Using this method, we also reconstructed the richness size spectrum and the relationship between abundance and richness with body mass classes. Similarly to the abundance size spectra, the reconstructed richness spectra better represented the observed data in 38% (Supplementary material, Figure S4.11) of surveys using method 1 and 33% of surveys using method 2 (Supplementary material, Figure S4.11).

The building up of size spectrum from species-level body size information opens new opportunities for similar studies in more data-poor situations. For example, abundance and richness size spectra can be reconstructed when only species' count data, or relative abundance, within a region are available. It is therefore possible to construct individual-level body size-based indicators (Blanchard et al., 2005, Graham et al., 2005, Shin et al., 2005) in the absence of individual-level body size information. Mechanistic approaches to food-web modelling are generally either species-based, where each species is represented by a set of trait values, or size-based, irrespective of species identity (e.g. the community size spectrum)(Blanchard et al., 2017, Brose et al., 2017). The reconstruction of size spectra from species-level information here brings together these approaches, maintaining species-level information and individual body size, which may aid in developing a mechanistic understanding of the contribution of species to individual-level community body size distributions (Andersen, 2019, Hartvig et al., 2011). This reconstruction method is now available as a R package for use in further community size spectra analyses (<https://github.com/FreddieJH/sbss>).

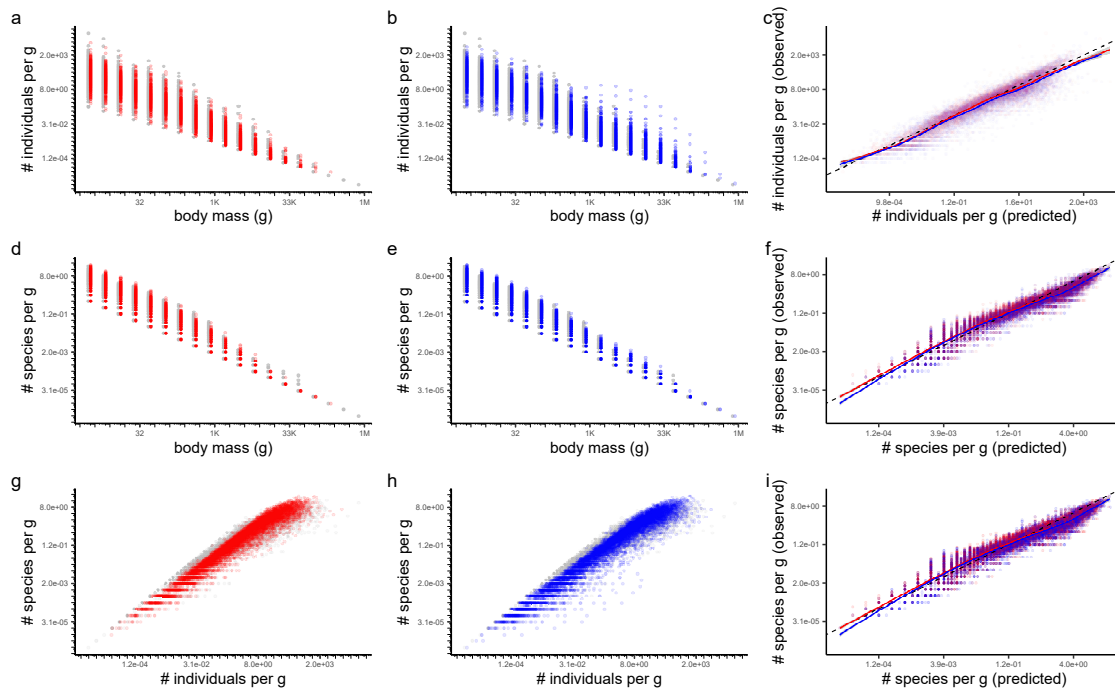


FIGURE 4.3: Reconstructed normalised abundance (a, b), normalised richness (e, f) size spectra, and the richness-abundance spectrum (g, h) based upon two levels of species-level body size information for 1000 test surveys; species-level body size distributions (red data points), and based upon a species-level asymptotic body size (blue data points). Predicted vs observed relationships for each of the three relationships are shown (c, f, i, respectively) with a LOESS smoothed line fit for each of the two reconstruction methods, compared to the 1:1 line shown as the dotted black line.

This study describes three important global-scale, empirical relationships linking individual body size to abundance and species richness in reefs. The similarity of these relationships with those observed in insect (Siemann et al., 1996) and other marine invertebrate communities (Fa and Fa, 2002, Labra et al., 2020, McClain, 2004) implies that the underlying mechanisms are potentially universal. Similar latitudinal variation in the slopes of the abundance and the richness size spectrum suggest that temperature may be a major driver in the three-way relationship between abundance, species richness and body size. Mechanistic approaches, combined with the empirical results here could help to elucidate the processes driving these observed patterns. Further, the reconstructed relationships here provide a means to analyse these relationships in other ecological realms, and where individual-level body size information is not readily available.

4.7 Methods

4.7.1 Data collection

Data on individual body length and abundance on reefs were obtained from the Reef Life Survey (see <https://reeflifesurvey.com>). Trained SCUBA divers swim along a 50 m transect and identify to species-level the fishes and invertebrates they encounter (Edgar

et al., 2020, Edgar and Stuart-Smith, 2014). A single survey ($n = 11,935$) consists of two separate methods undertaken on the same transect line. Method 1 involves recording any fish species ($n = 2,608$) within 5 m wide blocks either side of the line, whilst method 2 involves searching along the bottom, underneath kelp and in cracks in 1 m wide blocks either side of the line, recording invertebrates ($n = 1,184$) and cryptic fish species ($n = 951$). The abundance of each species within the defined block area is counted directly or estimated when necessary for highly abundant species. Size is usually estimated for fishes only. Fishes are binned into one of 13 size bins (2.5, 5, 7.5, 10, 12.5, 15, 20, 25, 30, 35, 40, 50, 62.5 cm), and lengths greater than 62.5 cm estimated to the nearest 12.5cm (see <https://reeflifesurvey.com> for a full description of the survey methods). Abundance from method 2 records were standardised to the equivalent area covered by method 1 (i.e. creating abundance per 500 m²) by multiplying abundance by five. A site ($n = 3,369$) usually contained multiple surveys undertaken at different depths on the same day.

4.7.2 Body mass estimation

Where body size was not estimated by the diver, as was the case for many large mobile invertebrate species, body size was estimated using estimated body-size probability distributions derived from species asymptotic body length. For full methods see Heather et al. (2021a).

Body mass was estimated from body length using published length-weight relationships (Fishbase (Froese and Pauly, 2010) and Sealifebase (Palomares and Pauly, 2019)) using the rfishbase package (Boettiger et al., 2012). Where species-level information was unavailable, body mass was estimated from one of two linear regression models: a class-level and an overall length-weight regression model. See Heather et al. (2021a) for full methods.

4.7.3 Fitting abundance size spectra

For each survey, abundance was calculated as the total number of individuals within a logarithmic (base = 2) body mass bin. A linear mixed effects model was fitted to the observed data predicting $\log_2(\text{abundance})$ from $\log_2(\text{body mass})$ and a random intercept term for surveyID nested within siteID (Figure 4.1a, Equation 4.1). To fit this model we used the lme4 (Bates et al., 2015) package in R.

$$\log_2(N) = \beta_1 + u_{0,\text{site}} + u_{0,\text{surv}|\text{site}} + \log_2(M) \cdot (\beta_1 + u_{1,\text{site}} + u_{1,\text{surv}|\text{site}}) \quad (4.1)$$

Where N is abundance, M is the middle of the body mass bin, u_0 is the random intercept term, and u_1 is the random slope term, β_0 is the overall intercept and β_1 is the overall slope term.

We calculated the normalised abundance by dividing the abundance within the logarithmic bin by the natural width of the bin. Normalisation of size spectra is a common procedure in abundance and biomass size spectra analyses (Kerr and Dickie, 2001). By dividing by the bin width we account for variation in width of the logarithmic size bins (Platt

and Denman, 1977), which results in an estimate of abundance density (aka. ‘normalised’ abundance), and a slope value one less than non-normalised size spectra (Edwards et al., 2017). We also fit Equation 4.1 to the normalised abundance size spectra (Figure 4.1b).

Survey-level estimates of the abundance size spectrum slope were estimated by summing the overall slope value (β_1), the random slope effect of the site for which the survey belongs ($u_{1,site}$) and the random slope effect of the survey ($u_{1,surv|site}$).

4.7.4 Fitting richness size spectra

For each survey, the number of unique species was calculated for each logarithmic size bin. We fit a linear model to the relationship between $\log_2(\text{species richness})$ and $\log_2(\text{body mass})$ with surveyID nested within siteID as a random intercept and slope term (Equation 4.2). To fit this model we used the lme4 (Bates et al., 2015) package in R.

$$\log_2(R) = \beta_1 + u_{0,site} + u_{0,surv|site} + \log_2(M) \cdot (\beta_1 + u_{1,site} + u_{1,surv|site}) \quad (4.2)$$

Where R is the species richness, and all other parameters are the same as those presented in equation 4.1.

We also modelled normalised richness (aka. richness density) using Equation 4.2. Where R then refers to the richness per unit body mass, as calculated by the number of species within a log body mass bin at the survey by the natural width of the log bin.

Survey-level estimates of the richness size spectrum slope were estimated by summing the overall slope value (β_1), the random slope effect of the site for which the survey belongs ($u_{1,site}$) and the random slope effect of the survey ($u_{1,surv|site}$).

4.7.5 Fitting richness-abundance spectra

We modelled the relationship between log abundance within a logarithmic bin class and the richness within the bin with a linear mixed effects model (Figure 4.1e, Equation 4.3). To fit this model we used the lme4 (Bates et al., 2015) package in R.

$$\log_2(R_m) = \beta_1 + u_{0,site} + u_{0,surv|site} + \log_2(N_m) \cdot (\beta_1 + u_{1,site} + u_{1,surv|site}) \quad (4.3)$$

where R_m is the total number of species within the log body mass bin m , and N_m is the total abundance of all individuals within the bin. For the normalised relationship, m refers not to the logarithmic bin, but the abundance and richness per unit body mass (abundance density and richness density) within the mass bin.

4.7.6 Size spectrum reconstruction methods

For reconstruction methods we split the data into a training ($n = 10935$ surveys) and a testing ($n = 1000$ surveys) dataset. From this test dataset we removed all body size information, maintaining speciesID, surveyID, siteID and abundance. We then performed two separate approaches (method 1 and 2) based upon the two-levels of body size data

availability for each species. Test surveys were randomly selected from surveys with > 90% of total abundance comprising fish species ($n = 3754$ surveys), therefore minimising comparisons of reconstructed size spectra with data including a reasonable portion of predicted data (invertebrate body size data), and thus with goodness-of-fit statistics artificially inflated.

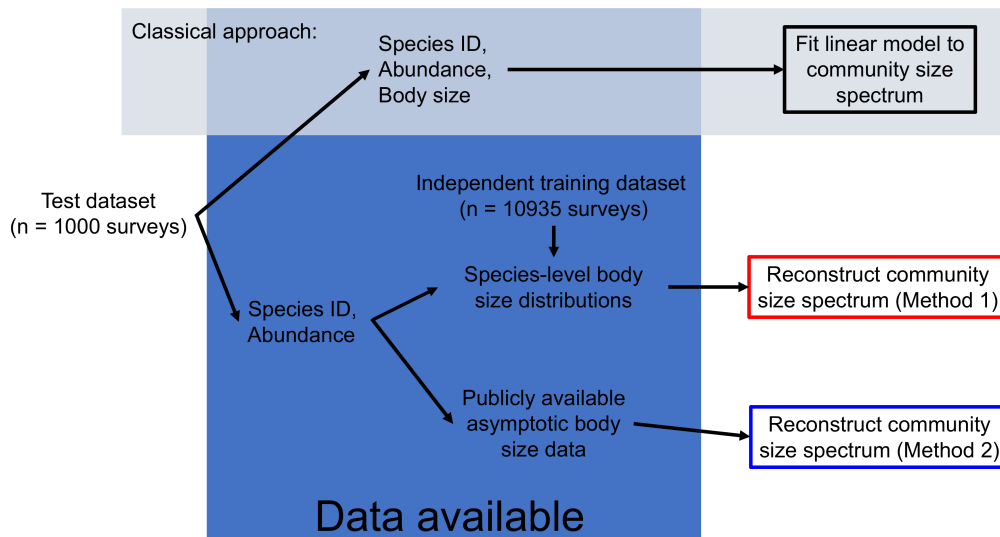


FIGURE 4.4: Summary of the approach of reconstructing size spectra based on limited body size data.

Method 1 (One body size distribution per species)

Method 1 refers to when a single body mass distribution per species is available. To obtain a single body mass distribution for each species we fitted a lognormal distribution to the observed body sizes from the training dataset (in survey size bins) using the ‘fitdistcens’ function within the ‘fitdistrplus’ package (Delignette-Muller and Dutang, 2015) in R (R Core Team, 2020). This function is specifically designed for fitting univariate binned data to a parametric distribution (Delignette-Muller and Dutang, 2015). Body length distributions were well represented as a lognormal distribution, consistent with previous literature (e.g. Blackburn and Gaston, 1994).

To convert these species body length distributions to body mass distributions, we used published species-level length-weight relationships (Froese and Pauly, 2010). If each species length distribution is lognormally distributed,

$$\log(p(l)) \sim \mathcal{N}(\mu_l, \sigma_l^2) \quad (4.4)$$

and the relationship between body mass (m) and body length (l) follows a power law relationship, $m = a \cdot l^b$, then the species mass distribution is lognormally distributed as,

$$\log(p(m)) \sim \mathcal{N}(\mu_m, \sigma_m^2) \quad (4.5)$$

where,

$$\begin{aligned}\mu_m &= b \cdot \mu_l + \log(a) \\ \sigma_m^2 &= b \cdot \sigma_l^2\end{aligned}\tag{4.6}$$

Method 2 (Asymptotic size for each species)

The second approach involved estimating the lognormal body mass distribution based upon the asymptotic length of the species (L) and the length-weight parameters, a and b , from the equation $m = a \cdot l^b$. These parameters (L , a , b) are publicly available from Sealifebase and Fishbase (Froese and Pauly, 2010, Palomares and Pauly, 2019). For each of the three parameters, if species-level information was unavailable, a mean genus-level estimate was used, else a family-level, order-level, class-level or phylum-level. By allowing broad-scale estimates of the three parameters, this method of species size distribution estimation is applicable even in the absence of any higher taxonomic-level body size information.

Following the methods of Heather et al. (2021a) to estimate the species body mass distribution based on the asymptotic mass of the species, we fit two linear models. Each model predicted one of the two parameters of the lognormal distribution (μ_m, σ_m^2) from the asymptotic mass, which is estimated from the asymptotic length, $M_\infty = a \cdot (L_\infty)^b$ (Supplementary material S4.1). Since the deviation in body mass (σ_m^2) appeared not to vary with increasing asymptotic body mass we used the mean (μ_m) for all species.

4.7.7 Building the community size spectrum

Following the methods outlined by Rinaldo et al. (2002), the community size spectrum was calculated as the weighted sum of the species' size distributions that make up the community, weighted by the abundance of the species in the community (see Rinaldo et al., 2002):

$$f(m; \mu_1, \dots, \mu_n, \sigma_1^2, \dots, \sigma_n^2) = \sum_k^m N_k \cdot p(m; \mu_k, \sigma_k^2)\tag{4.7}$$

where, N_k is the abundance of the k^{th} species in the community, m is the body mass, and $p(m; \mu_k, \sigma_k^2)$ is the lognormal probability density function for the k^{th} species.

To estimate the slope of the community size spectrum and allow for comparison with the observed data, we integrated the individual probability density for the community into \log_2 mass bins and multiplied the probability of occurrence of each bin by the total observed abundance at the survey. Estimated abundances in each \log_2 mass bin were rounded to the nearest whole number and to zero if < 1 . This resulted in an abundance estimate for each \log_2 mass bin at each survey, which can then be used with common linear modelling methods.

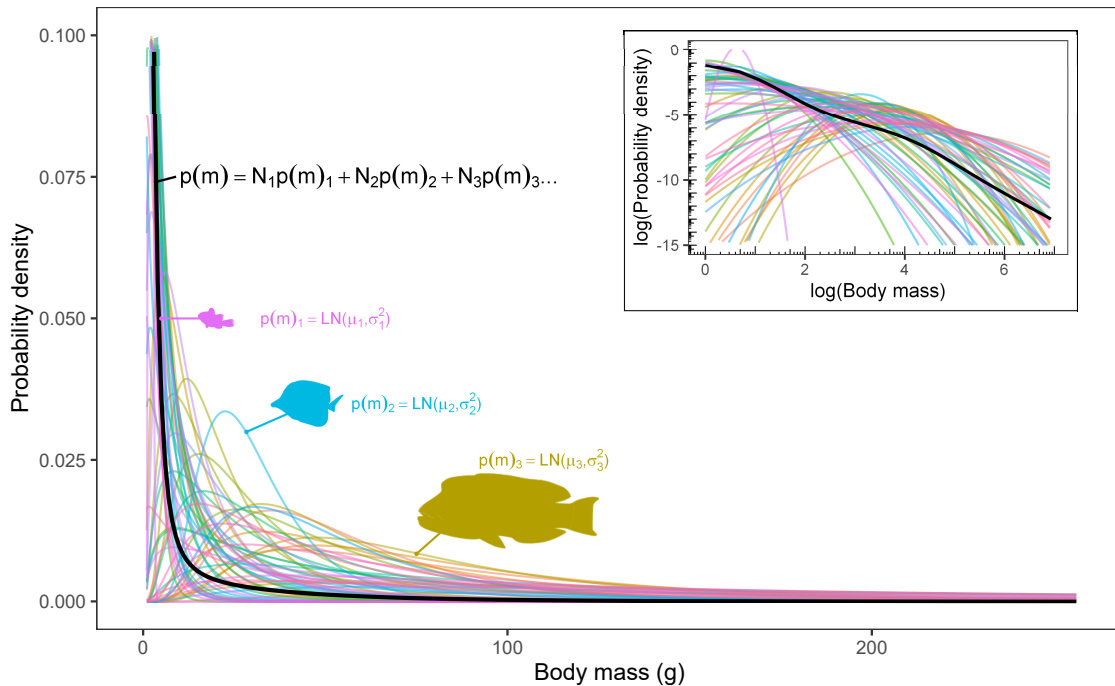


FIGURE 4.5: A power-law relationship emerges between body size and probability of occurrence by the summation of lognormal species mass distributions. The community size spectrum (black line) is calculated as the weighted sum of the species mass distributions (coloured lines). Inset shows the same relationship on the log-log scale; axes in the main plot have been cropped for visualisation purposes. Species silhouettes have been chosen for illustrative purposes only.

4.7.8 Validating reconstructed size spectra

For comparison with observed data, we integrate the continuous size distribution into \log_2 body mass bins, to give a probability of occurrence within a given mass bin per m^2 . We multiply this probability by the total abundance at the survey to obtain an estimate of abundance per mass bin per m^2 , and then multiply this by the area of a single transect (500 m^2) to obtain estimated abundance at the transect-level. We regard mass bins as empty when abundance estimates at the transect level are < 1 . From this we have species counts within log mass bins, and therefore species richness within each mass bin.

For both the abundance and richness size spectra, we tested the effectiveness of the size spectra reconstruction methods using the root mean squared error (RMSE) and the R^2 values of the observed vs expected response variables (abundance, richness, and abundance-richness). For each survey we calculated the root mean squared error (RMSE) between the reconstruction estimates of normalised abundance and the observed normalised abundance (Figure 4.3c), repeating for the normalised richness (Figure 4.3f) and normalised abundance-richness (Figure 4.3i) relationships. We also calculated the RMSE and R^2 values of a linear model fit estimate vs the observed data for the 1000 test surveys. These linear models refer to equations 4.1, 4.2, 4.3 for the abundance size spectrum, richness size spectrum and the richness-abundance spectra, respectively. RMSE is calculated

as $\sqrt{\frac{\sum_{i=1}^N \text{obs}_i - \text{exp}_i}{N}}$ for each mass-bin survey combination (i). RMSE is a positive number, with smaller RMSE values representing a better fitting model and 0 representing a perfect fit. We also calculated the R^2 of the linear relationship of the observed vs. expected normalised abundance (Figure 4.3c), normalised richness (Figure 4.3f), and normalised richness within a body mass bin (Figure 4.3i).

4.8 Acknowledgements

This research was supported by the Marine Biodiversity Hub, a collaborative partnership supported through funding from the Australian Government’s National Environmental Science Program, and data management support from Australia’s Integrated Marine Observing System (IMOS) – IMOS is enabled by the National Collaborative Research Infrastructure Strategy (NCRIS). This research was also made possible by funding of the Australian Research Council (ARC), and contributions from numerous participants in the Reef Life Survey program. The authors also thank data support from Antonia Cooper, Just Berkhout, Scott Ling, Ella Clausius and Elizabeth Oh.

4.9 Supplementary material

S4.1 Estimating the body mass distribution from asymptotic mass

In the absence of species-level body size distributions, we can estimate the distribution based on the asymptotic mass of the species. We assume body mass distributions are lognormally distributed (Blackburn and Gaston, 1994), with two parameters describing the distribution (μ, σ^2).

To estimate μ , given the asymptotic mass of the species (m_∞), we fit the linear model,

$$\mu_m = \beta_0 + \beta_1 \cdot \log(m_\infty) \quad (\text{S4.8})$$

to 698 species where we had estimates for both asymptotic mass and an estimate of mean body mass (μ_m). We found asymptotic body mass to explain 66% of the variation in mean body mass (Figure S4.6).

The fitted parameters are:

$$\begin{aligned} \beta_0 &= -0.95 \\ \beta_1 &= 0.77 \end{aligned} \quad (\text{S4.9})$$

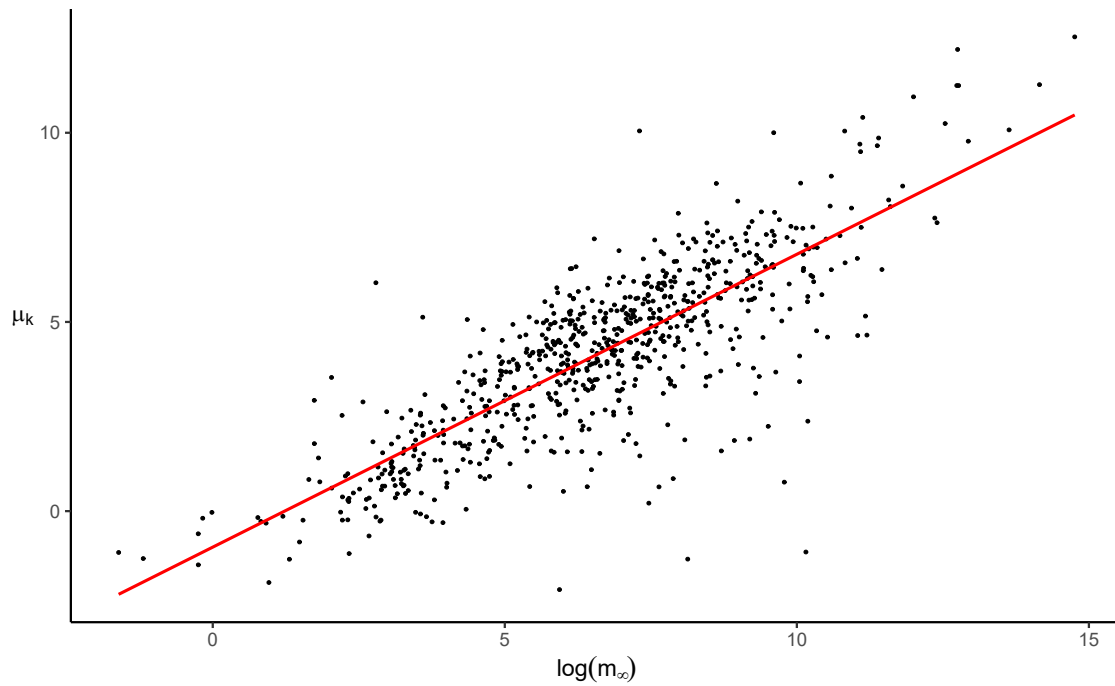


FIGURE S4.6: The mean of lognormally distributed body mass (μ_m) of a species is strongly correlated to its asymptotic mass (m_∞) (adjusted $R^2=66\%$). Each datapoint represents a single species ($n = 698$), and the red line shows the fitted linear model ($\mu_m = \beta_0 + \beta_1 \cdot m_\infty$, $p < 0.001$).

There appeared to be no significant relationship between deviation of body mass (σ_m^2) and the asymptotic mass (m_∞) of the species (Figure S4.7). We therefore chose a constant estimate of σ_m^2 as the mean of the 698 species, $\sigma_m^2 = 0.99$.

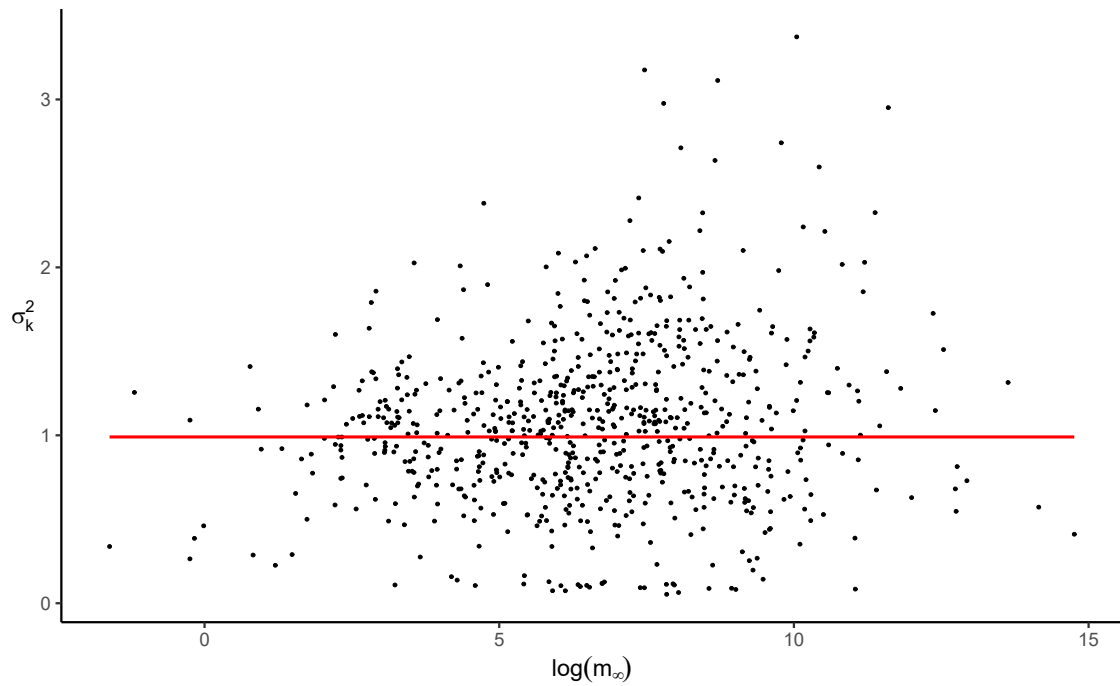


FIGURE S4.7: The variance of lognormally distributed body mass (σ_m^2) of a species is independent of asymptotic mass (m_∞). Each datapoint represents a single species ($n = 698$). A red line at 0.99 represents the mean of all species, and will be used at the variance parameter in the estimated lognormal body size distributions.

S4.2 Survey-level abundance size spectra

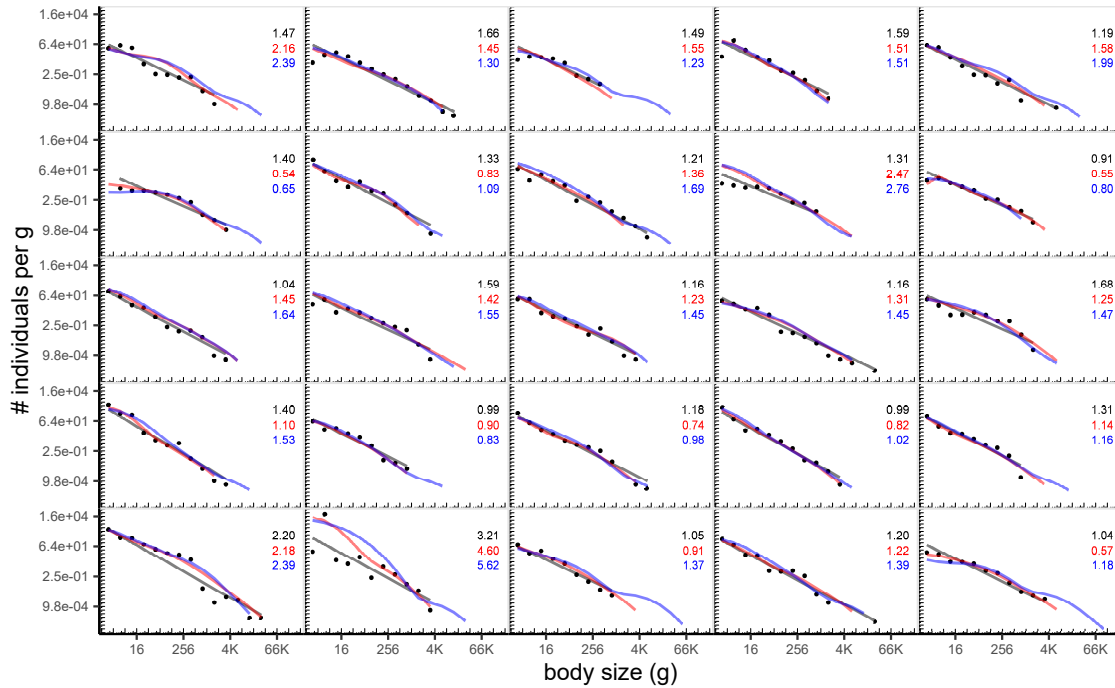


FIGURE S4.8: Abundance size spectra for a random sample of 25 surveys with three models. Black data points are the observed data. The black line represents the linear model fit to these observed data. The red line represents the estimated size spectrum based on knowledge of a single body size distribution for each species (Method 1). The blue line represents the estimated size spectrum based on species' size distributions reconstructed from the asymptotic mass of the species (Method 2). Numbers at the top right of each panel correspond to the root mean square error (RMSE) of each model, with smaller values representing a better fitting model.

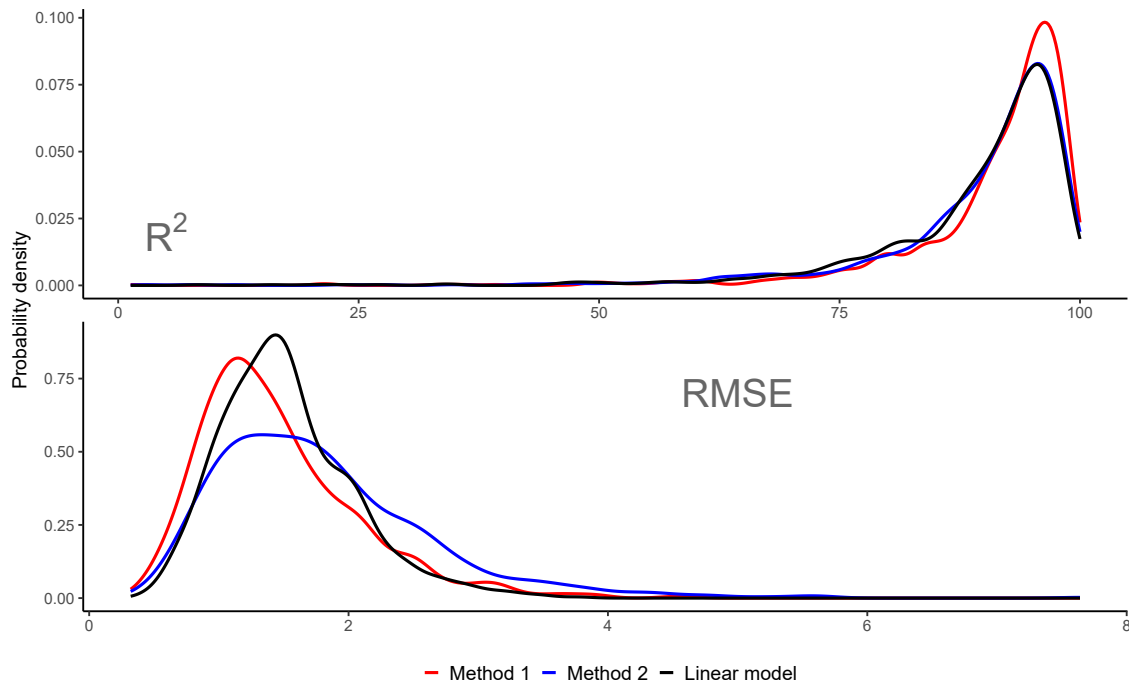


FIGURE S4.9: Comparison of the goodness of fit estimates for three abundance size spectra models for 1000 test surveys: 1) A linear model fit to the observed data (black line), 2) reconstructed abundance size spectrum based on global-average species' size distribution (Method1, red line) and 3) reconstructed abundance size spectrum based on information on the asymptotic mass (M_∞) of the species (Method 2, blue line). The top panel shows the adjusted R^2 estimate, and the bottom panel shows the root mean square error (RMSE) estimate for the observed vs modelled normalised abundance estimate.

S4.3 Survey-level richness size spectra

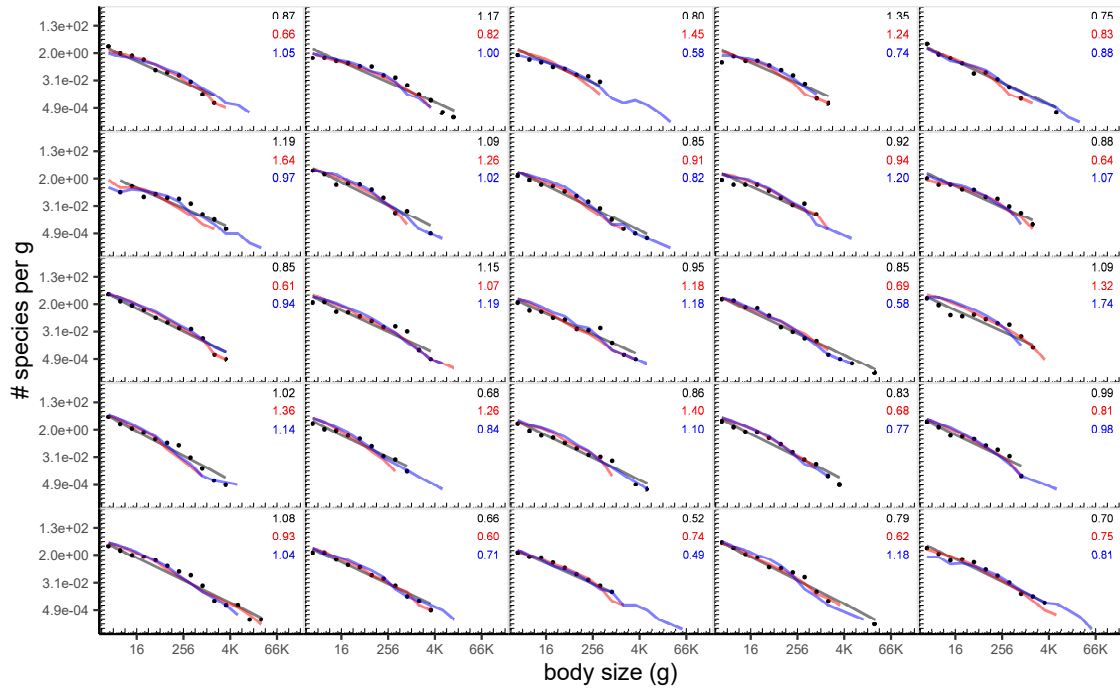


FIGURE S4.10: Richness size spectra for a random sample of 25 surveys with three models. Black data points are the observed data. The black line represents the linear model fit to these observed data. The red line represents the estimated size spectrum based on knowledge of a single body size distribution for each species (Method 1). The blue line represents the estimated size spectrum based on species' size distributions reconstructed from the asymptotic mass of the species (Method 2). Numbers at the top right of each panel correspond to the root mean square error (RMSE) of each model, with smaller values representing a better fitting model.

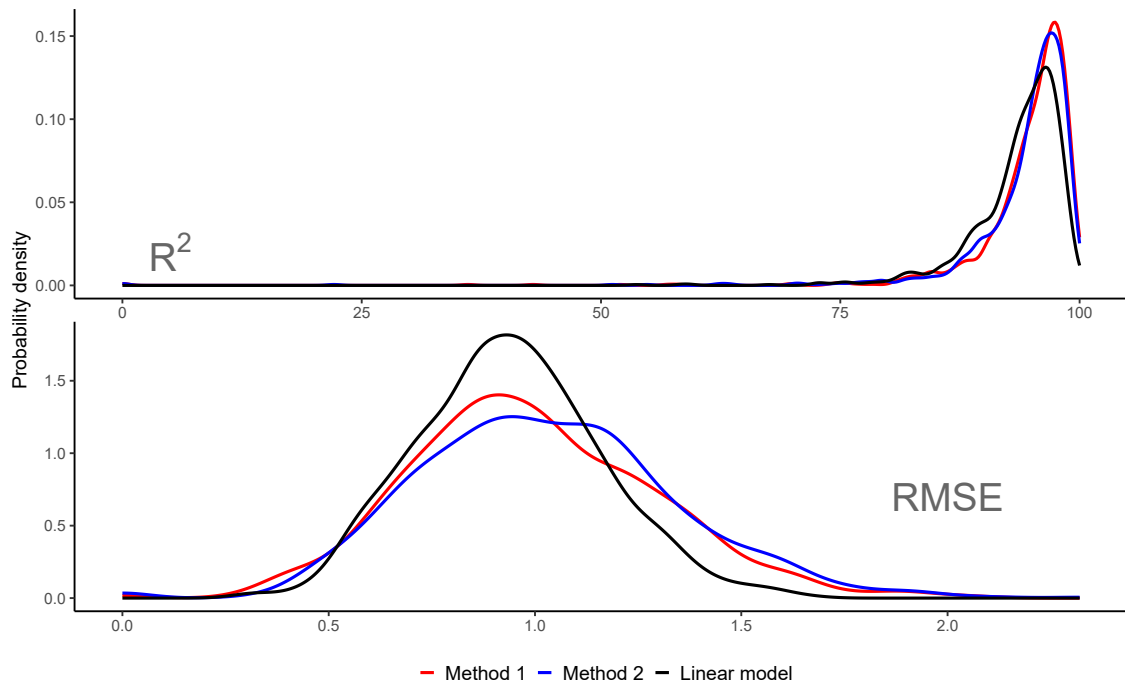


FIGURE S4.11: Comparison of the goodness of fit estimates for three species richness size spectra models for 1000 test surveys: 1) A linear model fit to the observed data (black line), 2) reconstructed abundance size spectrum based on global-average species' size distribution (Method1, red line) and 3) reconstructed richness size spectrum based on information on the asymptotic mass (m_∞) of the species (Method 2, blue line). The top panel shows the adjusted R^2 estimate, and the bottom panel shows the root mean square error (RMSE) estimate for the observed vs modelled species richness estimate.

S4.4 Survey-level richness-abundance spectrum

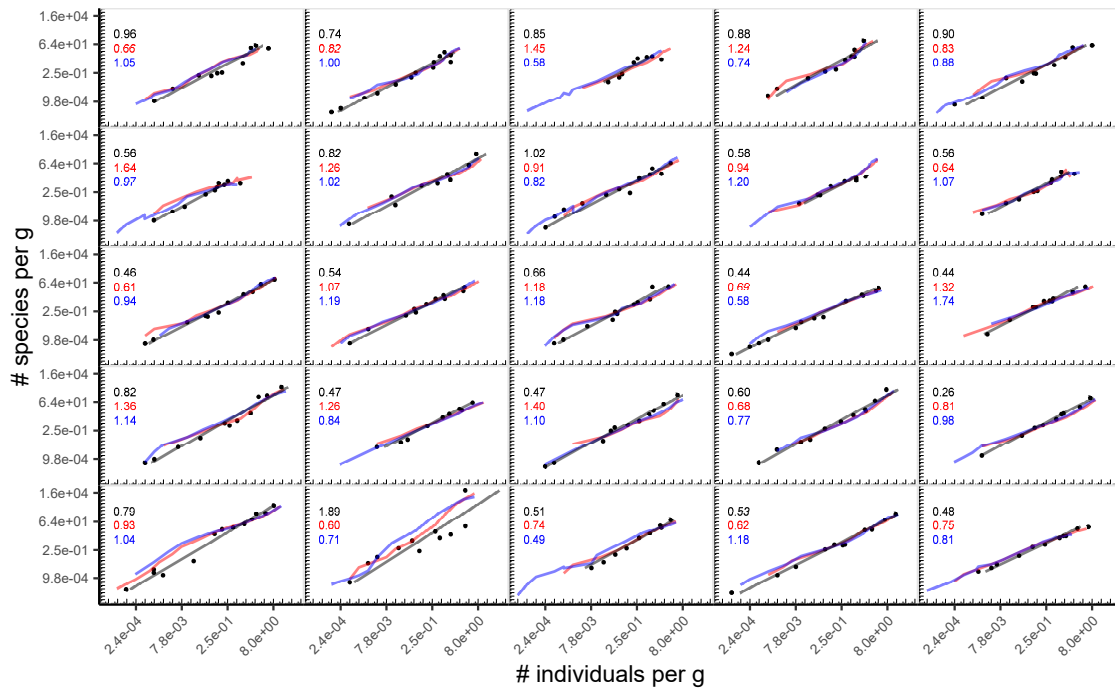


FIGURE S4.12: The relationship between the number of individuals (per unit g) within a logarithmic mass bin, and the number of species within the mass bin for a random sample of 25 surveys with three models. Black data points are the observed data. The black line represents the linear model fit to these observed data. The red line represents the estimated size spectrum based on knowledge of a single body size distribution for each species (Method 1). The blue line represents the estimated size spectrum based on species' size distributions reconstructed from the asymptotic mass of the species (Method 2). Numbers at the top right of each panel correspond to the root mean square error (RMSE) of each model, with smaller values representing a better fitting model.

Chapter 5

Synthesis & future research

Macroecological studies are based on the premise that broad-scale ecological patterns reflect the net outcomes of a complex combination of underlying processes (Brown et al., 2002, Brown and Maurer, 1989). By empirically describing these patterns, we are better informed to develop process-based mechanistic models with predictive capabilities under a range of scenarios. The distribution of individual body sizes within an ecological community is not only a measure of energetics but also of ecosystem structure (Marquet et al., 2005). This thesis has focused on the global-scale empirical relationships between body size, abundance, and species richness within reefs; integrating body size into the ongoing investigation of the enigmatic link between biodiversity and ecosystem functioning (Maureaud et al., 2020, Schneider et al., 2016). The consistency of the relationships described in this thesis with those across both aquatic and terrestrial realms, as well as across biological kingdoms, suggest that underlying universal ‘laws’ are at play. The methods presented in Chapter 4, for example, advances methods based on protist body size distributions (Giometto et al., 2013, Rinaldo et al., 2002) and the results support insect abundance-richness relationships (Siemann et al., 1996).

The ecological implications of body size by Robert H. Peters (Peters, 1983) describes the many empirical relationships with body size. In a paragraph on community size structure, Peters states that “Perhaps we will someday be able to measure the size spectrum of a pelagic site simply by driving across it in a boat”. This quote relates to the then recent development of sampling technologies, specifically the coulter counter, sonar, and radar technology. I would take this idea further and suggest that perhaps one day we would be able to measure the size spectrum of any ecological community, aquatic or terrestrial, from a laptop with access to appropriate remotely sensed data. Before this is possible, however, we must improve our understanding on how both broad- and fine-scale environmental and ecological drivers are changing community body size distributions.

5.1 The size spectrum as an ecological indicator of reef health

One of the overarching goals of this thesis was to improve our understanding of how the abundance of organisms is distributed across individual body sizes in reef communities. Body size is often described as the single most important trait defining how an individual interacts within the community and with the environment (Brown et al., 2002, Peters,

1983, Schmidt-Nielsen, 1984). The frequency distribution of body size in a community (the abundance size spectrum) therefore provides insights into the distribution and movement of energy within the food web (Brown and Gillooly, 2003, Trebilco et al., 2013). Since human disturbance to ecological communities is often size based (Reynolds et al., 2001), the size spectrum can be used to detect ecosystem disturbance. For its use as an ecological indicator, we must have an estimate of an expected 'baseline' size spectrum from which to compare and therefore be able to quantify deviations. Since all reefs globally are impacted by some form of human activity (Jackson et al., 2001, Knowlton and Jackson, 2008), we must have a predictive understanding of disturbances on size spectra if we are to determine the size spectrum in the absence of human pressure. One method is to compare relative slope values across a temporal (Wilson et al., 2010) or spatial (Robinson et al., 2017) range of disturbances (e.g., fishing pressure), yet this requires controlling or accounting for external environmental variables (e.g., seasonal and spatial variation in primary production).

Descriptions of the size spectrum of reef communities tend to focus on local-scale tropical coral reefs and are usually concentrated on fishes (Dulvy et al., 2004, Graham et al., 2005, Robinson et al., 2017, Wilson et al., 2010); however, recent work led by a PhD colleague, for which I contributed, extended analyses of size spectra from tropical to temperate realms, and to epifaunal invertebrates inhabiting a range of common reef habitat types (Fraser et al., 2020). Chapter 2 ("Globally consistent size spectra integrating fishes and invertebrates") of this thesis describes the empirical size spectrum of reefs globally, incorporating both fishes and large mobile invertebrates. The incorporation of invertebrates into reef size spectra steepens the slope estimates, bringing the estimates closer to theoretical expectations of -2 for biomass equivalence. This work improves our understanding of a baseline for reefs and describes the spatial variations in slope values. Chapter 3 ("Reef communities show predictable undulations in linear abundance size spectra from copepods to sharks") further develops the understanding of a baseline reef size spectrum by addressing the assumption that unimodal size spectra, commonly observed in reefs (e.g., Ackerman et al., 2004), are the result of sampling biases. The work presented in Chapter 3 suggests these nonlinear patterns are a true feature of the underlying size spectra of reefs, with deviations most likely driven by trophic cascades, supporting the mechanistic-based theory in lakes (Rossberg et al., 2019). To further test this theory, a destructive approach such as clove oil or rotenone sampling (Ackerman and Bellwood, 2002) may fill in the gap of individuals in the 22-50mm range absent in Heather et al. (2021b). The approach of ignoring small-bodied species that do not conform to the linear expectations of the size spectrum is commonly done in reef studies (Trebilco et al., 2015, Wilson et al., 2010), including in the study presented in Chapter 2 (Heather et al., 2021a). This does not mean that the descending limb of the size spectrum does not provide important information (e.g., quantifying fishing pressure Robinson et al., 2017), but suggests that it should be considered in the full context, i.e., as a component of an underlying nonlinear spectrum (Figure 5.1). Whilst the relative slope value of the size spectrum provides information about relative disturbance, an understanding of the

magnitude of the slope is also important to validate mechanistic approaches and improve inference on the movement of energy through the food web.

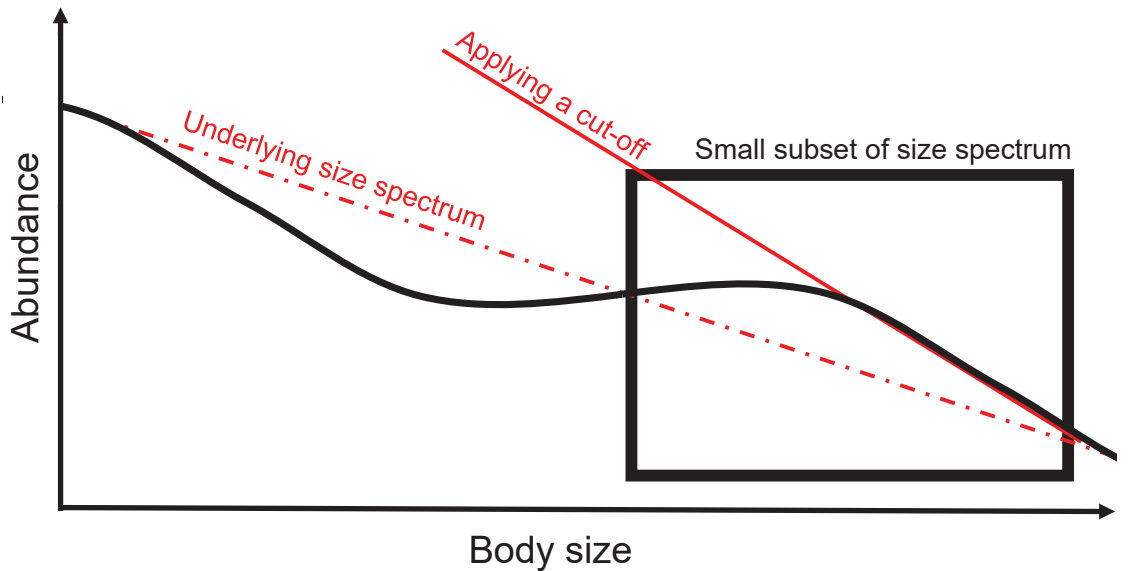


FIGURE 5.1: The importance of interpreting the size spectrum in the full context. By focusing on a small subset of the size spectrum (inside rectangular box), we may be ignoring the underlying pattern of the size spectrum. The solid red line indicates the linear model that would be fitted to the data if only the small subset of data is available (inside box), and a cut-off is applied (ignoring individuals in the abundance-dip). The red dashed line indicates the linear model that would be fitted with additional data exposing the underlying size spectrum.

As discussed throughout this thesis, the magnitude of the size spectrum slope can provide important information about the partitioning and movement of energy throughout the food web. For example, the metabolic theory of ecology (Brown et al., 2004) would suggest that if all individuals within a closed community are feeding upon a single basal trophic level (i.e., are herbivorous), one might expect abundance to scale with body mass to the power of 0.75. Steeper slopes would be expected situations where energy is lost through inefficient trophic energy transfer and feeding is size based (i.e., large eat small; Jennings et al., 2001). Chapter 3 highlights that a simple linear model is likely to exclude ecologically important information and may also influence what we regard as a baseline reef size spectrum, including the expected slope value (see Figure 5.1). A better understanding of the empirical size spectrum allows for process-based (e.g., food web models) and mechanistic models to test predictions. Below I outline some of the future directions that I think would be exciting to explore to gain a better understanding of the processes that give rise to the empirical size spectrum observed.

5.2 Where to next?

This thesis, with the aim of shedding light on the size structured nature of reefs, has opened many new questions and avenues for further research (Figure 5.2). This synthesis outlines the implications of the current research and the newly opened doors for exploration. Figure 5.2 shows a selection of 10 questions that have arisen as the result of the three papers presented in this thesis. I will further detail these questions below.

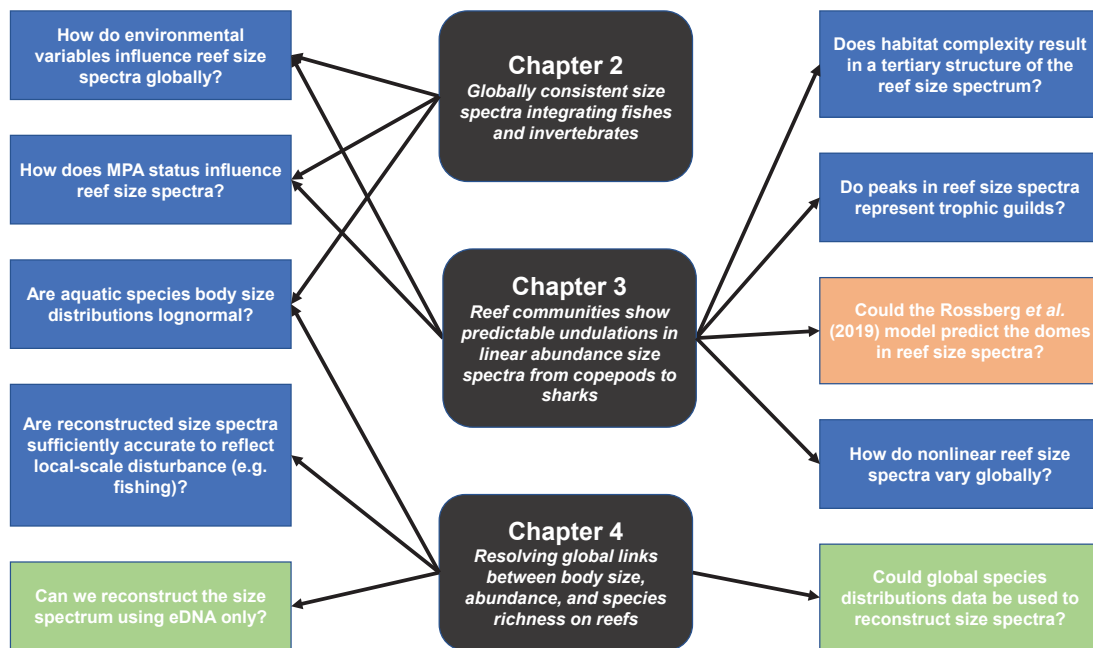


FIGURE 5.2: Potential directions for further research into reef size spectra and their links to the current works presented in this thesis. The colours of boxes represent the expected type of study required: blue = statistical approaches, orange = mechanistic or process-driven modelling, green = method application.

5.2.1 Question 1. How do environmental variables influence reef size spectra globally?

Chapter 2 describes the linear size spectrum of reefs globally. The study reports remarkable consistency in reef size spectra across broad-scale latitudinal gradients when invertebrates are included, yet variation in the slopes of size spectra at the local-scale still exist (Figure 2.4 in Chapter 2). These variations are likely driven by local-scale processes, such as site conditions and intensity of human disturbance (see also [Yen et al., 2017](#)). Further, Chapter 3 shows that nonlinear patterns in the size spectra are also likely driven by local site conditions. Combining the results of these two studies leads to the question of how environmental variables are statistically related to the linear (slope and intercept) and nonlinear (amplitude, wavelength) size spectrum parameters. This analysis would require fine-resolution, yet broad-scale, data on environmental conditions and human disturbance

(e.g., coastal human population) across the globe. To explain the variation in nonlinear parameters with environmental variables would require the estimation of nonlinear size spectra globally, expanding upon the spatial scale of the work of Chapter 3 (see Question 7 below). Outcomes should allow calculation of baseline curves that predict patterns in the absence of human impacts.

5.2.2 Question 2. How does MPA status influence reef size spectra?

Reef size spectra analyses relating human pressure (e.g., fishing) to the size spectrum slope often focus on local scale disturbances. Chapter 2 describes the empirical size spectrum of reefs globally. This includes reefs from outside and within marine protected areas, with a range of protection statuses. These data allow further investigation into the empirical relationship between size spectrum slope and ecological condition, and to therefore test the effectiveness of the size spectrum as an ecological indicator of reef health. Similar to Question 1, relating size spectra parameters to environmental conditions, a relatively simple analysis would be to statistically relate the linear size spectrum parameters (slope, intercept) to the protection status of the site, such as the five important characteristics of a protected area (NEOLI features in [Edgar et al., 2014](#)). This could also be expanded to nonlinear size spectra given a global description of the nonlinear size spectrum (see Question 7 below).

5.2.3 Question 3. Does habitat complexity result in a tertiary structure of the reef size spectrum?

The term secondary structure is generally used in size spectrum literature to describe the residuals of the fit of a linear model to the size spectrum. These deviations from linearity are usually assumed to represent some ecologically important variable, such as habitat complexity ([Rogers et al., 2014](#)). Chapter 3 quantifies the secondary structure of reef size spectra across a latitudinal gradient using an additional sine-wave component to the linear size spectrum. The results from Chapter 3 show broad-scale wave-like patterns are common in reef size spectra. The scale of body sizes for which these patterns span suggests they may be driven by trophic cascades. One might therefore expect that finer-scale deviations, such as the size-based refugia provided by reef habitat, could be detected by deviations from this wave-like size spectrum (i.e., the residuals of the nonlinear size spectrum). This would require fine-resolution data of reef habitat complexity and could be statistically analysed by the relationship between habitat complexity and the nonlinear size spectrum residuals, or incorporated into a mechanistic approach (e.g., [Rogers et al., 2014](#)).

5.2.4 Question 4. Do peaks in reef size spectra represent trophic guilds?

Chapter 3 postulates that wave-like patterns in reef size spectra arise from trophic cascades. If this is correct, then one might expect the removal of individuals within specific trophic guilds will predictably change the shape of the size spectrum. For example, if the peaks

and troughs are driven by a trophic interaction based on an adjacent peak or trough then a specific peak may predominately comprise a specific trophic group (e.g., macro-invertivores), and neighbour a trough dominated by a corresponding prey taxa (e.g., micro-invertebrates). This question could provide evidence for (or against) trophic cascades driving the wave-like patterns in reef size spectra. Further, the taxonomic composition of neighbouring peaks and troughs may shed light on food web interactions, although evidence of direct interactions may require a more in-depth mechanistic or process-based approach.

5.2.5 Question 5. Are aquatic species body size distributions lognormal?

One of the basic assumptions of studies outlined in Chapters 2 and 4 is that species' body sizes are lognormally distributed and can be reasonably predicted from asymptotic body size. This assumption is based upon both empirical patterns (e.g., [Giometto et al., 2013](#)) and population growth involving a multiplicative process ([Dennis and Patil, 1988](#)). Whilst the lognormal distribution does appear to provide a reasonable statistical representation of the underlying body size distribution at the broad scale explored in the studies presented within this thesis, uncertainty still exists on the drivers of the shape of species' body size distributions. For example, no consensus exists on whether species body size distributions are controlled by physiological constraints ([Pauly and Cheung, 2018](#)) or reflect adaptation to local site conditions (e.g., temperature; [Audzijonyte et al., 2020](#)). An answer to this question would require a large volume of body size data from various sources extending across a range of environmental conditions, and need to account for data-source biases.

5.2.6 Question 6. Could the [Rossberg et al. \(2019\)](#) model predict the domes in reef size spectra?

[Rossberg et al. \(2019\)](#) developed a mechanistic model to show that the wave-like patterns (also termed 'domes') observed in lake size spectra are likely driven by trophic cascades. The study fits a linear model with a sinusoidal component to these (empirical and simulated) wave-like patterns. The study presented in chapter 3 observes similar wave-like patterns in the empirical size spectrum of reefs when examined across a wide range of body sizes (epifauna and macrofauna). We showed that the sinusoidal size spectrum model provides a better fit than a linear model at more than 90% of the reefs studied. Combined with this, the distance between adjacent peaks and troughs was consistent with theoretical expectations based on trophic interactions. Both of these results support the hypothesis of trophic cascades driving the nonlinear patterns. [Rossberg et al. \(2019\)](#) also statistically related phosphorus availability to the nonlinear model parameters (e.g., amplitude, wavelength). Due to differences in nutrient availability between reef and freshwater lake ecosystems ([Howarth, 1988](#)), other variables (e.g., nitrogen availability) may possibly drive the nonlinear size spectrum patterns in reefs. The question therefore arises as to whether the mechanistic model in [Rossberg et al. \(2019\)](#) is applicable to reef

ecosystems, and if so, are the drivers of nonlinear patterns in reefs similar to those in lakes?

5.2.7 Question 7. How do nonlinear reef size spectra vary globally?

Due to the limited availability of epifaunal data, a relatively small number of sites ($n = 45$ sites) were analysed in Chapter 3, compared to the total number of visually surveyed sites ($n > 3000$) from the Reef Life Survey (Edgar et al., 2020, Edgar and Stuart-Smith, 2014, RLS, 2021). However, epifaunal assemblages vary consistently with microhabitat (Fraser et al., 2020), and data on the percentage cover of habitat (e.g., macroalgal, coral, sponge) are available globally from photo-quadrat data as part of the Reef Life Survey methods (Edgar et al., 2020). Using the empirical data on habitat composition at each site and extrapolating the habitat vs. epifaunal abundance relationships, it may be possible to provide an estimate of the epifaunal (Fraser et al., 2021), and therefore combined epifaunal and macrofaunal (see Chapter 3), size spectrum globally. This estimate would allow us to better test the drivers of the nonlinear patterns in reef size spectra. This extrapolation however would likely require additional epifaunal sampling across a broader range of ecosystems than those analysed in Chapter 3.

5.2.8 Question 8. Are reconstructed size spectra sufficiently accurate to broadly reflect local-scale disturbance (e.g., fishing)?

Chapter 4 shows that we can accurately reconstruct broad-scale abundance and richness size spectra using relative abundance measures and a single, global-scale, body size distribution for each species, even when this distribution is based only on asymptotic body size. Despite evidence that species' size distributions can reflect environmental conditions (Audzijonyte et al., 2020), the question remains whether the representation of a species by a single body size distribution globally is too coarse to detect changes in the size spectrum due to local disturbance. Since reconstructed size spectra are based upon a single body size distribution per species across the globe, then strong relationships between reconstructed size spectrum parameters and environmental conditions may suggest that either relative abundance of species (i.e., species composition), the species richness, or a combination of both is the primary driver of the shape of the size spectrum (Figure 5.3A, B).

The process of reconstructing the size spectrum in Chapter 4 can be broken down into 1) obtaining species asymptotic body size estimates, 2) using regression relationships to estimate a probability distribution of body size for each species, 3) summing up the probability distributions based on the relative abundances. The first step assumes a single asymptotic size per species in all locations. The second step assumes a single relationship between asymptotic body size and the lognormal distribution parameters, but also that all species body size distributions are lognormally distributed across locations and under various disturbances (Figure 5.3A, B). I could therefore imagine an extension of this work, combined with the ideas gained from the question of lognormally distributed body size

(See question 5: Are aquatic species body size distributions lognormal?), that would not assume a constant asymptotic body size or a constant relationship between asymptotic body size and the body size distribution (Figure 5.3C). Exploring this question would lead us to a more process-based understanding of how environmental conditions are linked to species' size distributions and thus to the overall community size spectrum. Stochastic events are likely to play a major role in determining local scale species distributions, and therefore make predictions based on local fishing pressure difficult. An analysis across many sites, however, may allow us to determine how species asymptotic size, species body size distributions, and species composition vary across a range of fishing pressures.

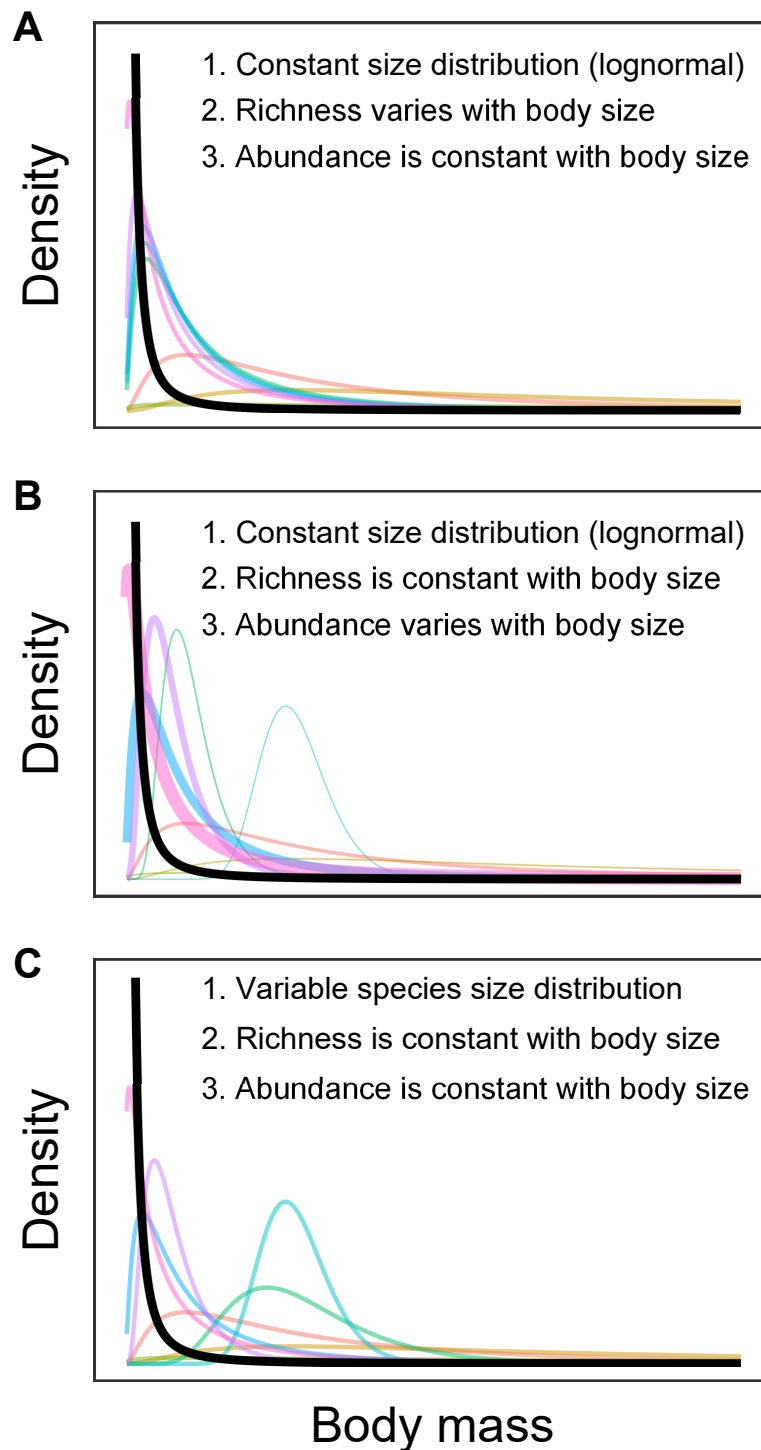


FIGURE 5.3: How variation in species' size distributions could give rise to the observed community size distribution (black line) – fewer individuals with increasing body size. Each coloured line represents a single species' size distribution, the thickness of the line represents the relative abundance of the species. Variation in the community size spectrum can be driven by (A) the number of species (richness) varying with body size, (B) the relative abundance within species varying with body size, and (C) the non-constant shapes of the species body size distributions. A constant size distribution refers to a single lognormal distribution based on a constant relationship between species asymptotic size and size distribution.

5.2.9 Question 9. Can we reconstruct the size spectrum using eDNA only?

The studies presented in this thesis have had the benefit of access to a global-scale dataset of reef faunal abundance and body size. Such a breadth of body size information is rarely available in other ecosystems. However, as I show throughout this thesis, body size follows strong and predictable patterns that can inform further study in the absence of such data. Most significantly, Chapter 4 shows that a simple estimate of asymptotic body mass is sufficient to reconstruct the abundance and richness size spectrum of reef communities.

Chapter 4 shows that with species' relative abundance, and publicly available information on species asymptotic body length and length-weight relationships, i.e., from Fish Base (Froese and Pauly, 2010) and Sea Life Base (Palomares and Pauly, 2019), we can reconstruct both abundance and richness size spectra. Any sources of relative abundances of species, in combination with mean or asymptotic size estimates, could therefore allow for reconstruction of size spectra. Environmental DNA (eDNA) refers to DNA that is sampled from the general environment (e.g., water, soil, air) as opposed to a specific organism (Bohmann et al., 2014). Lacoursière-Roussel et al. (2016) show, in Lake Trout, that the concentration of eDNA can be related to relative abundance, however the accuracy of eDNA to determine relative abundances is debated due to errors involved with DNA amplification (Fonseca, 2018). Despite this, advances in this field are exciting, and one day may provide a way to estimate the size spectrum, and therefore a measure of ecosystem health, simply by collecting eDNA in water samples.

5.2.10 Question 10. Could global species distribution data be used to reconstruct size spectra?

Global species geographical distributions, such as provided by the Global Biodiversity Information Facility (GBIF; <https://gbif.org>) or Ocean Biodiversity Information System (OBIS; <http://obif.org>), are extremely valuable data sources. In some cases, relative abundance data are available, which would allow for size spectrum reconstruction following similar methods to those described for estimating size spectra based on eDNA (Question 9). However, distributional data alone will be sufficient to reconstruct very coarse size spectra only. By better understanding the nature of the relationship between asymptotic body size and abundance (i.e., the diversity size spectrum; Reuman et al., 2014) and the processes that drive spatial variation in that relationship, we may be able to combine species abundance estimates (based on asymptotic size) with estimated global species body size distributions. This approach would be coarse but would allow us to tease apart the question of how much variation in the community size spectrum is driven by the richness alone (Figure 5.3A), i.e., when the relative abundance of the species and the shape of the size distribution are held constant.

5.3 Concluding remarks

This research presented in this thesis capitalised on a global dataset of abundance and body size estimates of reef-associated fauna (Edgar et al., 2020, Edgar and Stuart-Smith, 2014), unparalleled in taxonomic and geographical scale. This dataset has permitted the exploration of global-scale relationships between body size, abundance and species richness; three cornerstones of macroecology (Gaston and Blackburn, 2000). This thesis provides the first global test of the biomass equivalence rule for any ecosystem (Polishchuk and Blanchard, 2019), showing that reef size spectra are consistent across latitudes and in-line with theoretical expectations, but only when large mobile invertebrates are accounted for. This is an important step in understanding the baseline size spectrum of reefs and highlights the connectivity of the energy pathways between invertebrates and fishes (Barneche et al., 2014, Blanchard et al., 2011).

A common feature of these global reef size spectra was the unintuitive increase in abundance with body size for the smallest-bodied fishes (i.e., the ‘abundance dip’). Although previously described in reef size spectra (Ackerman et al., 2004), this feature is often assumed to be a result of sampling biases associated with visual survey methods. Chapter 3 provides empirical evidence against this idea of sampling biases as the primary driver of the dip in abundance, suggesting that it is a true feature of size spectra – a component of a broader-scale wave-like pattern in size spectra (see Figure 5.1) that is likely driven by trophic interactions. This nonlinear size spectrum of reefs opens up many new questions (Figure 5.2) about whether this pattern holds globally, and whether these wave-like are related to ecosystem disturbance.

The study of these macroecological relationships requires large amounts of available data. A lack of body size data is usually a prohibiting factor in the construction of size spectra, yet the consistency of the empirical relationship between asymptotic body size and body size distributions allows size spectra to be estimated where minimal body size information is available. The methods developed in Chapter 4 enable the reconstruction of size spectra in situations of varying levels of data-availability. I am currently developing a freely available package in R (<https://github.com/FreddieJH/sbss>) that enables a user to reconstruct a community size spectrum based on species-level information: 1) The relative abundance of the species, and 2) the species asymptotic size (with capabilities of estimating asymptotic size from publicly available sources when not provided). This package will facilitate further exploration of the relationships described in this thesis, not only in reef ecosystems but for any ecological community.

5.4 Code availability

The R code to reproduce all figures in Chapters 2 - 4 are available on [Github](#), as well as the package to build size spectra from species-level information:

- Chapter 2 - https://github.com/FreddieJH/inverts_size_spec

-
- Chapter 3 - https://github.com/FreddieJH/sinusoidal_size_spec
 - Chapter 4 - https://github.com/FreddieJH/building_size_spec
 - Species based size spectrum (sbss) package - <https://github.com/FreddieJH/sbss>

Bibliography

Ackerman, J. L. and D. R. Bellwood

2000. Reef fish assemblages: A re-evaluation using enclosed rotenone stations. *Marine Ecology Progress Series*, 206(1954):227–237.

Ackerman, J. L. and D. R. Bellwood

2002. Comparative efficiency of clove oil and rotenone for sampling tropical reef fish assemblages. *Journal of Fish Biology*, 60(4):893–901.

Ackerman, J. L., D. R. Bellwood, and J. H. Brown

2004. The contribution of small individuals to density-body size relationships: Examination of energetic equivalence in reef fishes. *Oecologia*, 139(4):568–571.

Akaike, H.

1974. A new look at the statistical model identification. *IEEE Transactions on Automatic Control*, 19(6):716–723.

Andersen, K. H.

2019. *Fish ecology, evolution, and exploitation: a new theoretical synthesis*. Princeton University Press.

Andersen, K. H. and J. E. Beyer

2006. Asymptotic size determines species abundance in the marine size spectrum. *American Naturalist*, 168(1):54–61.

Andersen, K. H. and M. Pedersen

2010. Damped trophic cascades driven by fishing in model marine ecosystems. *Proceedings of the Royal Society B: Biological Sciences*, 277(1682):795–802.

Anticamara, J., R. Watson, A. Gelchu, and D. Pauly

2011. Global fishing effort (1950–2010): Trends, gaps, and implications. *Fisheries Research*, 107(1-3):131–136.

Audzijonyte, A., S. A. Richards, R. D. Stuart-Smith, G. Pecl, G. J. Edgar, N. S. Barrett, N. Payne, and J. L. Blanchard

2020. Fish body sizes change with temperature but not all species shrink with warming. *Nature Ecology and Evolution*, 4(June). Publisher: Springer US.

Azzurro, E., M. Matiddi, E. Fanelli, P. Guidetti, G. L. Mesa, A. Scarpato, and V. Axiak

2010. Sewage pollution impact on Mediterranean rocky-reef fish assemblages. *Marine Environmental Research*, 69(5):390–397.

- Azzurro, E., A. Pais, P. Consoli, and F. Andaloro
2007. Evaluating day–night changes in shallow Mediterranean rocky reef fish assemblages by visual census. *Marine Biology*, 151(6):2245–2253.
- Barneche, D. R., M. Kulbicki, S. R. Floeter, A. M. Friedlander, and A. P. Allen
2016. Energetic and ecological constraints on population density of reef fishes. *Proceedings of the Royal Society B: Biological Sciences*, 283(1823):20152186–20152186.
- Barneche, D. R., M. Kulbicki, S. R. Floeter, A. M. Friedlander, J. Maina, and A. P. Allen
2014. Scaling metabolism from individuals to reef-fish communities at broad spatial scales. *Ecology Letters*, 17(9):1067–1076.
- Bates, D., M. Mächler, B. M. Bolker, and S. C. Walker
2015. Fitting Linear Mixed-Effects Models Using lme4. *Journal of Statistical software*, 67(1).
- Benoît, E. and M. J. Rochet
2004. A continuous model of biomass size spectra governed by predation and the effects of fishing on them. *Journal of Theoretical Biology*, 226(1):9–21.
- Bianchi, G., H. Gislason, K. Graham, L. Hill, X. Jin, K. Koranteng, S. Manickchand-Heileman, I. Payá, K. Sainsbury, F. Sanchez, and K. Zwanenburg
2000. Impact of fishing on size composition and diversity of demersal fish communities. *ICES Journal of Marine Science*, 57(3):558–571.
- Blackburn, T. M. and K. J. Gaston
1994. Animal body size distributions: patterns, mechanisms and implications. *Trends in Ecology and Evolution*, 9(12):471–474.
- Blackburn, T. M. and K. J. Gaston
1997. A Critical Assessment of the Form of the Interspecific Relationship between Abundance and Body Size in Animals. *The Journal of Animal Ecology*, 66(2):233–233.
- Blanchard, J. L., K. H. Andersen, F. Scott, N. T. Hintzen, G. Piet, and S. Jennings
2014. Evaluating targets and trade-offs among fisheries and conservation objectives using a multispecies size spectrum model. *Journal of Applied Ecology*, 51(3):612–622.
- Blanchard, J. L., N. K. Dulvy, S. Jennings, J. R. Ellis, J. K. Pinnegar, A. Tidd, and L. T. Kell
2005. Do climate and fishing influence size-based indicators of Celtic Sea fish community structure? *ICES Journal of Marine Science*, 62:405–411. Issue: 3.
- Blanchard, J. L., R. F. Heneghan, J. D. Everett, R. Trebilco, and A. J. Richardson
2017. From Bacteria to Whales: Using Functional Size Spectra to Model Marine Ecosystems. *Trends in Ecology and Evolution*, 32(3):174–186. Publisher: Elsevier Ltd.
- Blanchard, J. L., R. Law, M. D. Castle, and S. Jennings
2011. Coupled energy pathways and the resilience of size-structured food webs. *Theoretical Ecology*, 4(3):289–300.

- Boettiger, C., D. T. Lang, and P. C. Wainwright
2012. rfishbase: exploring, manipulating and visualizing FishBase data from R. *Journal of Fish Biology*, 81(6):2030–2039.
- Bohmann, K., A. Evans, M. T. P. Gilbert, G. R. Carvalho, S. Creer, M. Knapp, D. W. Yu, and M. de Bruyn
2014. Environmental DNA for wildlife biology and biodiversity monitoring. *Trends in Ecology & Evolution*, 29(6):358–367.
- Boudreau, P., L. Dickie, and S. Kerr
1991. Body-size spectra of production and biomass as system-level indicators of ecological dynamics. *Journal of Theoretical Biology*, 152(3):329–339.
- Boudreau, P. R. and L. M. Dickie
1992. Biomass spectra of aquatic ecosystems in relation to fisheries yield. *Canadian Journal of Fisheries and Aquatic Sciences*, 49(8):1528–1538.
- Bozec, Y. M., M. Kulbicki, F. Laloë, G. Mou-Tham, and D. Gascuel
2011. Factors affecting the detection distances of reef fish: Implications for visual counts. *Marine Biology*, 158(5):969–981.
- Brose, U., J. L. Blanchard, A. Eklöf, N. Galiana, M. Hartvig, M. R. Hirt, G. Kalinkat, M. C. Nordström, E. J. O’Gorman, B. C. Rall, F. D. Schneider, E. Thébault, and U. Jacob
2017. Predicting the consequences of species loss using size-structured biodiversity approaches: Consequences of biodiversity loss. *Biological Reviews*, 92(2):684–697.
- Brown, J. H.
1995. *Macroecology*. University of Chicago Press.
- Brown, J. H.
2014. Why are there so many species in the tropics? *Journal of Biogeography*, 41(1):8–22.
- Brown, J. H. and J. F. Gillooly
2003. Ecological food webs: High-quality data facilitate theoretical unification. *Proceedings of the National Academy of Sciences*, 100(4):1467–1468.
- Brown, J. H., J. F. Gillooly, A. P. Allen, V. M. Savage, and G. B. West
2004. Toward a metabolic theory of ecology. *Ecology*, 85(7):1771–1789.
- Brown, J. H., J. F. Gillooly, and G. B. West
2002. The next step in Macroecology: from general empirical patterns to universal ecological laws. P. 20.
- Brown, J. H. and B. A. Maurer
1989. Macroecology: The Division of Food and Space Among Species on Continents. *Science*, 243(4895):1145–1150.

- Brown, J. H. and P. F. Nicoletto
1991. Spatial Scaling of Species Composition: Body Masses of North American Land Mammals. *The American Naturalist*, 138(6):1478–1512.
- Campbell, S. J., E. S. Darling, S. Pardede, G. Ahmadia, S. Mangubhai, Amkieltiela, Estradivari, and E. Maire
2020. Fishing restrictions and remoteness deliver conservation outcomes for Indonesia's coral reef fisheries. *Conservation Letters*, 13(2).
- Cardillo, M.
2003. Biological determinants of extinction risk: why are smaller species less vulnerable? *Animal Conservation*, 6(1):63–69.
- Cheal, A. J., M. A. MacNeil, M. J. Emslie, and H. Sweatman
2017. The threat to coral reefs from more intense cyclones under climate change. *Global Change Biology*, 23(4):1511–1524.
- Cohen, J. E., S. L. Pimm, P. Yodzis, and J. Saldaña
1993. Body Sizes of Animal Predators and Animal Prey in Food Webs. *Journal of Animal Ecology*, 62(1):67–78.
- Connolly, S. R., S. A. Keith, R. K. Colwell, and C. Rahbek
2017. Process, Mechanism, and Modeling in Macroecology. *Trends in Ecology & Evolution*, 32(11):835–844.
- Cresswell, A. K., G. J. Edgar, R. D. Stuart-Smith, R. J. Thomson, N. S. Barrett, and C. R. Johnson
2017. Translating local benthic community structure to national biogenic reef habitat types. *Global Ecology and Biogeography*, 26(10):1112–1125.
- Cyr, H., R. H. Peters, J. A. Downing, and H. Cyr
1997. Population Density and Community Size Structure: Comparison of Aquatic and Terrestrial Systems. *Oikos*, 80(1):139.
- Daan, N., H. Gislason, J. G. Pope, and J. C. Rice
2005. Changes in the North Sea fish community: Evidence of indirect effects of fishing? *ICES Journal of Marine Science*, 62(2):177–188.
- Damuth, J.
1981. Population density and body size in mammals. *Nature*, 290(23):699–700.
- Delignette-Muller, M. L. and C. Dutang
2015. fitdistrplus: An R Package for Fitting Distributions. *Journal of Statistical Software*, 64(4):1–34.
- Dennis, B. and G. Patil
1988. Applications in Ecology. In *Lognormal distributions: Theory and applications*.

- Dickie, L. M., S. R. Keer, and P. R. Boudreau
1987. Size-dependent processes underlying regularities in ecosystem structure. *Ecological Monographs*, 57(3):233–250.
- Dinmore, T. A. and S. Jennings
2004. Predicting abundance-body mass relationships in benthic infaunal communities. *Marine Ecology Progress Series*, 276(1):289–292.
- Donovan, M. K., A. M. Friedlander, J. Lecky, J. B. Jouffray, G. J. Williams, L. M. Wedding, L. B. Crowder, A. L. Erickson, N. A. J. Graham, J. M. Gove, C. V. Kappel, K. Karr, J. N. Kittinger, A. V. Norström, M. Nyström, K. L. L. Oleson, K. A. Stamoulis, C. White, I. D. Williams, and K. A. Selkoe
2018. Combining fish and benthic communities into multiple regimes reveals complex reef dynamics. *Scientific Reports*, 8(1):1–11.
- Dulvy, N. K., N. V. Polunin, A. C. Mill, and N. A. Graham
2004. Size structural change in lightly exploited coral reef fish communities: Evidence for weak indirect effects. *Canadian Journal of Fisheries and Aquatic Sciences*, 61(3):466–475.
- Eddy, T. D., J. R. Bernhardt, J. L. Blanchard, W. W. Cheung, M. Colléter, H. du Pontavice, E. A. Fulton, D. Gascuel, K. A. Kearney, C. M. Petrik, T. Roy, R. R. Rykaczewski, R. Selden, C. A. Stock, C. C. Wabnitz, and R. A. Watson
2020. Energy Flow Through Marine Ecosystems: Confronting Transfer Efficiency. *Trends in Ecology & Evolution*, P. S0169534720302573.
- Edgar, G. J.
1994. Observations on the size-structure of macrofaunal assemblages. *Journal of Experimental Marine Biology and Ecology*, 176(2):227–243.
- Edgar, G. J., T. J. Alexander, J. S. Lefcheck, A. E. Bates, S. J. Kininmonth, R. J. Thomson, E. Duffy, M. J. Costello, and R. D. Stuart-Smith
2017. Abundance and local-scale processes contribute to multi-phyla gradients in global marine diversity. *Science Advances*, 3(10).
- Edgar, G. J., G. J. Edgar, A. Cooper, S. C. Baker, W. Barker, N. S. Barrett, M. A. Becerro, A. E. Bates, D. Brock, D. M. Ceccarelli, E. Clausius, M. Davey, T. R. Davis, P. B. Day, A. Green, S. R. Griffiths, J. Hicks, I. A. Hinojosa, B. K. Jones, S. Kininmonth, M. F. Larkin, N. Lazzari, J. S. Lefcheck, S. D. Ling, P. Mooney, E. Oh, A. Pérez-Matus, J. B. Pocklington, R. Riera, J. A. Sanabria-Fernandez, Y. Seroussi, I. Shaw, D. Shields, J. Shields, M. Smith, G. A. Soler, J. Stuart-Smith, J. Turnbull, and R. D. Stuart-Smith
2020. Establishing the ecological basis for conservation of shallow marine life using Reef Life Survey. *Biological conservation*, v. 252:2020 v.252.
- Edgar, G. J. and C. Shaw
1995. The production and trophic ecology of shallow-water fish assemblages in southern Australia I. Species richness, size-structure and production of fishes in Western Port, Victoria. *Journal of Experimental Marine Biology and Ecology*, 194(1):53–81.

- Edgar, G. J. and R. D. Stuart-Smith
2009. Ecological effects of marine protected areas on rocky reef communities-A continental-scale analysis. *Marine Ecology Progress Series*, 388(4):51–62.
- Edgar, G. J. and R. D. Stuart-Smith
2014. Systematic global assessment of reef fish communities by the Reef Life Survey program. *Scientific Data*, 1:1–8.
- Edgar, G. J., R. D. Stuart-Smith, T. J. Willis, S. Kininmonth, S. C. Baker, S. Banks, N. S. Barrett, M. A. Becerro, A. T. F. Bernard, J. Berkhout, C. D. Buxton, S. J. Campbell, A. T. Cooper, M. Davey, S. C. Edgar, G. Försterra, D. E. Galván, A. J. Irigoyen, D. J. Kushner, R. Moura, P. E. Parnell, N. T. Shears, G. A. Soler, E. M. A. Strain, and R. J. Thomson
2014. Global conservation outcomes depend on marine protected areas with five key features. *Nature*, 506(7487):216–20.
- Edwards, A. M., J. P. Robinson, M. J. Plank, J. K. Baum, and J. L. Blanchard
2017. Testing and recommending methods for fitting size spectra to data. *Methods in Ecology and Evolution*, 8(1):57–67.
- Elton, C. S.
1927. *Animal ecology*. University of Chicago Press.
- Fa, D. A. and J. E. Fa
2002. Species diversity, abundance and body size in rocky-shore Mollusca. *Journal of Molluscan Studies*, 68(1):95–100.
- Fine, P. V.
2015. Ecological and Evolutionary Drivers of Geographic Variation in Species Diversity. *Annual Review of Ecology, Evolution, and Systematics*, 46(1):369–392.
- Fonseca, V. G.
2018. "Pitfalls in relative abundance estimation using eDNA metabarcoding". *Molecular Ecology Resources*, 18(5):923–926.
- Fraser, K., R. Stuart-Smith, S. Ling, F. Heather, and G. Edgar
2020. Taxonomic composition of mobile epifaunal invertebrate assemblages on diverse benthic microhabitats from temperate to tropical reefs. *Marine Ecology Progress Series*, 640(Taylor 1998):31–43.
- Fraser, K. M., R. D. Stuart-Smith, S. D. Ling, and G. J. Edgar
2021. Small invertebrate consumers produce consistent size spectra across reef habitats and climatic zones. *Oikos*, 130(1):156–170.
- Froese, R. and D. Pauly
2010. Fish Base.
- Gaston, K. J. and T. M. Blackburn
1995. Birds, body size and the threat of extinction. P. 8.

- Gaston, K. J. and T. M. Blackburn
2000. *Pattern and Process in Macroecology*.
- Ghilarov, M.
1944. Correlation between size and number of soil animals. *Comptes Rendus (Doklady) de l'Academie des Sciences de l'URSS XLIII*, 6:267–269.
- Gillooly, J. F., E. L. Charnov, G. B. West, V. M. Savage, and J. H. Brown
2002. Effects of size and temperature on developmental time. *Nature*, 417(6884):70–73.
- Giometto, A., F. Altermatt, F. Carrara, A. Maritan, and A. Rinaldo
2013. Scaling body size fluctuations. *Proceedings of the National Academy of Sciences of the United States of America*, 110(12):4646–4650.
- Gislason, H., J. Collie, B. R. MacKenzie, A. Nielsen, M. d. F. Borges, T. Bottari, C. Chaves, A. V. Dolgov, J. Dulčić, D. Duplisea, H. O. Fock, D. Gascuel, L. Gil de Sola, J. G. Hiddink, R. Hofstede, I. Isajlović, J. P. Jonasson, O. Jørgensen, K. Kristinsson, G. Marteinsdottir, H. Masski, S. Matić-Skoko, M. R. Payne, M. Peharda, J. Reinert, J. Sólmundsson, C. Silva, L. Stefansdottir, F. Velasco, and N. Vrgoč
2020. Species richness in North Atlantic fish: Process concealed by pattern. *Global Ecology and Biogeography*, 29(5):842–856.
- Graham, N. A. J., N. K. Dulvy, S. Jennings, and N. V. C. Polunin
2005. Size-spectra as indicators of the effects of fishing on coral reef fish assemblages. *Coral Reefs*, 24(1):118–124.
- Graham, N. A. J., S. K. Wilson, S. Jennings, N. V. C. Polunin, J. Robinson, J. P. Bijoux, and T. M. Daw
2007. Lag effects in the impacts of mass coral bleaching on coral reef fish, fisheries, and ecosystems. *Conservation Biology*, 21(5):1291–1300.
- Hartvig, M., K. H. Andersen, and J. E. Beyer
2011. Food web framework for size-structured populations. *Journal of Theoretical Biology*, 272(1):113–122.
- Heather, F. J., J. L. Blanchard, G. J. Edgar, R. Trebilco, and R. D. Stuart-Smith
2021a. Globally consistent reef size spectra integrating fishes and invertebrates. *Ecology Letters*, 24(3):572–579.
- Heather, F. J., R. D. Stuart-Smith, J. L. Blanchard, K. M. Fraser, and G. J. Edgar
2021b. Reef communities show predictable undulations in linear abundance size spectra from copepods to sharks. *Ecology Letters*, 24(10):2146–2154.
- Hebbali, A.
2020. *olsrr: Tools for Building OLS Regression Models*.

- Heenan, A., G. J. Williams, and I. D. Williams
2020. Natural variation in coral reef trophic structure across environmental gradients. *Frontiers in Ecology and the Environment*, 18(2):69–75.
- Hixon, M. A. and J. P. Beets
1989. Shelter Characteristics and Caribbean Fish Assemblages: Experiments with Artificial Reefs. *Bulletin of Marine Science*, 44:15.
- Hixon, M. A. and J. P. Beets
1993. Predation, prey refuges, and the structure of coral-reef fish assemblages. *Ecological Monographs*, 63(1):77–101. Publisher: Ecological Society of America.
- Howarth, R. W.
1988. Nutrient Limitation Of Net Primary Production In Marine Ecosystems. P. 24.
- Hughes, T. P.
2003. Climate Change, Human Impacts, and the Resilience of Coral Reefs. *Science*, 301(5635):929–933.
- Hughes, T. P., K. D. Anderson, S. R. Connolly, S. F. Heron, J. T. Kerry, J. M. Lough, A. H. Baird, J. K. Baum, M. L. Berumen, T. C. Bridge, D. C. Claar, C. M. Eakin, J. P. Gilmour, N. A. J. Graham, H. Harrison, J.-P. A. Hobbs, A. S. Hoey, M. Hoogenboom, R. J. Lowe, M. T. McCulloch, J. M. Pandolfi, M. Pratchett, V. Schoepf, G. Torda, and S. K. Wilson
2018. Spatial and temporal patterns of mass bleaching of corals in the Anthropocene. *Science*, 359(6371):80–83.
- Hutchinson, G. E. and R. H. MacArthur
1959. A Theoretical Ecological Model of Size Distributions Among Species of Animals. *The American Naturalist*, 93(869):117–125.
- Huxley, J., R. E. Strauss, and F. B. Churchill
1932. *Problems of relative growth*.
- Jackson, J. B. C., M. X. Kirby, W. H. Berger, K. A. Bjorndal, L. W. Botsford, B. J. Bourque, R. H. Bradbury, R. Cooke, J. Erlandson, J. A. Estes, T. P. Hughes, S. Kidwell, C. B. Lange, H. S. Lenihan, J. M. Pandolfi, C. H. Peterson, R. S. Steneck, M. J. Tegner, and R. R. Warner
2001. Historical overfishing and the recent collapse of coastal ecosystems. *Science*, 293(5530):629–637.
- Jennings, S. and J. L. Blanchard
2004. Fish abundance with no fishing: predictions based on macroecological theory. *Journal of Animal Ecology*, 73(4):632–642.
- Jennings, S., S. P. R. Greenstreet, and J. D. Reynolds
1999. Structural change in an exploited fish community: a consequence of differential fishing effects on species with contrasting life histories. *Journal of Animal Ecology*, 68(3):617–627.

Jennings, S. and J. Lock

1996. Population and ecosystem effects of reef fishing. In *Reef Fisheries*.

Jennings, S. and S. Mackinson

2003. Abundance-body mass relationships in size-structured food webs. *Ecology Letters*, 6(11):971–974.

Jennings, S., J. K. Pinnegar, N. V. C. Polunin, and T. W. Boon

2001. Weak cross-species relationships between body size and trophic level belie powerful size-based trophic structuring in fish communities. *Journal of Animal Ecology*, 70(6):934–944.

Jennings, S., K. J. Warr, and S. Mackinson

2002. Use of size-based production and stable isotope analyses to predict trophic transfer efficiencies and predator-prey body mass ratios in food webs. *Marine Ecology Progress Series*, 240:11–20.

Kerr, S. R. and L. M. Dickie

2001. *The biomass spectrum: a predator-prey theory of aquatic production*. Columbia University Press.

Kleiber, M.

1932. Body size and metabolism. *Hilgardia: A Journal of Agricultural Science*, 6(11):315–353.

Knowlton, N. and J. B. C. Jackson

2008. Shifting Baselines, Local Impacts, and Global Change on Coral Reefs. *PLoS Biology*, 6(2):e54.

Koenker, R.

2010. Quantile Regression in R: A Vignette. *Quantile Regression*, Pp. 295–316.

Labra, F. A., E. Hernández-Miranda, and R. A. Quiñones

2020. Assessing how body size affects the species-time relationship in a shallow marine benthic megafauna community exposed to a strong hypoxia disturbance. *Marine Biology*, 167(2):15.

Lacoursière-Roussel, A., G. Côté, V. Leclerc, and L. Bernatchez

2016. Quantifying relative fish abundance with eDNA: a promising tool for fisheries management. *Journal of Applied Ecology*, 53(4):1148–1157.

Lindeman, R. L.

1942. The Trophic Dynamic of Ecology. *Ecology*, 23(4):399–417.

Loder, N., T. M. Blackburn, and K. J. Gaston

1997. The Slippery Slope: Towards an Understanding of the Body Size Frequency Distribution. *Oikos*, 78(1):195.

- Marquet, P. A., R. A. Quiñones, S. Abades, F. Labra, M. Tognelli, M. Arim, and M. Rivadeneira
2005. Scaling and power-laws in ecological systems. *Journal of Experimental Biology*, 208(9):1749–1769.
- Maureaud, A., K. H. Andersen, L. Zhang, and M. Lindegren
2020. Trait-based food web model reveals the underlying mechanisms of biodiversity–ecosystem functioning relationships. *Journal of Animal Ecology*, 89(6):1497–1510.
- Maxwell, T. A. D. and S. Jennings
2006. Predicting abundance–body size relationships in functional and taxonomic subsets of food webs. *Oecologia*, 150(2):282–290.
- May, R. M.
1986. The Search for Patterns in the Balance of Nature: Advances and Retreats. *Ecology*, 67(5):1115–1126.
- McClain, C. R.
2004. Connecting species richness, abundance and body size in deep-sea gastropods: Species richness, abundance and body size in deep-sea gastropods. *Global Ecology and Biogeography*, 13(4):327–334.
- Mellin, C., D. Mouillot, M. Kulbicki, T. R. McClanahan, L. Vigliola, C. J. Bradshaw, R. E. Brainard, P. Chabanet, G. J. Edgar, D. A. Fordham, A. M. Friedlander, V. Parravicini, A. M. Sequeira, R. D. Stuart-Smith, L. Wantiez, and M. J. Caley
2016. Humans and seasonal climate variability threaten large-bodied coral reef fish with small ranges. *Nature Communications*, 7:1–9. Publisher: Nature Publishing Group.
- Menge, B. A. and J. Lubchenco
1981. Community Organization in Temperate and Tropical Rocky Intertidal Habitats: Prey Refuges in Relation to Consumer Pressure Gradients. *Ecological Monographs*, 51(4):429–450.
- Morais, R. A. and D. R. Bellwood
2019. Pelagic Subsidies Underpin Fish Productivity on a Degraded Coral Reef. *Current Biology*, 29(9):1521–1527.e6.
- Morais, R. A., S. R. Connolly, and D. R. Bellwood
2020a. Human exploitation shapes productivity–biomass relationships on coral reefs. *Global Change Biology*, 26(3):1295–1305.
- Morais, R. A., M. Depczynski, C. Fulton, M. Marnane, P. Narvaez, V. Huertas, S. J. Brandl, and D. R. Bellwood
2020b. Severe coral loss shifts energetic dynamics on a coral reef. *Functional Ecology*, 34(7):1507–1518.

- Mumby, P. J.
2006. Fishing, Trophic Cascades, and the Process of Grazing on Coral Reefs. *Science*, 311(5757):98–101.
- Nash, K. L. and N. A. Graham
2016. Ecological indicators for coral reef fisheries management. *Fish and Fisheries*, 17(4):1029–1054.
- Nee, S., A. F. Read, J. J. D. Greenwood, and P. H. Harvey
1991. The relationship between abundance and body size in British birds. *Nature*, 351(May):312–313.
- Newman, M. E. J.
2005. Power laws, Pareto distributions and Zipf's law. *Contemporary Physics*, 46(5):323–351.
- Olden, J. D., Z. S. Hogan, and M. J. V. Zanden
2007. Small fish, big fish, red fish, blue fish: size-biased extinction risk of the world's freshwater and marine fishes. *Global Ecology and Biogeography*, 16(6):694–701.
- Palomares, M. L. D. and D. Pauly
2019. Sea Life Base.
- Pauly, D.
1998. Fishing Down Marine Food Webs. *Science*, 279(5352):860–863.
- Pauly, D. and W. W. L. Cheung
2018. Sound physiological knowledge and principles in modeling shrinking of fishes under climate change. *Global Change Biology*, 24(1):e15–e26.
- Petchey, O. L. and A. Belgrano
2010. Body-size distributions and size-spectra: universal indicators of ecological status? *Biology Letters*, 6(4):434–437.
- Peters, R. H.
1983. *The ecological implications of body size*, volume 2. Cambridge University Press.
- Platt, T. and K. Denman
1977. Organisation in the pelagic ecosystem. *Helgoländer Wissenschaftliche Meeresuntersuchungen*, 30(1-4):575–581.
- Polishchuk, L. V.
2019. M.S. Ghilarov's Principle, or Biomass Equivalence Rule, as a Conservation Law in Ecology. *Biology Bulletin Reviews*, 9(3):215–229.
- Polishchuk, L. V. and J. L. Blanchard
2019. Uniting Discoveries of Abundance-Size Distributions from Soils and Seas. *Trends in Ecology & Evolution*, 34(1):2–5.

- Pope, J. and B. Knights
1982. Comparison of length distributions of combined catches of all demersal fishes in surveys in the North Sea and at Faroe Bank. In *Multispecies approaches to fisheries management advice*, volume 59, Pp. 116–118.
- Purves, D. W.
2013. Time to model all life on earth. *Nature*, 493:295–297.
- R Core Team
2020. R: A Language and Environment for Statistical Computing.
- Rahbek, C.
2004. The role of spatial scale and the perception of large-scale species-richness patterns: Scale and species-richness patterns. *Ecology Letters*, 8(2):224–239.
- Reuman, D. C., H. Gislason, C. Barnes, F. Mélin, and S. Jennings
2014. The marine diversity spectrum. *Journal of Animal Ecology*, 83(4):963–979.
- Reuman, D. C., C. Mulder, D. Raffaelli, and J. E. Cohen
2008. Three allometric relations of population density to body mass: Theoretical integration and empirical tests in 149 food webs. *Ecology Letters*, 11(11):1216–1228.
- Reynolds, J. D., S. Jennings, and N. K. Dulvy
2001. Life histories of fishes and population responses to exploitation. In *Conservation of Exploited Species*, Pp. 148–168. Cambridge University Press, Cambridge.
- Rice, J. C. and H. Gislason
1996. Patterns of change in the size spectra of numbers and diversity of the North Sea fish assemblage, as reflected in surveys and models. *ICES Journal of Marine Science*, 53(6):1214–1225.
- Rinaldo, A., A. Maritan, K. K. Cavender-Bares, and S. W. Chisholm
2002. Cross-scale ecological dynamics and microbial size spectra in marine ecosystems. *Proceedings of the Royal Society B: Biological Sciences*, 269:2051–2059.
- RLS
2021. Reef Life Survey.
- Robinson, J. P. W., J. K. Baum, and H. Giacomini
2016. Trophic roles determine coral reef fish community size structure. *Canadian Journal of Fisheries and Aquatic Sciences*, 73(4):496–505.
- Robinson, J. P. W., S. K. Wilson, S. Jennings, and N. A. J. Graham
2019a. Thermal stress induces persistently altered coral reef fish assemblages. *Global Change Biology*, 25(8):2739–2750.

- Robinson, J. P. W., S. K. Wilson, J. Robinson, C. Gerry, J. Lucas, C. Assan, R. Govinden, S. Jennings, and N. A. J. Graham
2019b. Productive instability of coral reef fisheries after climate-driven regime shifts. *Nature Ecology & Evolution*, 3(2):183–190.
- Robinson, J. W., I. D. Williams, A. M. Edwards, J. McPherson, L. A. Yeager, L. Vigliola, R. E. Brainard, and J. K. Baum
2017. Fishing degrades size structure of coral reef fish communities. *Global Change Biology*, 23(3):1009–1022.
- Rodriguez, J. and M. M. Mullin
1986. Relation between biomass and body weight of plankton in a steady state oceanic ecosystem1: Biomass and size of plankton. *Limnology and Oceanography*, 31(2):361–370.
- Rogers, A., J. L. Blanchard, and P. J. Mumby
2014. Vulnerability of coral reef fisheries to a loss of structural complexity. *Current Biology*, 24(9):1000–1005. Publisher: Elsevier Ltd.
- Rossberg, A. G., U. Gaedke, and P. Kratina
2019. Dome patterns in pelagic size spectra reveal strong trophic cascades. *Nature Communications*, 10(1):1–11. Publisher: Springer US.
- Salomon, A. K., S. K. Gaichas, N. T. Shears, J. E. Smith, E. M. P. Madin, and S. D. Gaines
2010. Key Features and Context-Dependence of Fishery-Induced Trophic Cascades. *Conservation Biology*, 24(2):382–394.
- Schmidt-Nielsen, K.
1984. *Scaling: why is animal size so important?* Cambridge university press.
- Schneider, F. D., U. Brose, B. C. Rall, and C. Guill
2016. Animal diversity and ecosystem functioning in dynamic food webs. *Nature Communications*, 7(1):12718.
- Schwinghamer, P.
1981. Characteristic Size Distributions of Integral Benthic Communities. *Canadian Journal of Fisheries and Aquatic Sciences*, 38(10):1255–1263.
- Sheldon, R. W., T. P. T. Evelyn, and T. R. Parsons
1967. On the occurrence and formation of small particulates in seawater. *Limnology and Oceanography*, 12(July):367–375.
- Sheldon, R. W. and T. R. Parsons
1966. On some applications of the Coulter counter for marine research. *Oceanographic and Limnological*.
- Sheldon, R. W. and T. R. Parsons
1967. A Continuous Size Spectrum for Particulate Matter in the Sea. *Journal of the Fisheries Research Board of Canada*, 24(5):909–915.

- Sheldon, R. W., A. Prakash, and W. H. Sutcliffe
1972. The size distribution of particles in the ocean. *Limnology and Oceanography*, 17(May):327–340.
- Sheldon, R. W., W. H. Sutcliffe Jr., and M. a. Paranjape
1977. Structure of Pelagic Food Chain and Relationship Between Plankton and Fish Production. *Journal of the Fisheries Research Board of Canada*, 34(12):2344–2353.
- Shin, Y. J., M. J. Rochet, S. Jennings, J. G. Field, and H. Gislason
2005. Using size-based indicators to evaluate the ecosystem effects of fishing. *ICES Journal of Marine Science*, 62(3):384–396.
- Shulman, M. J.
1985. Coral reef fish assemblages: intra- and interspecific competition for shelter sites. *Environmental Biology of Fishes*, 13(2):81–92.
- Siemann, E., D. Tilman, and J. Haarstad
1996. Insect species diversity, abundance and body size relationships. *Nature*, 380(6576):704–706.
- Spalding, M. D., H. E. Fox, G. R. Allen, N. Davidson, Z. A. Ferdaña, M. Finlayson, B. S. Halpern, M. A. Jorge, A. Lombana, S. A. Lourie, K. D. Martin, E. McManus, J. Molnar, C. A. Recchia, and J. Robertson
2007. Marine Ecoregions of the World: A Bioregionalization of Coastal and Shelf Areas. *BioScience*, 57(7):573–583.
- Sprules, W. G. and L. E. Barth
2016. Surfing the biomass size spectrum: Some remarks on history, theory, and application. *Canadian Journal of Fisheries and Aquatic Sciences*, 73(4):477–495.
- Sprules, W. G., J. M. Casselman, and B. Shuter
1983. Size Distribution of Pelagic Particles in Lakes. *Canadian Journal of Fisheries and Aquatic Sciences*, 40(10):1761–1769.
- Sprules, W. G. and M. Munawar
1986. Plankton Size Spectra in Relation to Ecosystem Productivity, Size, and Perturbation. *Canadian Journal of Fisheries and Aquatic Sciences*, 43(9):1789–1794.
- Steneck, R. S., D. R. Bellwood, and M. E. Hay
2017. Herbivory in the marine realm. *Current Biology*, 27(11):R484–R489. Publisher: Elsevier.
- Stewart, B. and J. Beukers
2000. Baited technique improves censuses of cryptic fish in complex habitats. *Marine Ecology Progress Series*, 197:259–272.
- Stuart-Smith, R. D., G. J. Edgar, N. S. Barrett, A. E. Bates, S. C. Baker, N. J. Bax, M. A. Becerro, J. Berkhout, J. L. Blanchard, D. J. Brock, G. F. Clark, A. T. Cooper, T. R. Davis,

- P. B. Day, J. Emmett Duffy, T. H. Holmes, S. A. Howe, A. Jordan, S. Kininmonth, N. A. Knott, L. S. Jonathan, S. D. Ling, A. Parr, E. Strain, S. Hugh, and T. Russell
2017. Assessing national biodiversity trends for rocky and coral reefs through the integration of citizen science and scientific monitoring programs. *BioScience*, 67(2):134–146.
- Stuart-Smith, R. D., C. Mellin, A. E. Bates, and G. J. Edgar
2021. Habitat loss and range shifts contribute to ecological generalization among reef fishes. *Nature Ecology & Evolution*.
- Trebilco, R., J. K. Baum, A. K. Salomon, and N. K. Dulvy
2013. Ecosystem ecology: Size-based constraints on the pyramids of life. *Trends in Ecology and Evolution*, 28(7):423–431. Publisher: Elsevier Ltd.
- Trebilco, R., N. K. Dulvy, S. C. Anderson, and A. K. Salomon
2016. The paradox of inverted biomass pyramids in kelp forest fish communities. *Proceedings of the Royal Society B: Biological Sciences*, 283(1833).
- Trebilco, R., N. K. Dulvy, H. Stewart, and A. K. Salomon
2015. The role of habitat complexity in shaping the size structure of a temperate reef fish community. *Marine Ecology Progress Series*, 532:197–211.
- Turner, R. E.
2001. Some effects of eutrophication on pelagic and demersal marine food webs. In *Coastal and Estuarine Studies*, volume 58, Pp. 371–398. Washington, D. C.: American Geophysical Union.
- Tyberghein, L., H. Verbruggen, K. Pauly, C. Troupin, F. Mineur, and O. De Clerck
2012. Bio-ORACLE: a global environmental dataset for marine species distribution modelling: Bio-ORACLE marine environmental data rasters. *Global Ecology and Biogeography*, 21(2):272–281.
- Ware, D. M.
1978. Bioenergetics of Pelagic Fish: Theoretical Change in Swimming Speed and Ration with Body Size. *Journal of the Fisheries Research Board of Canada*, 35(2):220–228.
- White, E. P., B. J. Enquist, and J. L. Green
2008. On estimating the exponent of power law frequency distributions. *Ecology*, 89(4):905–912.
- White, E. P., S. K. Ernest, A. J. Kerkhoff, and B. J. Enquist
2007. Relationships between body size and abundance in ecology. *Trends in Ecology and Evolution*, 22(6):323–330.
- Willis, T. J.
2001. Visual census methods underestimate density and diversity of cryptic reef fishes. *Journal of Fish Biology*, 59(5):1408–1411.

- Wilson, S., R. Fisher, M. Pratchett, N. Graham, N. Dulvy, R. Turner, A. Cakacaka, and N. Polunin
2010. Habitat degradation and fishing effects on the size structure of coral reef fish communities. *Ecological Applications*, 20(2):442–451.
- Yamanaka, T., P. C. L. White, M. Spencer, and D. Raffaelli
2012. Patterns and processes in abundance-body size relationships for marine benthic invertebrates. *Journal of Animal Ecology*, 81(2):463–471.
- Yen, J. D. L., J. R. Thomson, J. M. Keith, D. M. Paganin, E. Fleishman, D. S. Dobkin, J. M. Bennett, R. Mac Nally, and M. Dornelas
2017. Balancing generality and specificity in ecological gradient analysis with species abundance distributions and individual size distributions. *Global Ecology and Biogeography*, 26(3):318–332.
- Zgliczynski, B. J. and S. A. Sandin
2017. Size-structural shifts reveal intensity of exploitation in coral reef fisheries. *Ecological Indicators*, 73:411–421.